

**Characteristic α -Acid Derivatives from *Humulus lupulus* with
Antineuroinflammatory Activities**

Jiayuan Li,[†] Ning Li,^{*,†} Xuezheng Li,[‡] Gang Chen,[†] Cungang Wang,[†] Bin Lin,[§] and Yue Hou^{*,[⊥]}

[†] School of Traditional Chinese Materia Medica, Shenyang Pharmaceutical University, Shenyang; Key Laboratory of Structure-Based Drug Design and Discovery, Ministry of Education, Wenhua Road 103, Shenyang 110016, People's Republic of China

[‡] Department of Pharmacy, Affiliated Hospital of Yanbian University, Yanji 133000, People's Republic of China

[§] School of Pharmaceutical Engineering, Shenyang Pharmaceutical University, Shenyang 110016, People's Republic of China

[⊥] College of Life and Health Sciences, Department of Biochemistry and Molecular Biology, Northeastern University, Shenyang, 110819, People's Republic of China

List of Supporting Information

- S1.** ^1H NMR (400 MHz, CDCl_3) spectrum of (3*R*, 8*S*)-humulone A (**1**).
- S2.** ^{13}C NMR (100 MHz, CDCl_3) spectrum of (3*R*, 8*S*)-humulone A (**1**).
- S3.** HSQC (600 MHz, CDCl_3) spectrum of (3*R*, 8*S*)-humulone A (**1**).
- S4.** HMBC (600 MHz, CDCl_3) spectrum of (3*R*, 8*S*)-humulone A (**1**).
- S5.** NOESY (600 MHz, CDCl_3) spectrum of (3*R*, 8*S*)-humulone A (**1**).
- S6.** HRESIMS spectrum of (3*R*, 8*S*)-humulone A (**1**).
- S7.** Selected structures and population of the low-energy B3LYP/6-31G (d) in *vacuo* conformers of (3*R*, 8*S*)-**1** based on experimental NOE correlations.
- S8.** ^1H NMR (400 MHz, CDCl_3) spectrum of (3*S*, 8*S*)-humulone A (**2**).
- S9.** ^{13}C NMR (100 MHz, CDCl_3) spectrum of (3*S*, 8*S*)-humulone A (**2**).
- S10.** HSQC (600 MHz, CDCl_3) spectrum of (3*S*, 8*S*)-humulone A (**2**).
- S11.** HMBC (600 MHz, CDCl_3) spectrum of (3*S*, 8*S*)-humulone A (**2**).
- S12.** NOESY (600 MHz, CDCl_3) spectrum of (3*S*, 8*S*)-humulone A (**2**).
- S13.** HRESIMS spectrum of (3*S*, 8*S*)-humulone A (**2**).
- S14.** Experimental CD spectrum of (3*S*, 8*S*)-humulone A (**2**).
- S15.** ^1H NMR (400 MHz, CDCl_3) spectrum of (3*S*, 8*S*)-cohumulone A (**3**).
- S16.** ^{13}C NMR (100 MHz, CDCl_3) spectrum of (3*S*, 8*S*)-cohumulone A (**3**).
- S17.** HSQC (600 MHz, CDCl_3) spectrum of (3*S*, 8*S*)-cohumulone A (**3**).
- S18.** HMBC (600 MHz, CDCl_3) spectrum of (3*S*, 8*S*)-cohumulone A (**3**).
- S19.** NOESY (600 MHz, CDCl_3) spectrum of (3*S*, 8*S*)-cohumulone A (**3**).
- S20.** HRESIMS spectrum of (3*S*, 8*S*)-cohumulone A (**3**).

- S21.** Experimental CD spectrum of (3*S*, 8*S*)-cohumulone A (**3**).
- S22.** ¹H NMR (400 MHz, CDCl₃) spectrum of (2*S*, 7*S*)-humulone B (**4**).
- S23.** ¹³C NMR (100 MHz, CDCl₃) spectrum of (2*S*, 7*S*)-humulone B (**4**).
- S24.** HSQC (600 MHz, CDCl₃) spectrum of (2*S*, 7*S*)-humulone B (**4**).
- S25.** HMBC (600 MHz, CDCl₃) spectrum of (2*S*, 7*S*)-humulone B (**4**).
- S26.** NOESY (600 MHz, CDCl₃) spectrum of (2*S*, 7*S*)-humulone B (**4**).
- S27.** HRESIMS spectrum of (2*S*, 7*S*)-humulone B (**4**).
- S28.** Selected structures and population of the low-energy B3LYP/6-31G (d) in *vacuo* conformers of (2*S*, 7*S*)-**4** based on experimental NOE correlations.
- S29.** ¹H NMR(400 MHz, CDCl₃) spectrum of (2*R*, 7*S*)-humulone B (**5**).
- S30.** ¹³C NMR(100 MHz, CDCl₃) spectrum of (2*R*, 7*S*)-humulone B (**5**).
- S31.** HSQC (600 MHz, CDCl₃) spectrum of (2*R*, 7*S*)-humulone B (**5**).
- S32.** HMBC (600 MHz, CDCl₃) spectrum of (2*R*, 7*S*)-humulone B (**5**).
- S33.** NOESY (600 MHz, CDCl₃) spectrum of (2*R*, 7*S*)-humulone B (**5**).
- S34.** HRESIMS spectrum of (2*R*, 7*S*)-humulone B (**5**).
- S35.** Selected structures and population of the low-energy B3LYP/6-31G (d) in *vacuo* conformers of (2*R*, 7*S*)-**5** based on experimental NOE correlations.
- S36.** ¹H NMR (400 MHz, CDCl₃) spectrum of (2*S*, 7*S*)-cohumulone B (**6**).
- S37.** ¹³C NMR (100 MHz, CDCl₃) spectrum of (2*S*, 7*S*)-cohumulone B (**6**).
- S38.** HSQC (600 MHz, CDCl₃) spectrum of (2*S*, 7*S*)-cohumulone B (**6**).
- S39.** HMBC (600 MHz, CDCl₃) spectrum of (2*S*, 7*S*)-cohumulone B (**6**).
- S40.** NOESY (600 MHz, CDCl₃) spectrum of (2*S*, 7*S*)-cohumulone B (**6**).

- S41.** HRESIMS spectrum of (2*S*, 7*S*)-cohumulone B (**6**).
- S42.** Experimental CD spectrum of (2*S*, 7*S*)-cohumulone B (**6**).
- S43.** ¹H NMR (400 MHz, CDCl₃) spectrum of (2*S*, 3*aS*)-humulone C (**7**).
- S44.** ¹³C NMR (100 MHz, CDCl₃) spectrum of (2*S*, 3*aS*)-humulone C (**7**).
- S45.** HSQC (600 MHz, CDCl₃) spectrum of (2*S*, 3*aS*)-humulone C (**7**).
- S46.** HMBC (600 MHz, CDCl₃) spectrum of (2*S*, 3*aS*)-humulone C (**7**).
- S47.** NOESY (600 MHz, CDCl₃) spectrum of (2*S*, 3*aS*)-humulone C (**7**).
- S48.** HRESIMS spectrum of (2*S*, 3*aS*)-humulone C (**7**).
- S49.** Structures and populations of the low-energy B3LYP/6-31G (d) in *vacuo* conformers (>2%) of (2*S*, 3*aS*)-**7**.
- S50.** ¹H NMR (600 MHz, CD₃OD) spectrum of (3*S*, 3'*R*, 5*R*)-humulone acid B (**8**).
- S51.** ¹³C NMR (150 MHz, CD₃OD) spectrum of (3*S*, 3'*R*, 5*R*)-humulone acid B (**8**).
- S52.** HSQC (600 MHz, CD₃OD) spectrum of (3*S*, 3'*R*, 5*R*)-humulone acid B (**8**).
- S53.** HMBC (600 MHz, CD₃OD) spectrum of (3*S*, 3'*R*, 5*R*)-humulone acid B (**8**).
- S54.** NOESY (600 MHz, CD₃OD) spectrum of (3*S*, 3'*R*, 5*R*)-humulone acid B (**8**).
- S55.** HRESIMS spectrum of (3*S*, 3'*R*, 5*R*)-humulone acid B (**8**).
- S56.** Selected structures and population of the low-energy B3LYP/6-31G (d) in *vacuo* conformers of (3*S*, 3'*R*)-**8** based on experimental NOE correlations.
- S57.** The molecular energy profiles of conformational flexibility of compound **8**
- S58.** ¹H NMR (400 MHz, CDCl₃) spectrum of lupulone H (**9**).
- S59.** ¹H NMR (600 MHz, CDCl₃) spectrum of (*R*)-lupulone H (**9a**).
- S60.** ¹H NMR (600 MHz, CDCl₃) spectrum of (*S*)-lupulone H (**9b**).

- S61.** ^{13}C NMR (100 MHz, CDCl_3) spectrum of lupulone H (**9**).
- S62.** HSQC (600 MHz, CDCl_3) spectrum of lupulone H (**9**).
- S63.** HMBC (600 MHz, CDCl_3) spectrum of lupulone H (**9**).
- S64.** NOESY (600 MHz, CDCl_3) spectrum of lupulone H (**9**).
- S65.** HRESIMS spectrum of lupulone H (**9**).
- S66.** The HPLC of chiral column analysis of lupulone H (**9**).
- S67.** Structures and populations of the low-energy B3LYP/6-31G (d) in *vacuo* conformers (>2%) of (2*S*)-**9**.
- S68.** ^1H NMR (400 MHz, $\text{DMSO}-d_6$) spectrum of lupulone G (**10**)
- S69.** ^1H NMR (600 MHz, $\text{DMSO}-d_6$) spectrum of (*R*)-lupulone G (**10a**)
- S70.** ^1H NMR (600 MHz, $\text{DMSO}-d_6$) spectrum of (*S*)-lupulone G (**10b**)
- S71.** ^{13}C NMR (100 MHz, $\text{DMSO}-d_6$) spectrum of lupulone G (**10**).
- S72.** Experimental CD spectra of (*R*)-lupulone G (**10a**) and (*S*)-lupulone G (**10b**).
- S73.** The HPLC of chiral column analysis of lupulone G (**10**).
- S74.** ^1H NMR (400 MHz, $\text{DMSO}-d_6$) spectrum of 5-deprenyllupulonol C (**11**).
- S75.** ^{13}C NMR (100 MHz, $\text{DMSO}-d_6$) spectrum of 5-deprenyllupulonol C (**11**).
- S76.** Experimental CD spectra of (*R*)-5-deprenyllupulonol C (**11a**) and (*S*)-5-deprenyllupulonol C (**11b**).
- S77.** The HPLC of chiral column analysis of 5-deprenyllupulonol C (**11**).
- S78.** ^1H NMR (400 MHz, $\text{DMSO}-d_6$) spectrum of 5,7-dihydroxy-2-isopropyl-8-prenylchromone (**12**).

S79. ^{13}C NMR (100 MHz, $\text{DMSO-}d_6$) spectrum of 5,7-dihydroxy-2-isopropyl-8-prenylchromone (**12**).

S80. HSQC (600 MHz, $\text{DMSO-}d_6$) spectrum of 5,7-dihydroxy-2-isopropyl-8-prenylchromone (**12**).

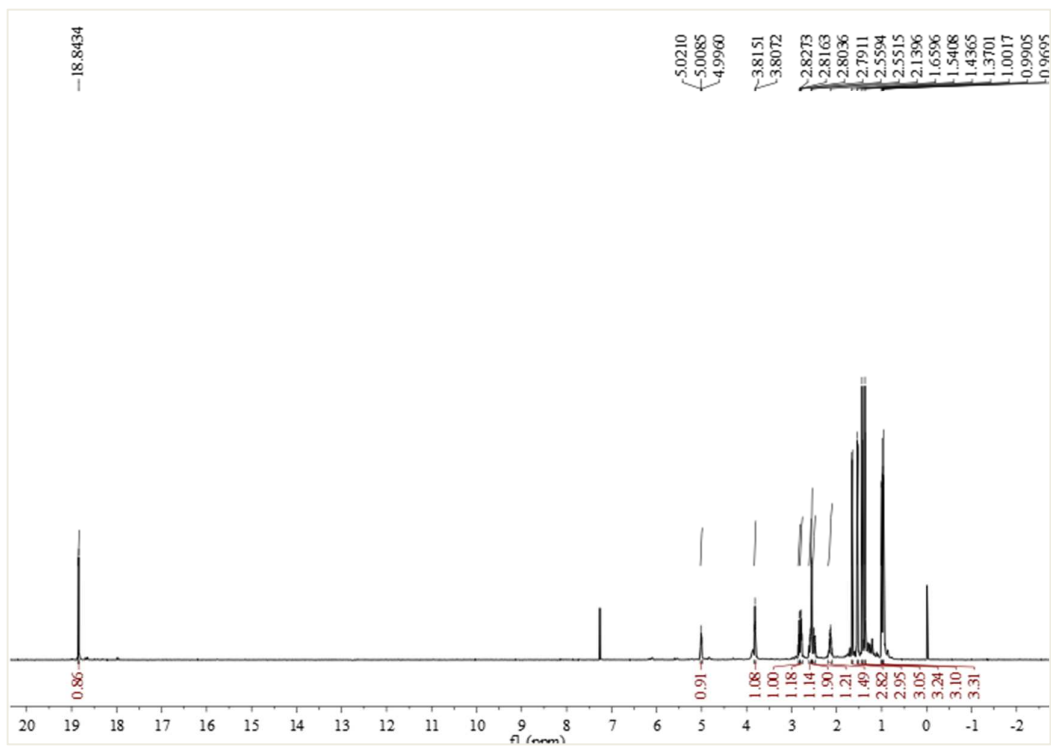
S81. HMBC (600 MHz, $\text{DMSO-}d_6$) spectrum of 5,7-dihydroxy-2-isopropyl-8-prenylchromone (**12**).

S82. HRESIMS spectrum of 5,7-dihydroxy-2-isopropyl-8-prenylchromone (**12**).

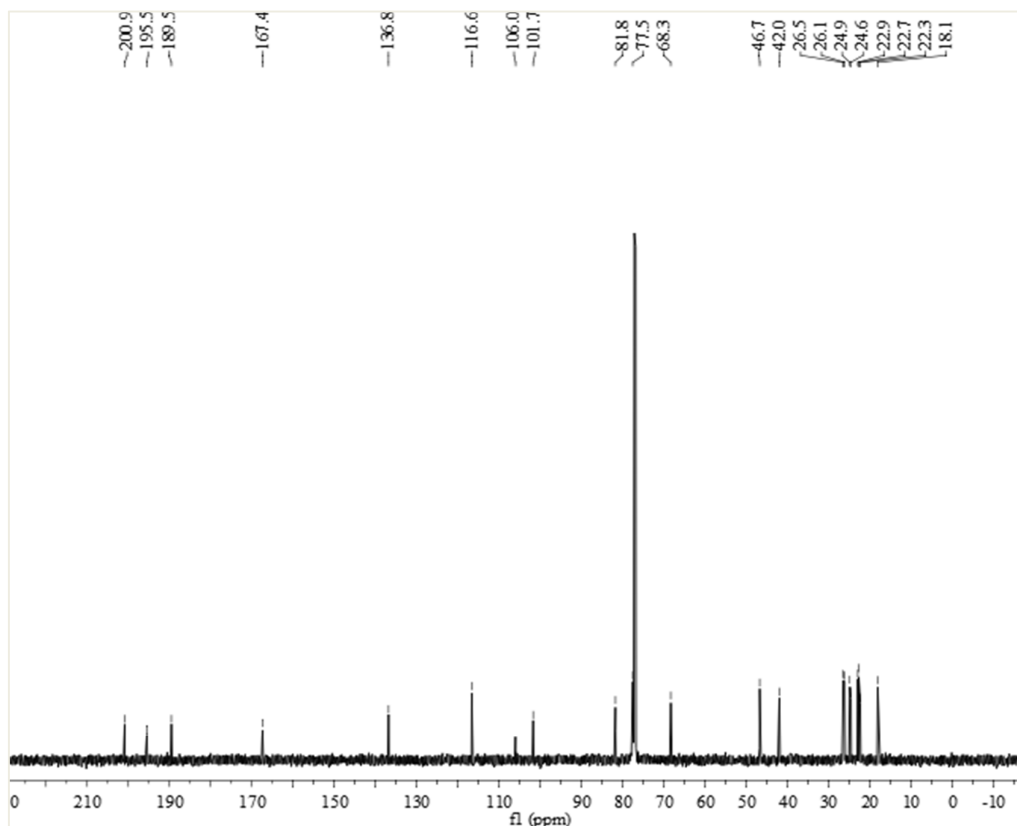
S83. The experimental method used for ECD calculations of compounds **1**, **4**, **5**, **7**, **8** and **9**.

S84. BV-2 cell viability assay and effect of the extracts and isolated compounds **1-8**, **13-17** on LPS-induced NO production in BV-2 microglial cells.

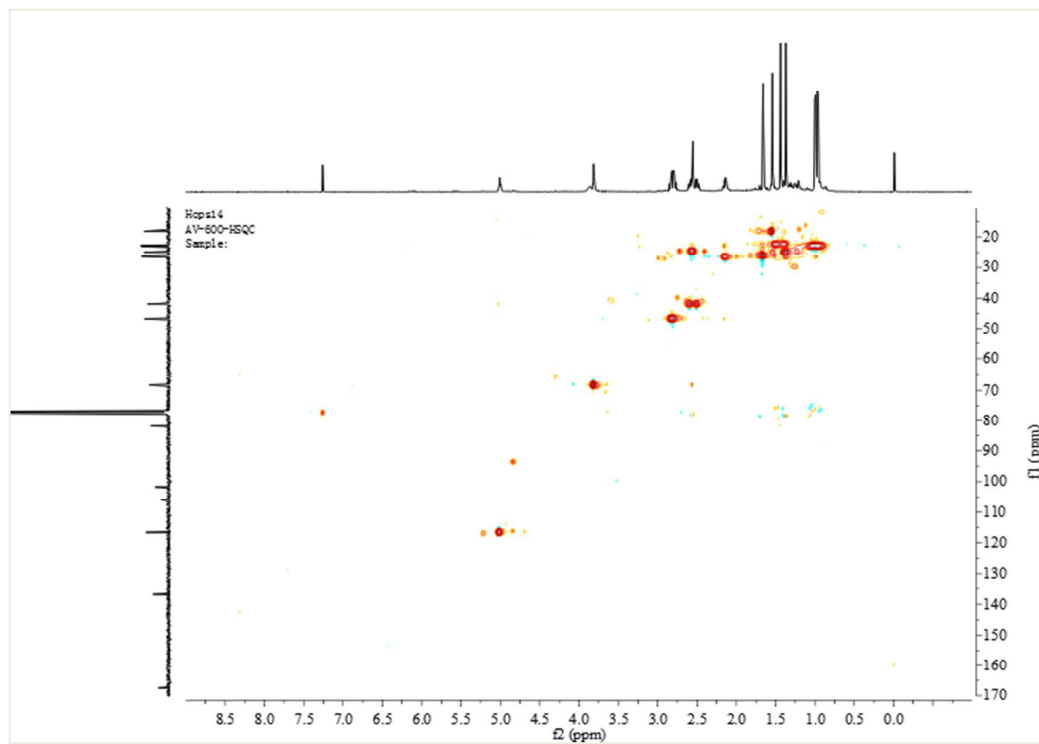
S1. ^1H NMR (400 MHz, CDCl_3) spectrum of (3*R*, 8*S*)-humulone A (**1**).



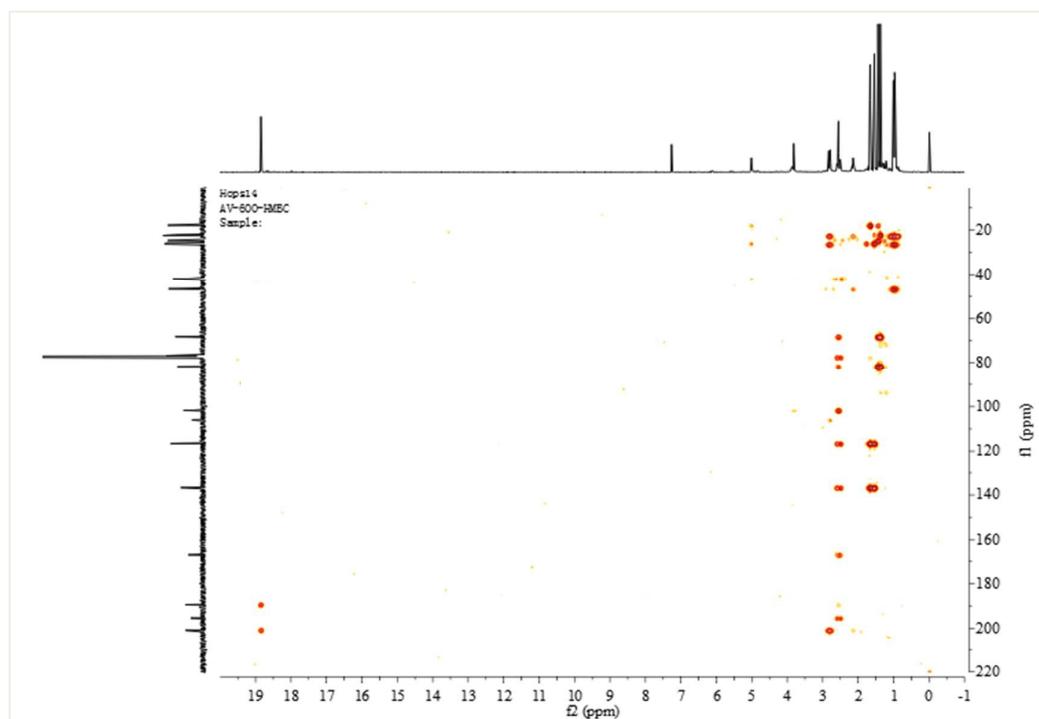
S2. ^{13}C NMR (100 MHz, CDCl_3) spectrum of (3*R*, 8*S*)-humulone A (**1**).



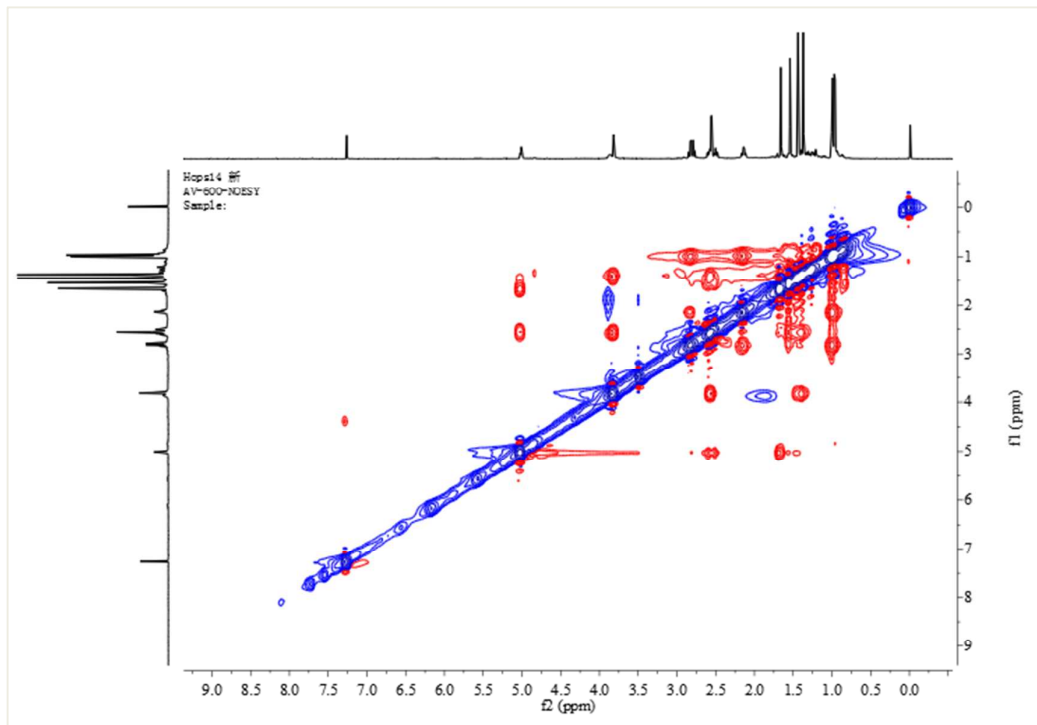
S3. HSQC (600 MHz, CDCl₃) spectrum of (3*R*, 8*S*)-humulone A (**1**).



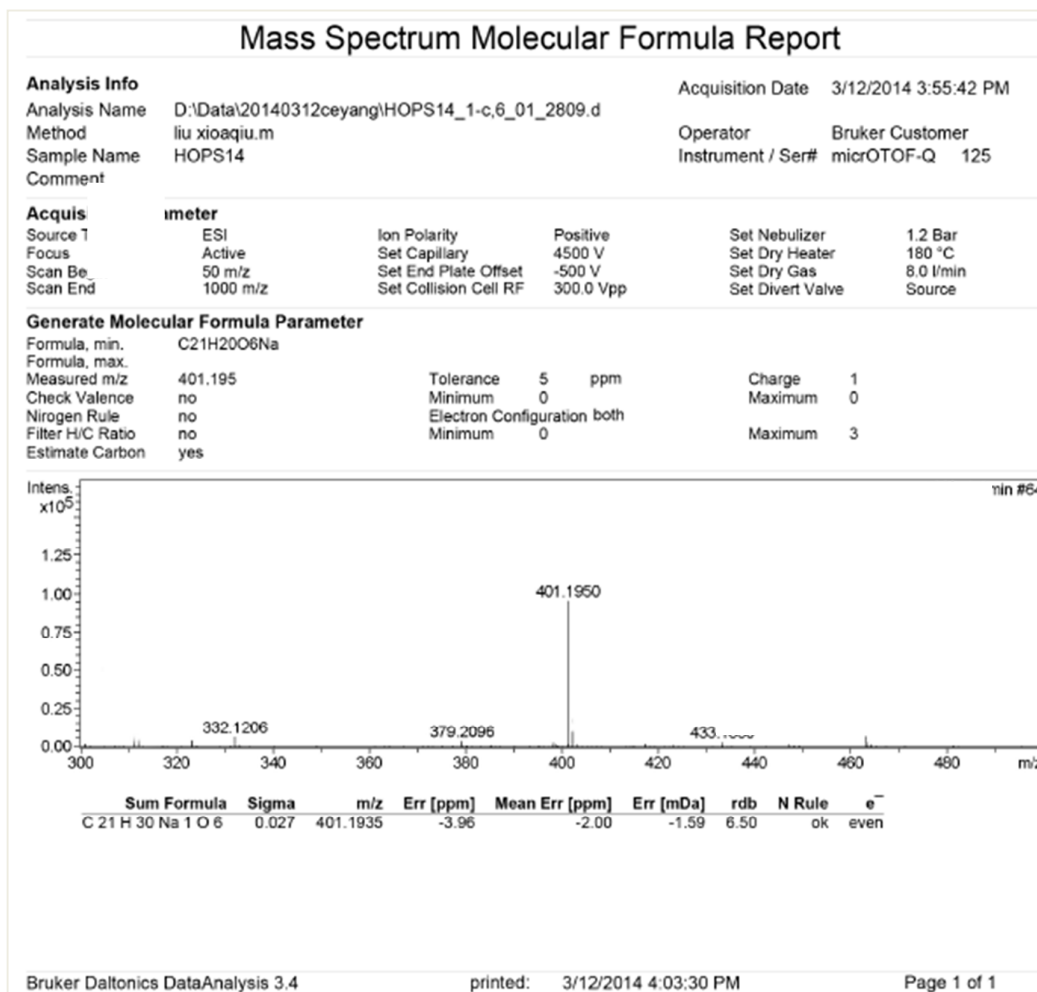
S4. HMBC (600 MHz, CDCl₃) spectrum of (3*R*, 8*S*)-humulone A (**1**).



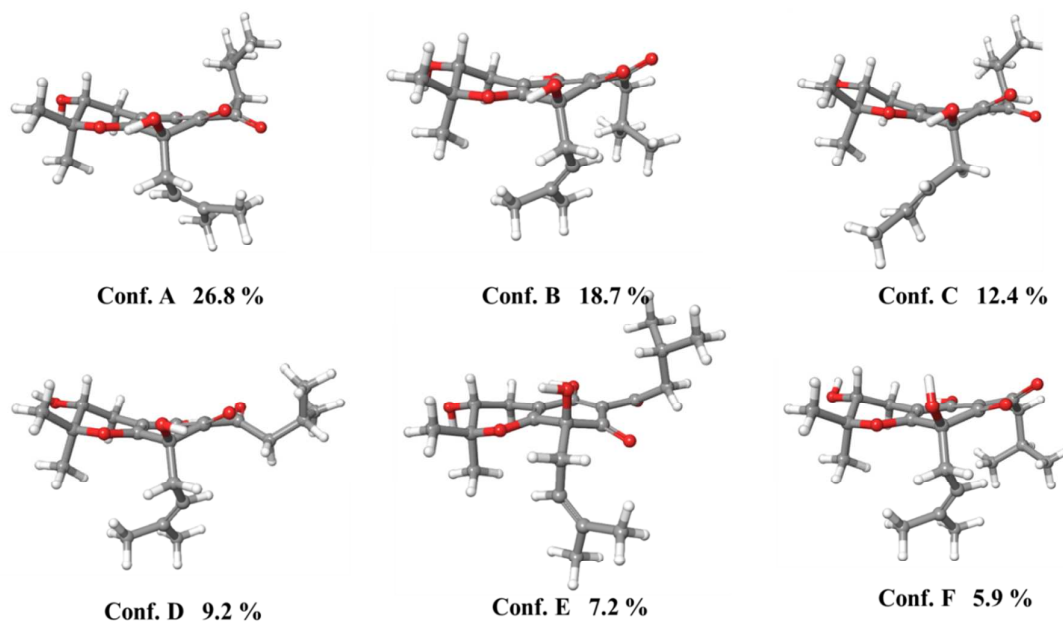
S5. NOESY (600 MHz, CDCl₃) spectrum of (3*R*, 8*S*)-humulone A (**1**).



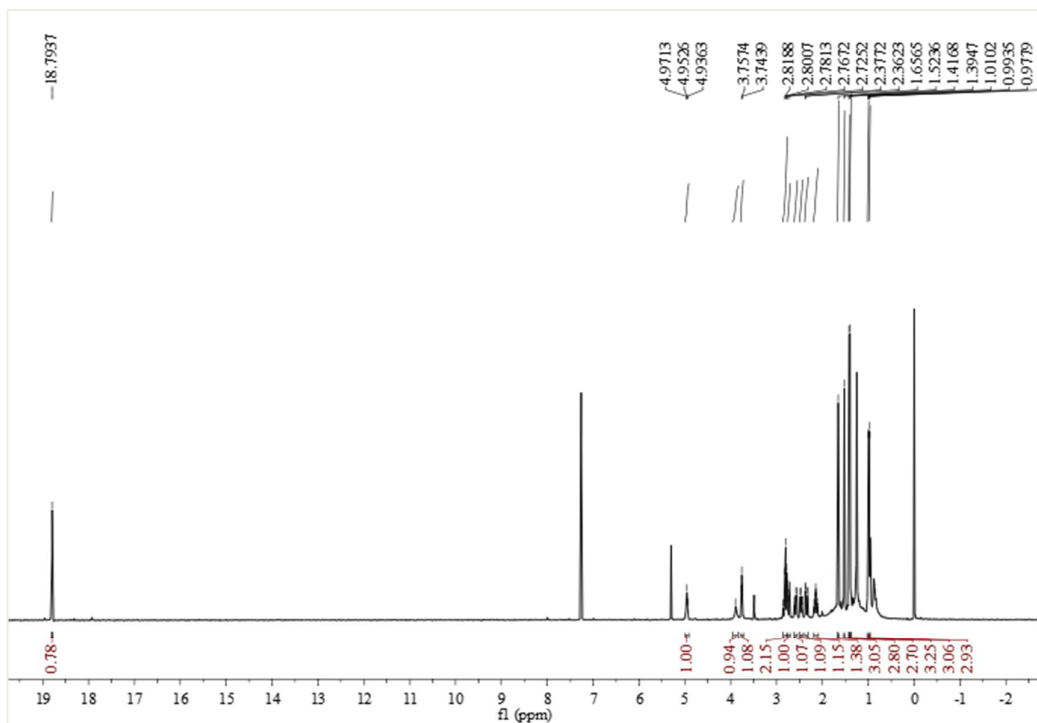
S6. HRESIMS spectrum of (3*R*, 8*S*)-humulone A (1).



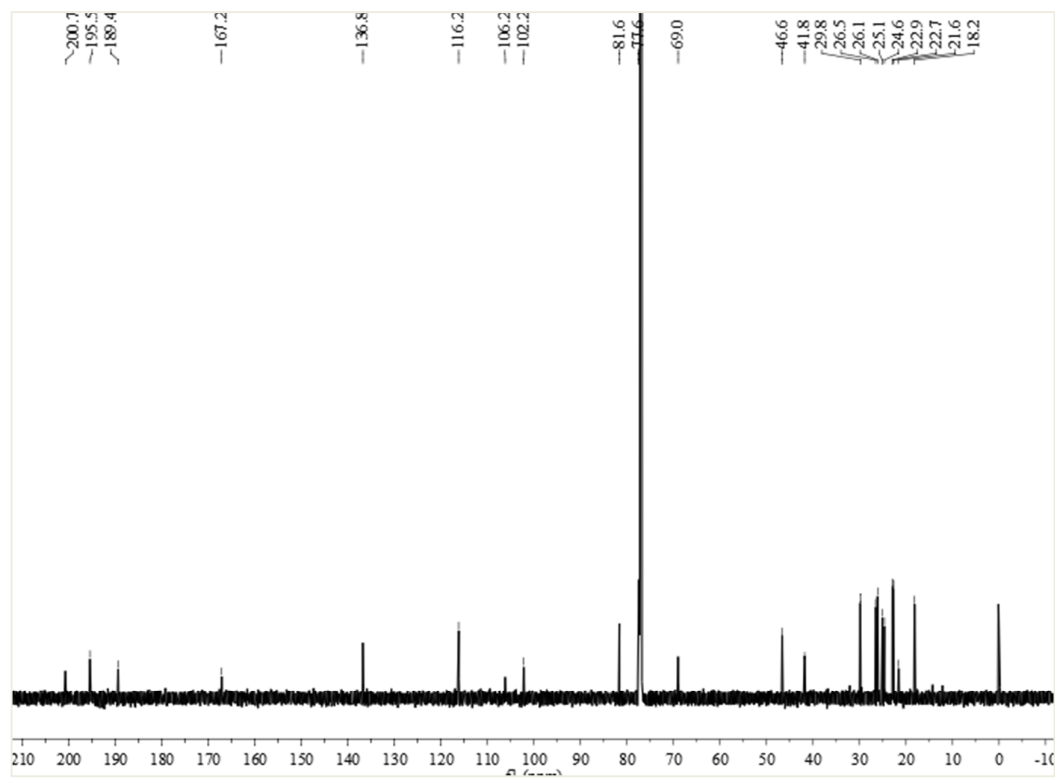
S7. Selected structures and population of the low-energy B3LYP/6-31G (d) in vacuo conformers of (3*R*, 8*S*)-**1** based on experimental NOE correlations.



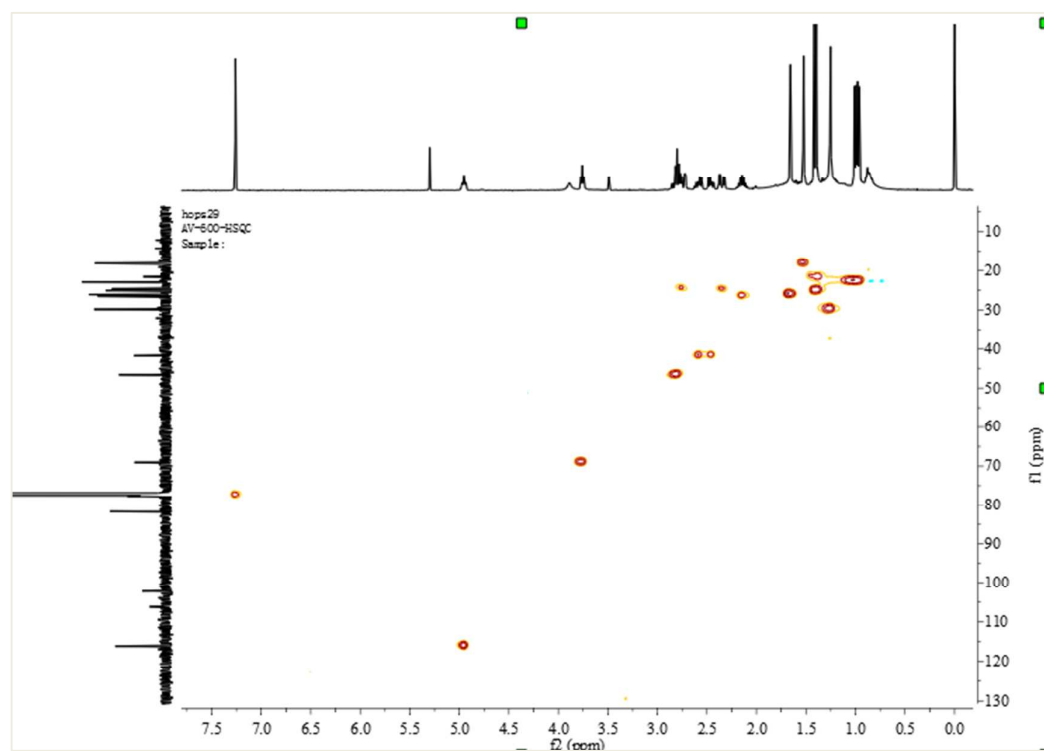
S8. ^1H NMR (400 MHz, CDCl_3) spectrum of (3*S*, 8*S*)-humulone A (**2**).



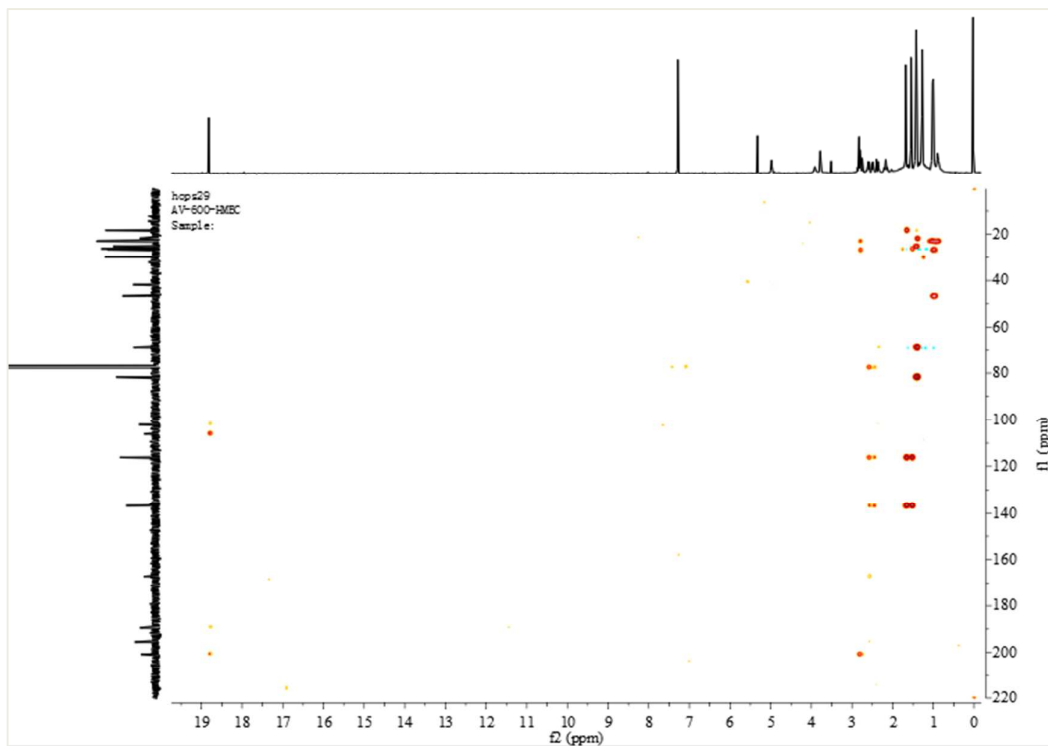
S9. ^{13}C NMR (100 MHz, CDCl_3) spectrum of (3*S*, 8*S*)-humulone A (**2**).



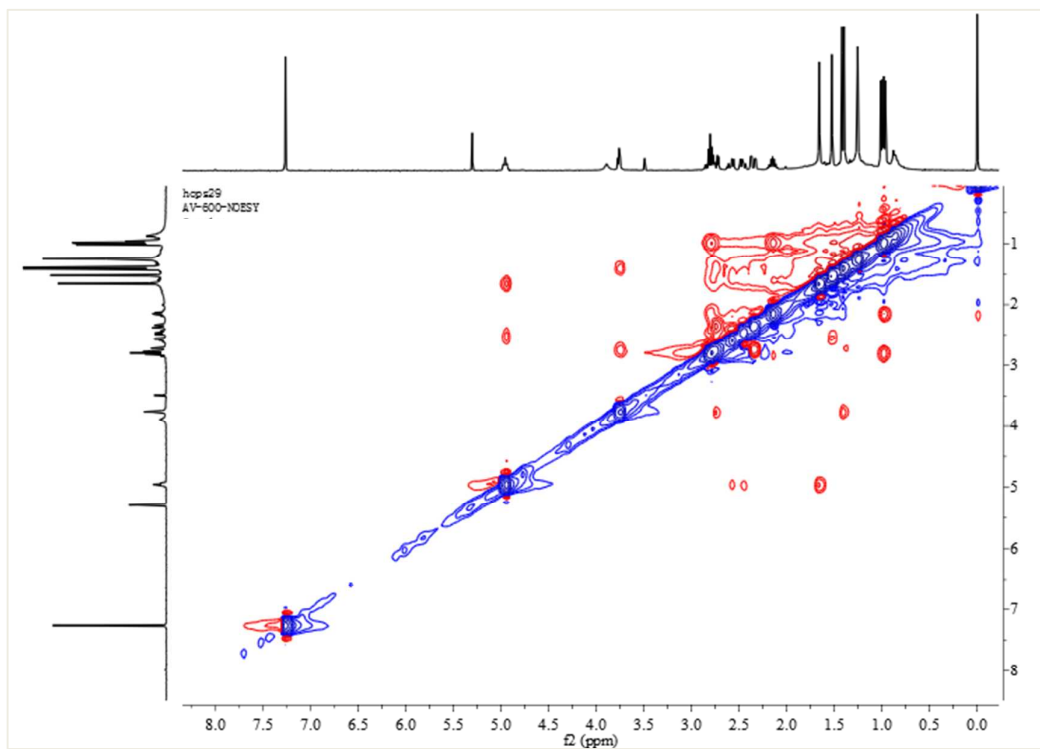
S10. HSQC (600 MHz, CDCl_3) spectrum of (3*S*, 8*S*)-humulone A (**2**).



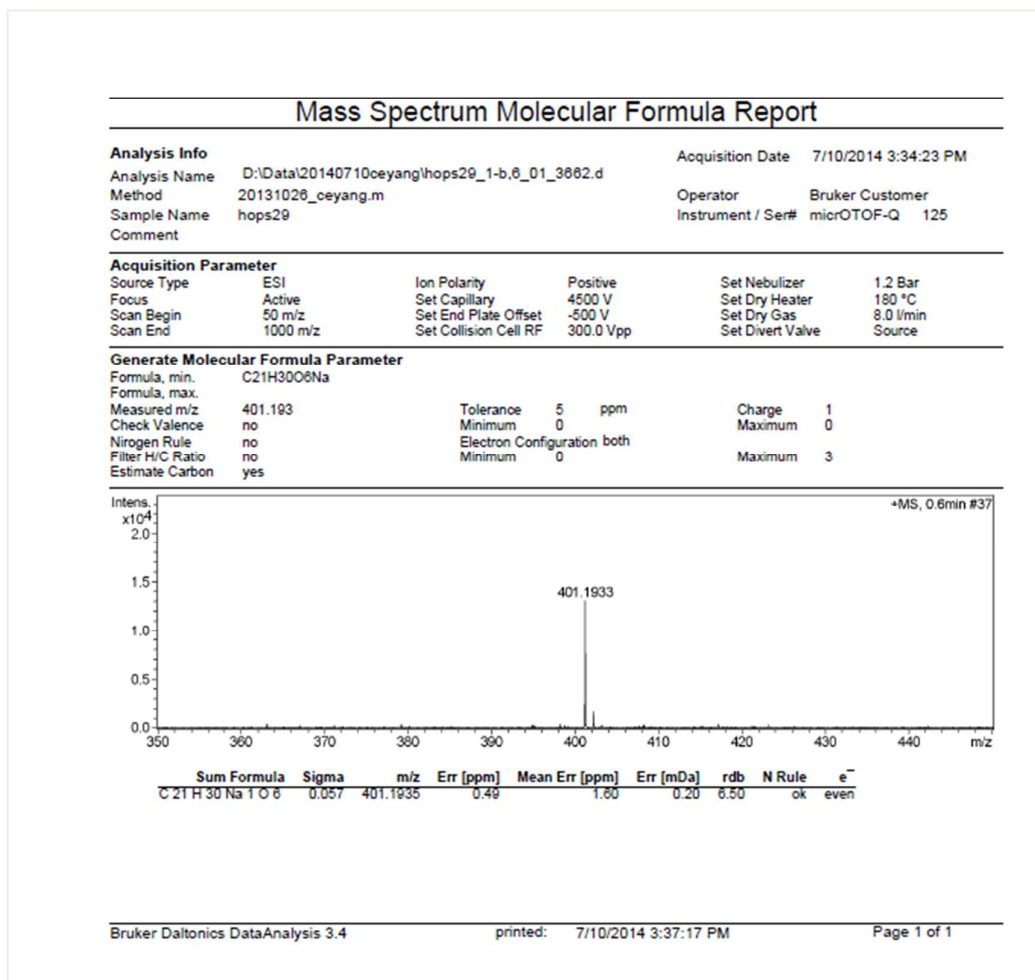
S11. HMBC (600 MHz, CDCl₃) spectrum of (3*S*, 8*S*)-humulone A (**2**).



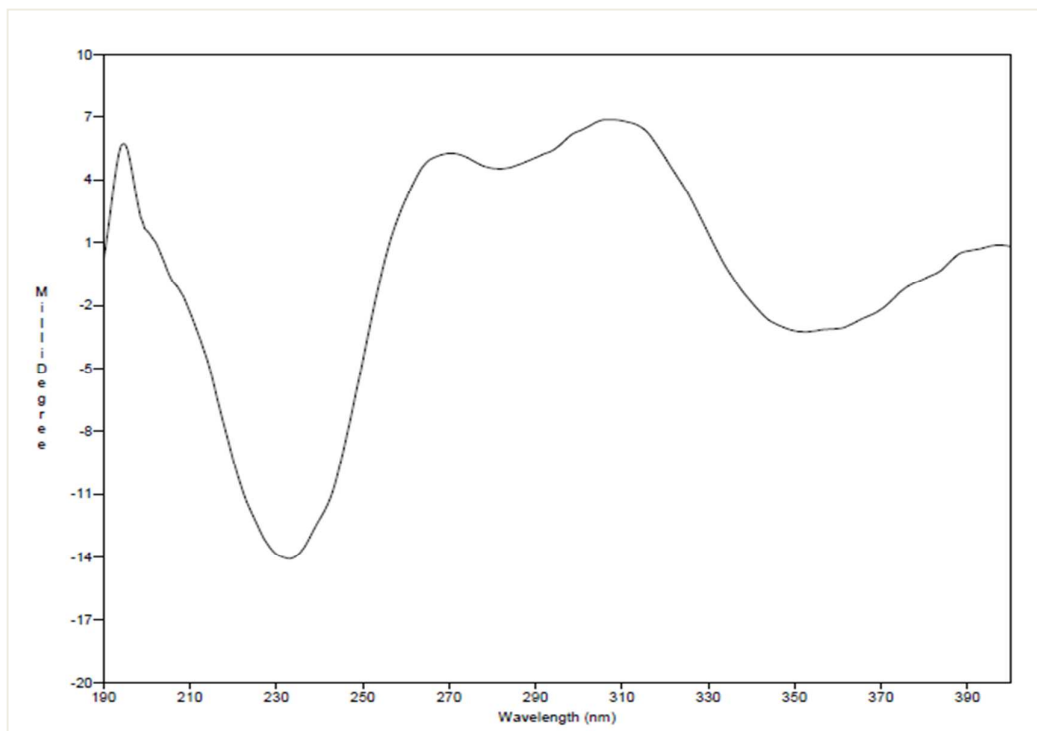
S12. NOESY (600 MHz, CDCl₃) spectrum of (3*S*, 8*S*)-humulone A (**2**).



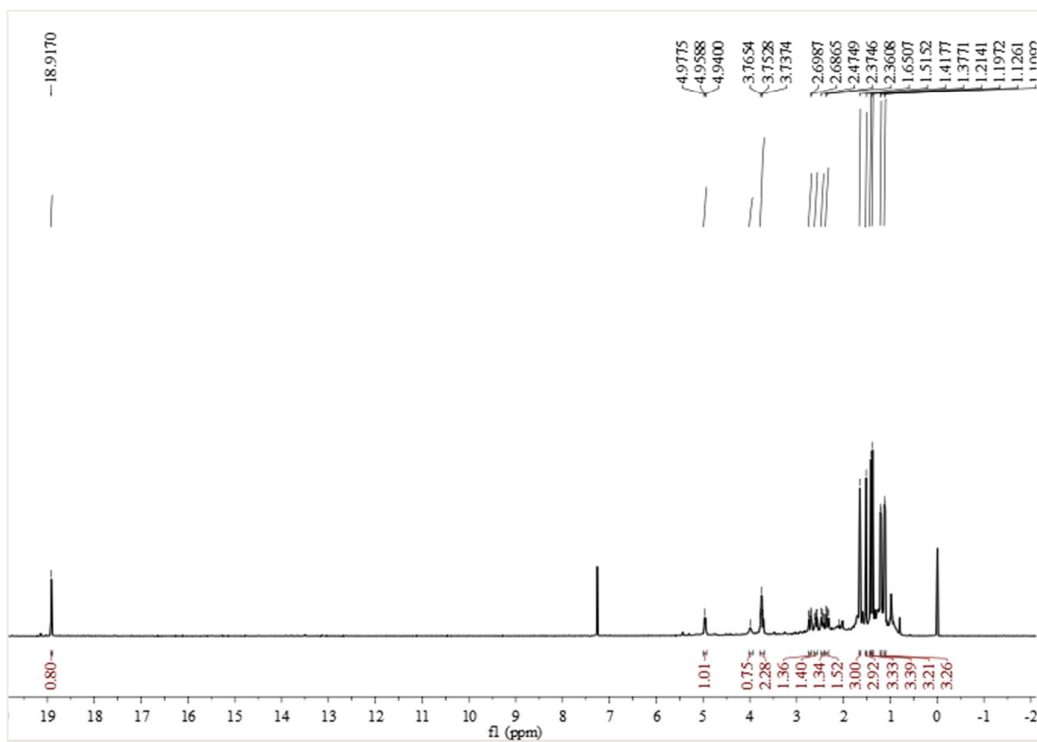
S13. HRESIMS spectrum of (3*S*, 8*S*)-humulone A (2).



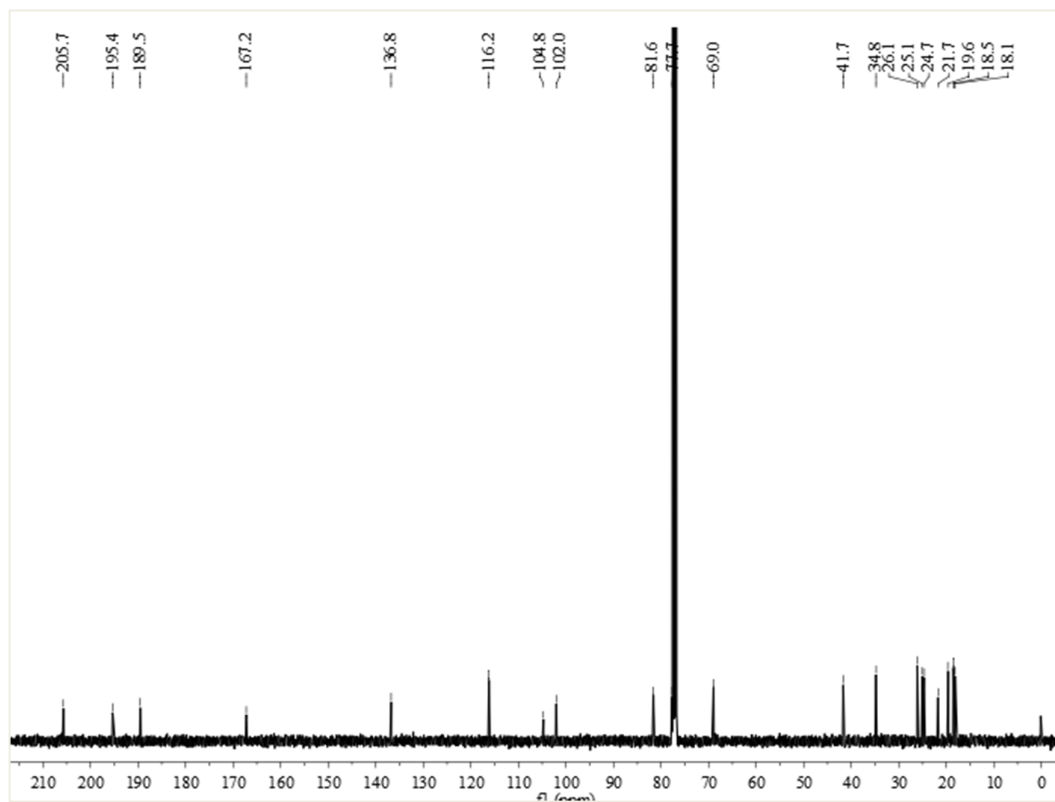
S14. Experimental CD spectrum of (3*S*, 8*S*)-humulone A (**2**).



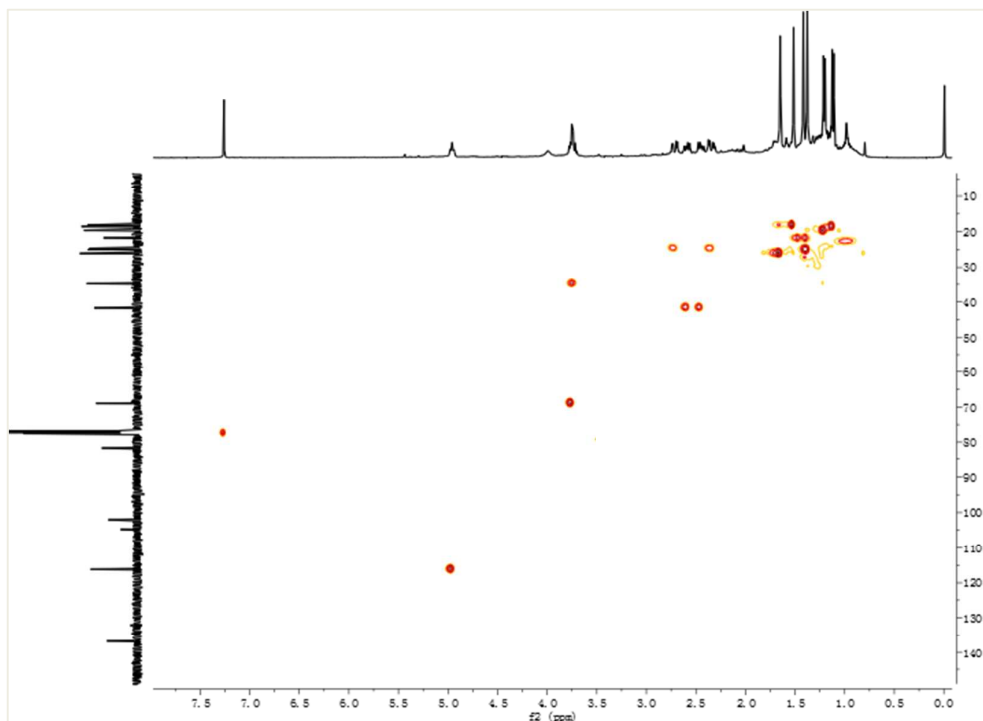
S15. ^1H NMR (400 MHz, CDCl_3) spectrum of (3*S*, 8*S*)-cohumulone A (**3**).



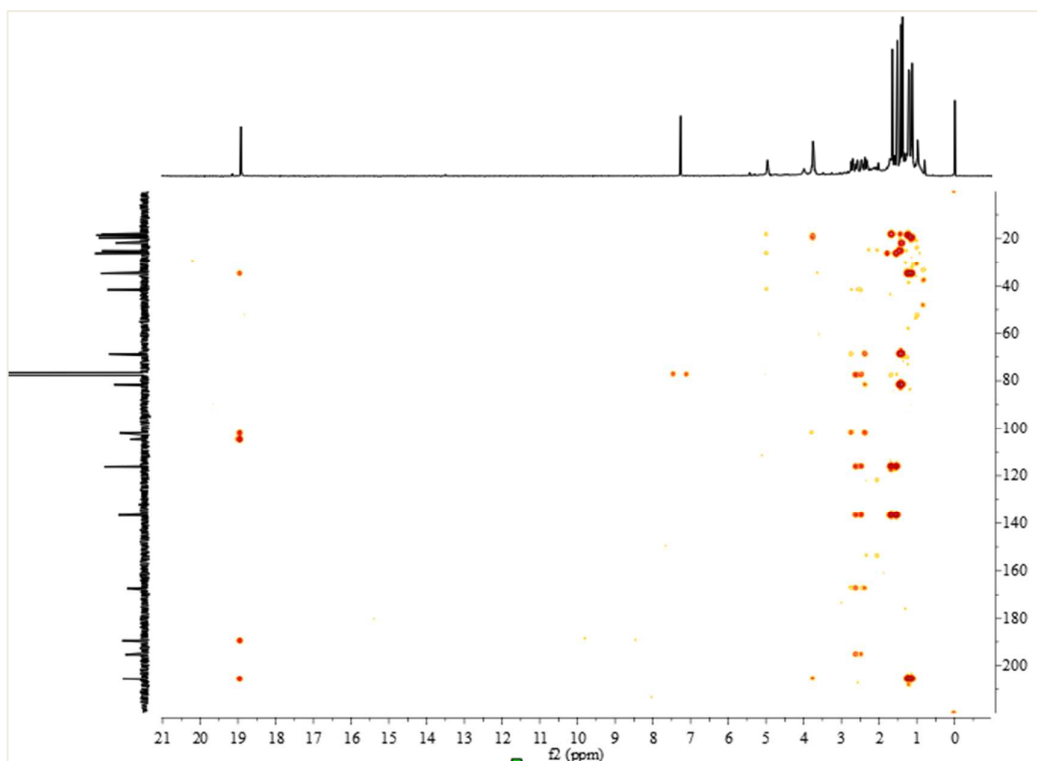
S16. ^{13}C NMR (100 MHz, CDCl_3) spectrum of (3*S*, 8*S*)-cohumulone A (**3**).



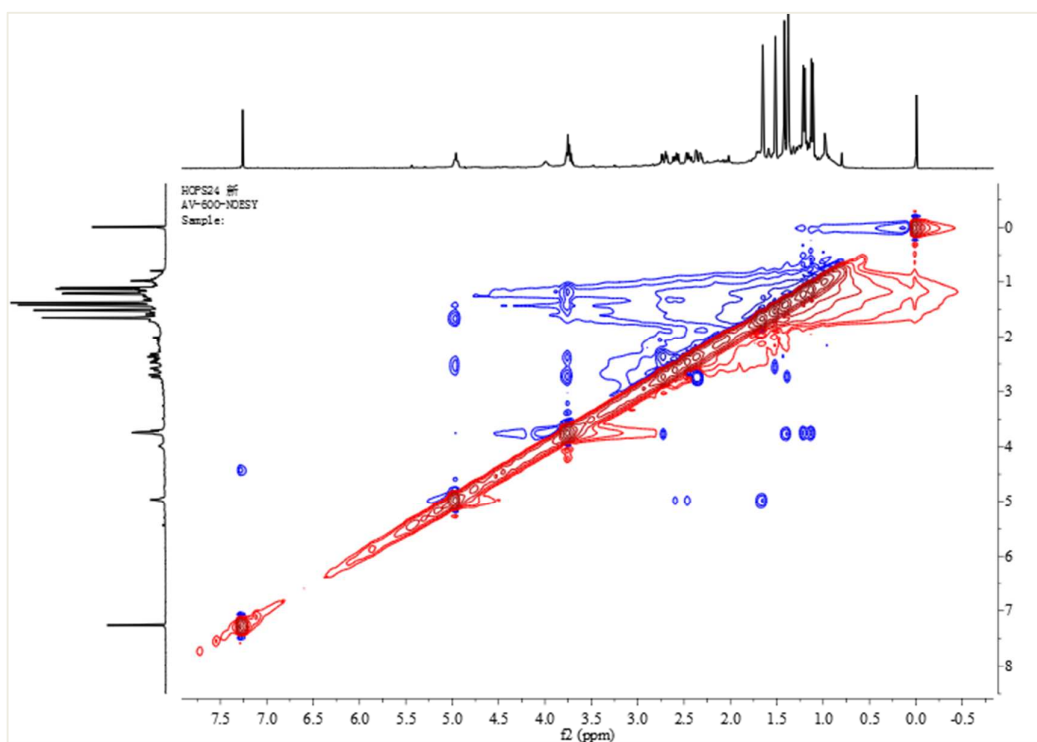
S17. HSQC (600 MHz, CDCl_3) spectrum of (3*S*, 8*S*)-cohumulone A (**3**).



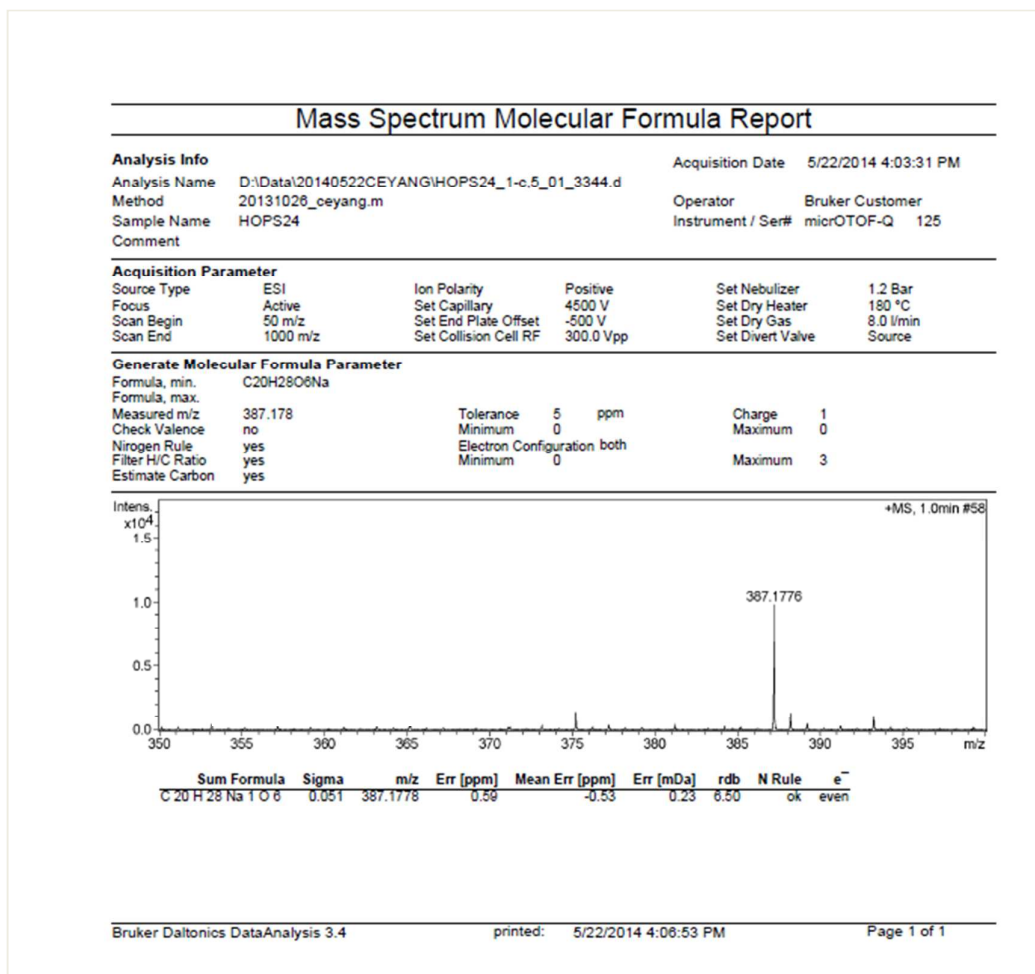
S18. HMBC (600 MHz, CDCl₃) spectrum of (3*S*, 8*S*)-cohumulone A (**3**).



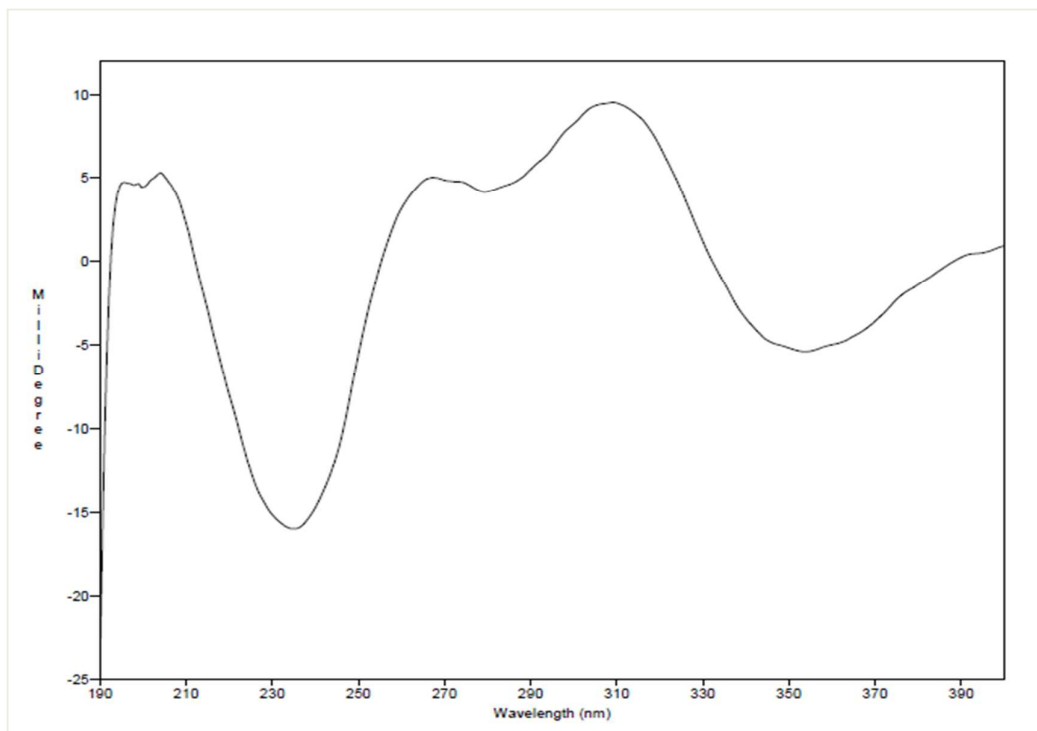
S19. NOESY (600 MHz, CDCl₃) spectrum of (3*S*, 8*S*)-cohumulone A (**3**).



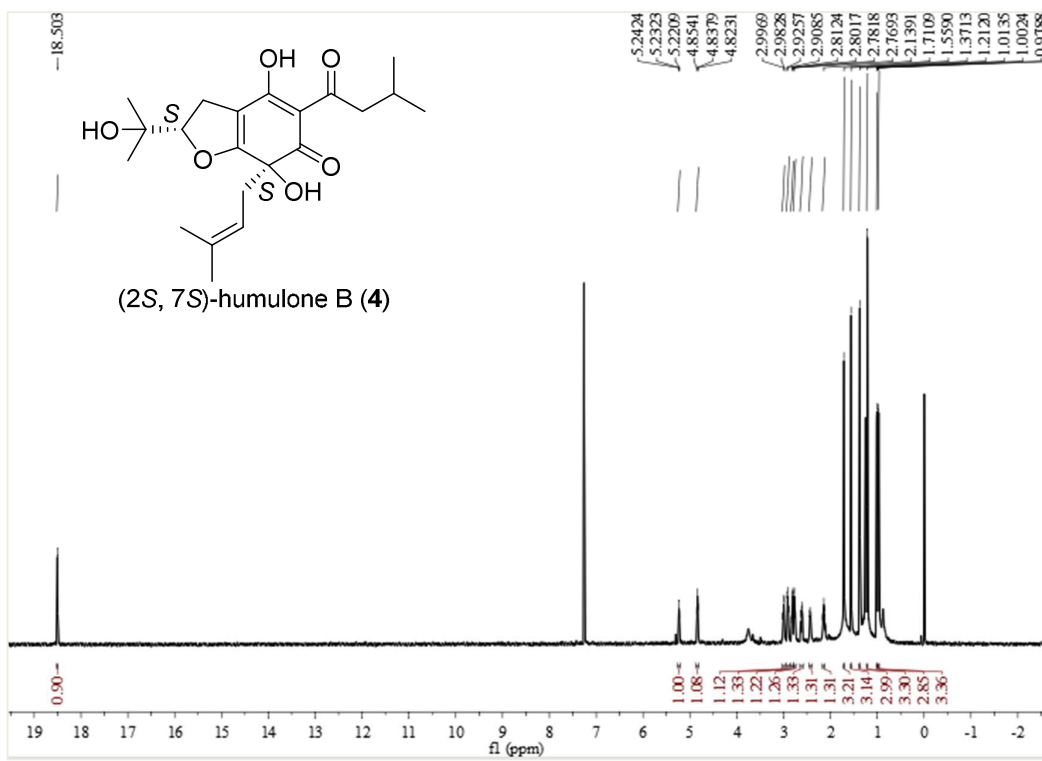
S20. HRESIMS spectrum of (3*S*, 8*S*)-cohumulone A (**3**).



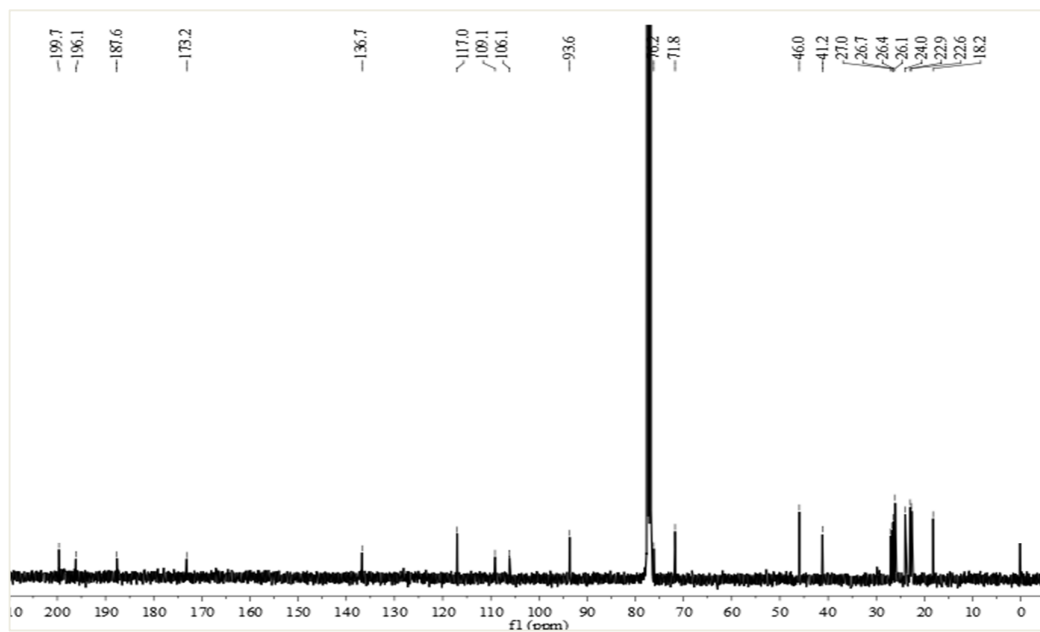
S21. Experimental CD spectrum of (3*S*, 8*S*)-cohumulone A (**3**).



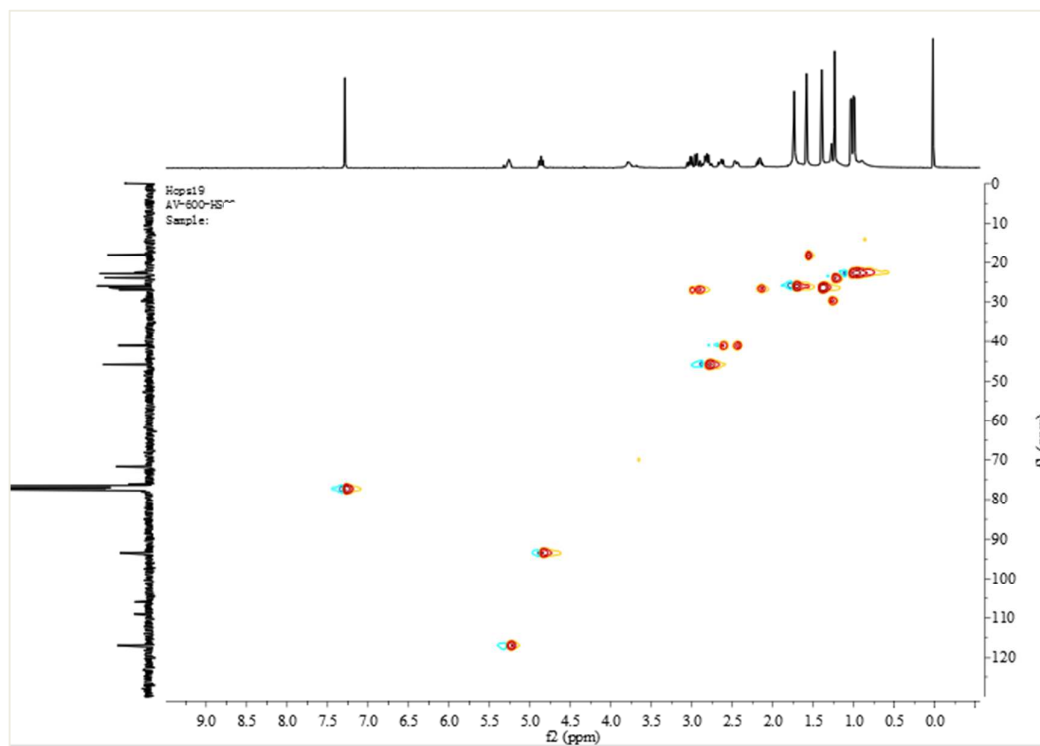
S22. ^1H NMR (400 MHz, CDCl_3) spectrum of (2*S*, 7*S*)-humulone B (**4**).



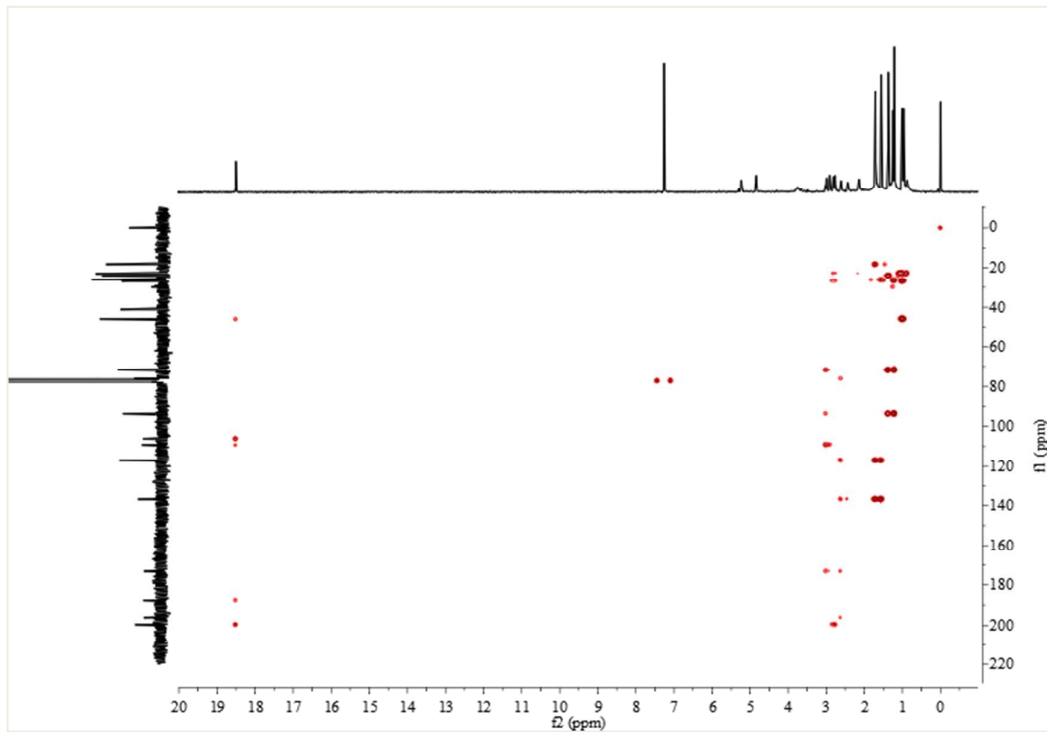
S23. ^{13}C NMR (100 MHz, CDCl_3) spectrum of (2*S*, 7*S*)-humulone B (**4**).



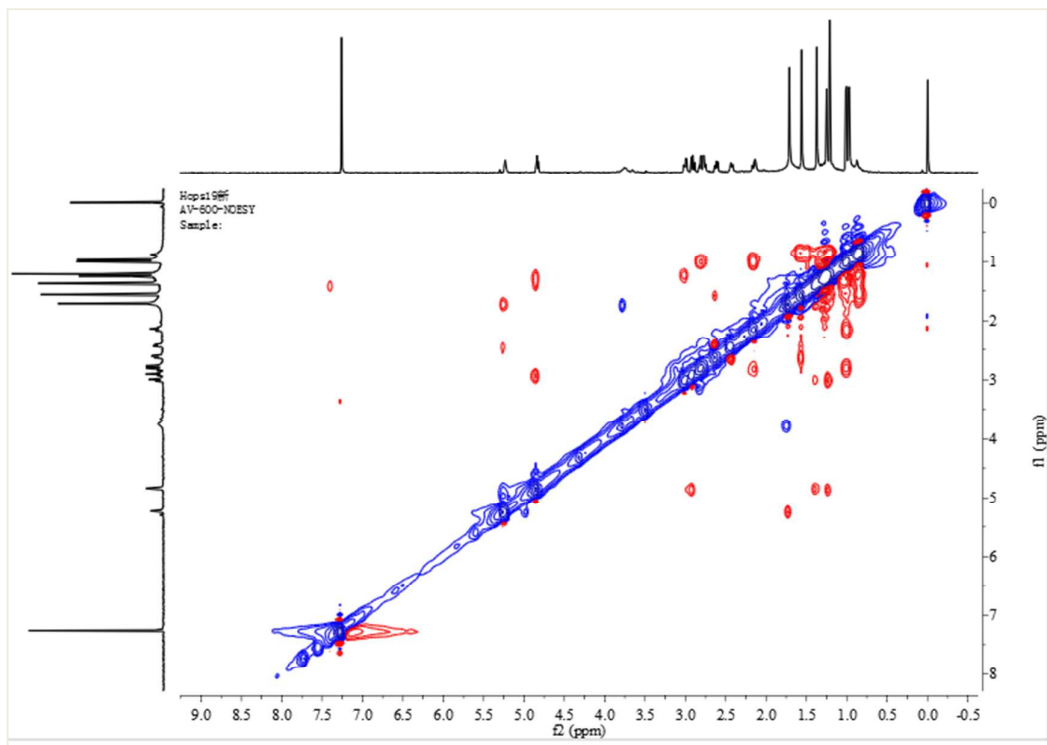
S24. HSQC (600 MHz, CDCl_3) spectrum of (2*S*, 7*S*)-humulone B (**4**).



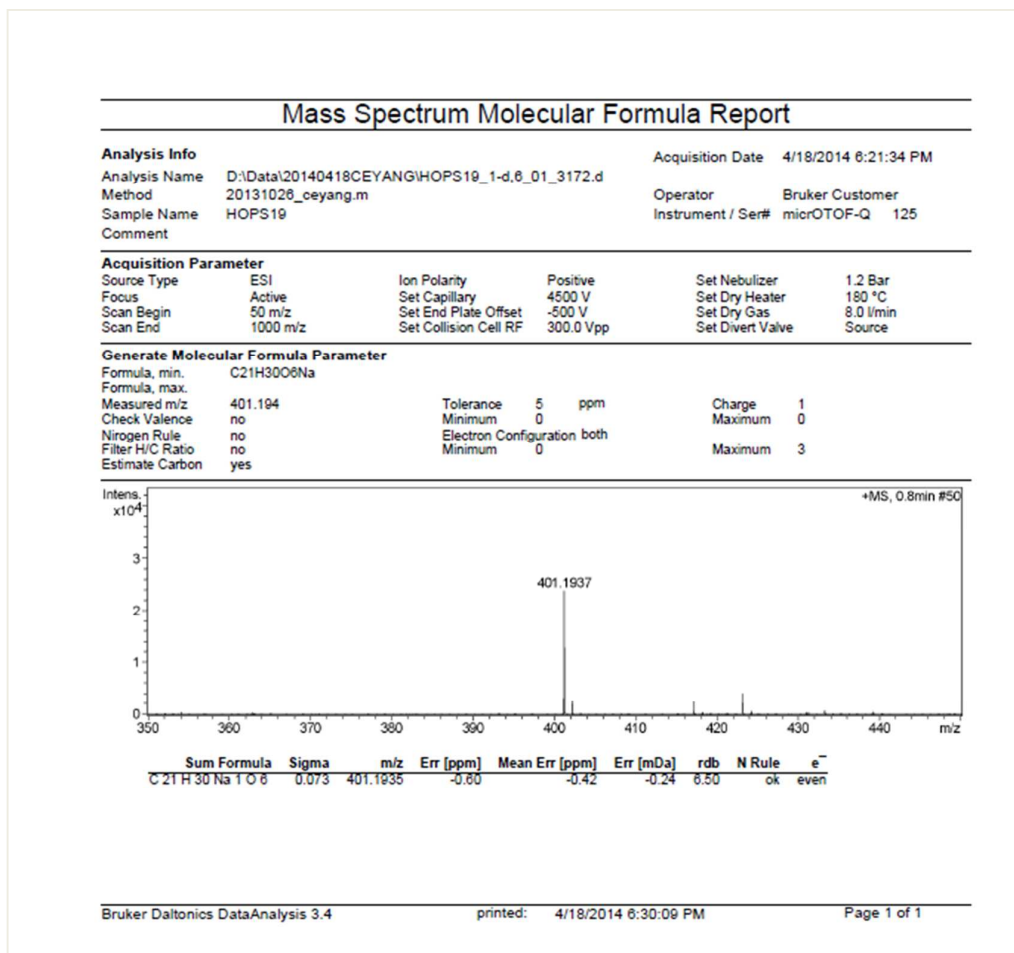
S25. HMBC (600 MHz, CDCl₃) spectrum of (2*S*, 7*S*)-humulone B (**4**).



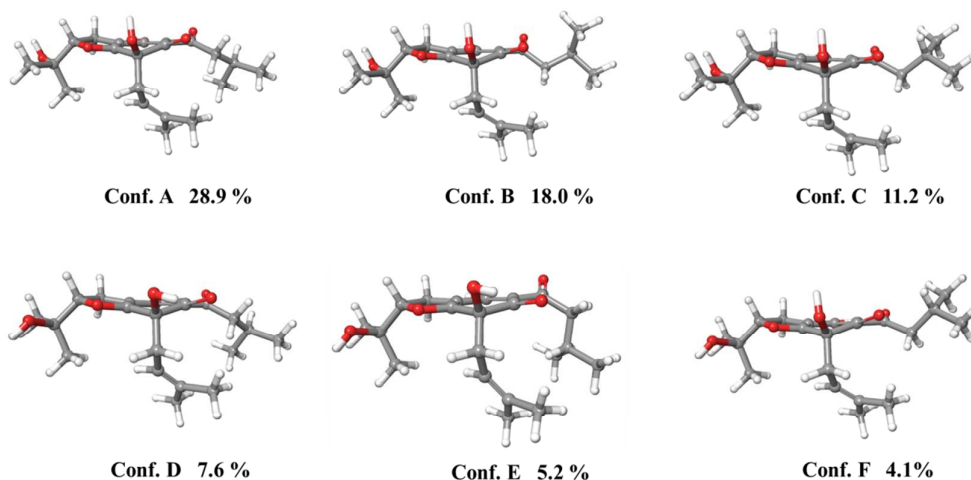
S26. NOESY (600 MHz, CDCl₃) spectrum of (2*S*, 7*S*)-humulone B (**4**).



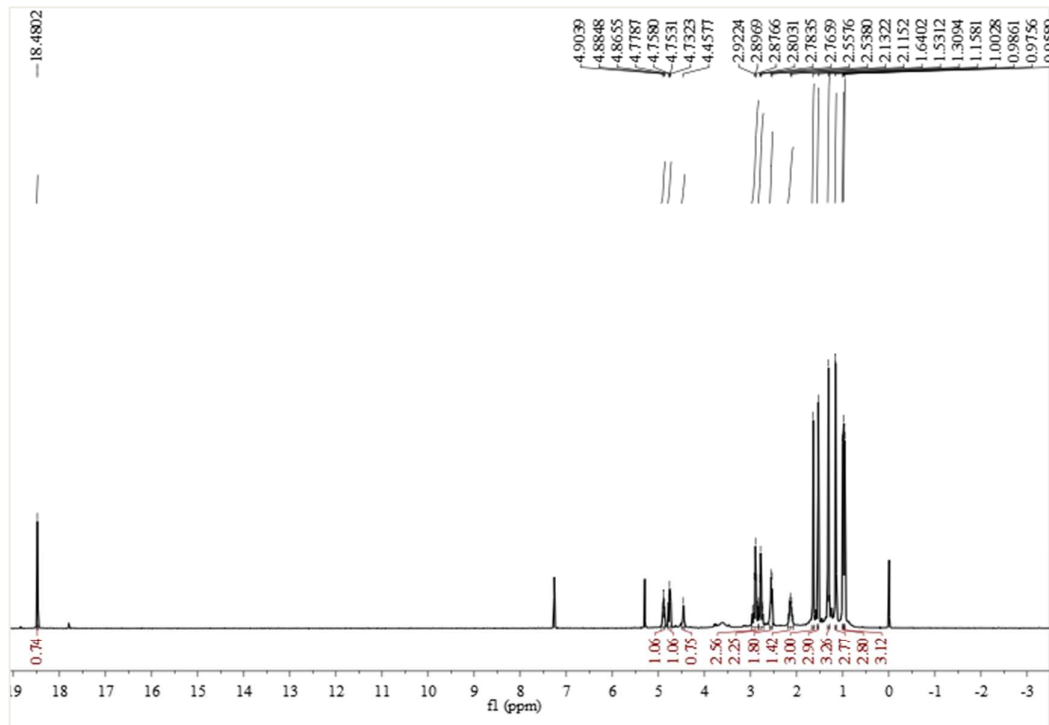
S27. HRESIMS spectrum of (2*S*, 7*S*)-humulone B (**4**).



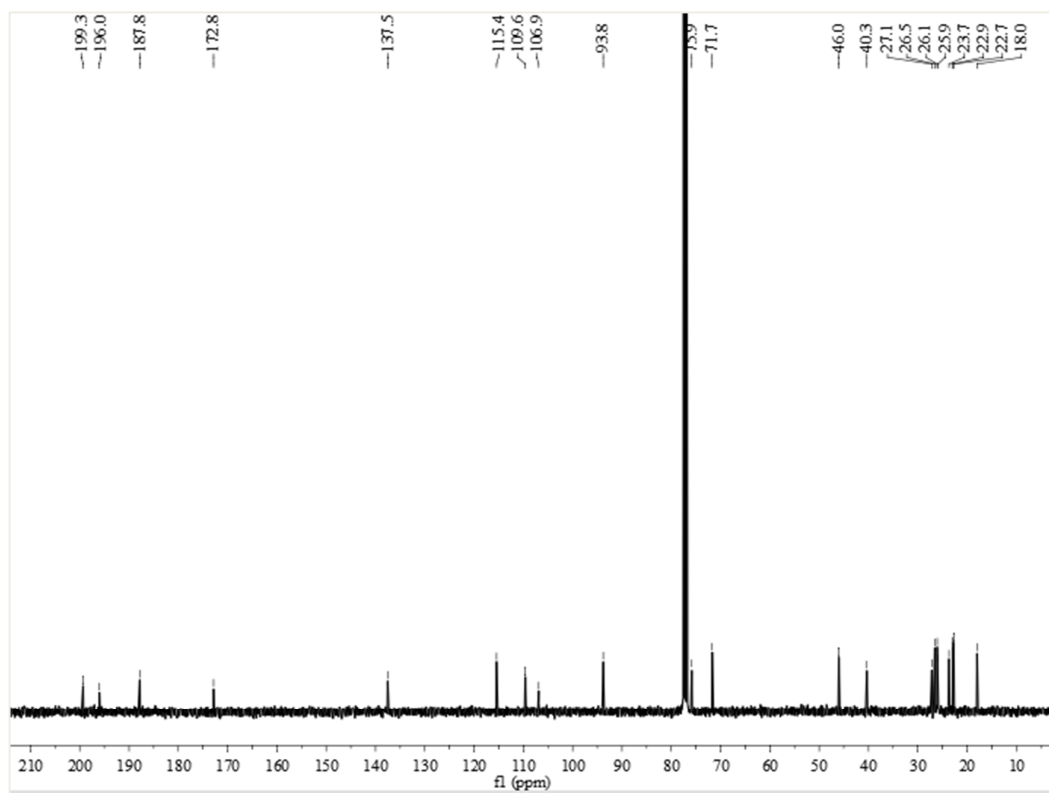
S28. Selected structures and population of the low-energy B3LYP/6-31G (d) *in vacuo* conformers of (2*S*, 7*S*)-**4** based on experimental NOE correlations.



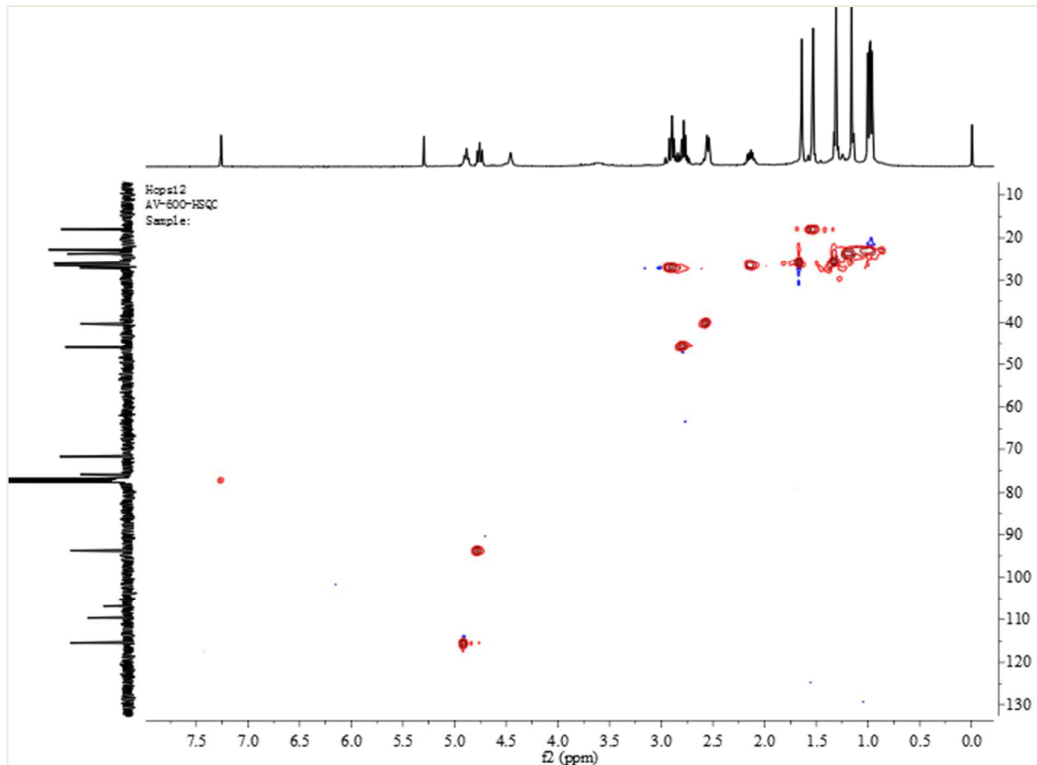
S29. ^1H NMR (400 MHz, CDCl_3) spectrum of (2*R*, 7*S*)-humulone B (**5**).



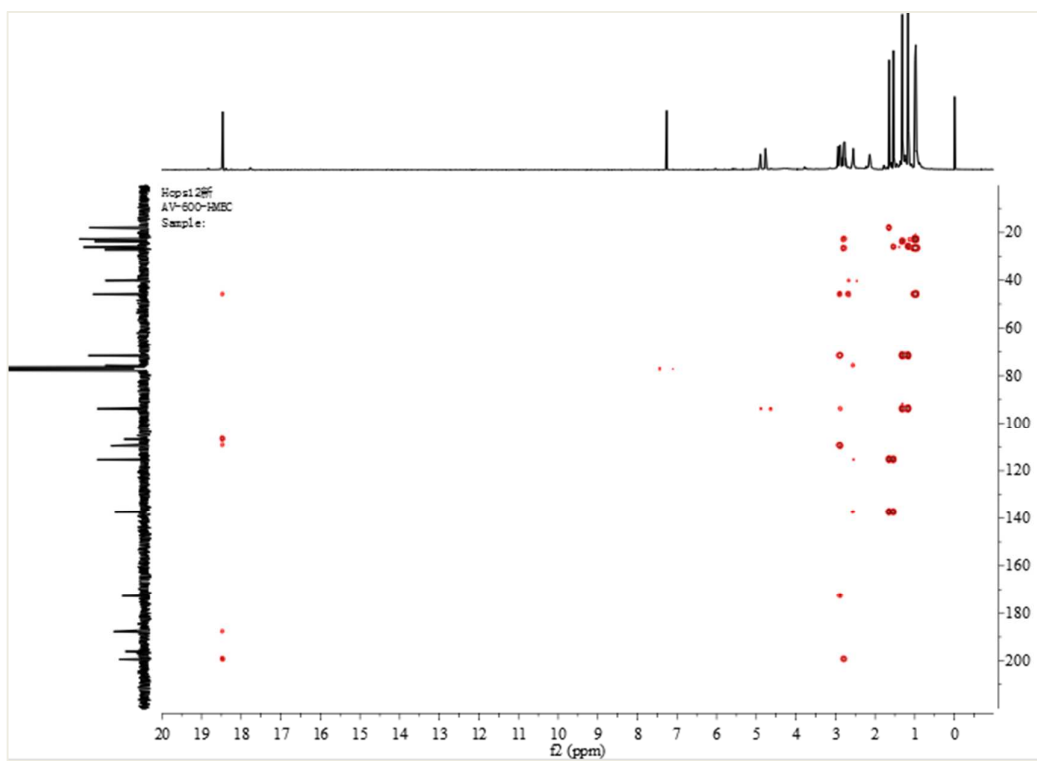
S30. ^{13}C NMR (100 MHz, CDCl_3) spectrum of (2*R*, 7*S*)-humulone B (**5**).



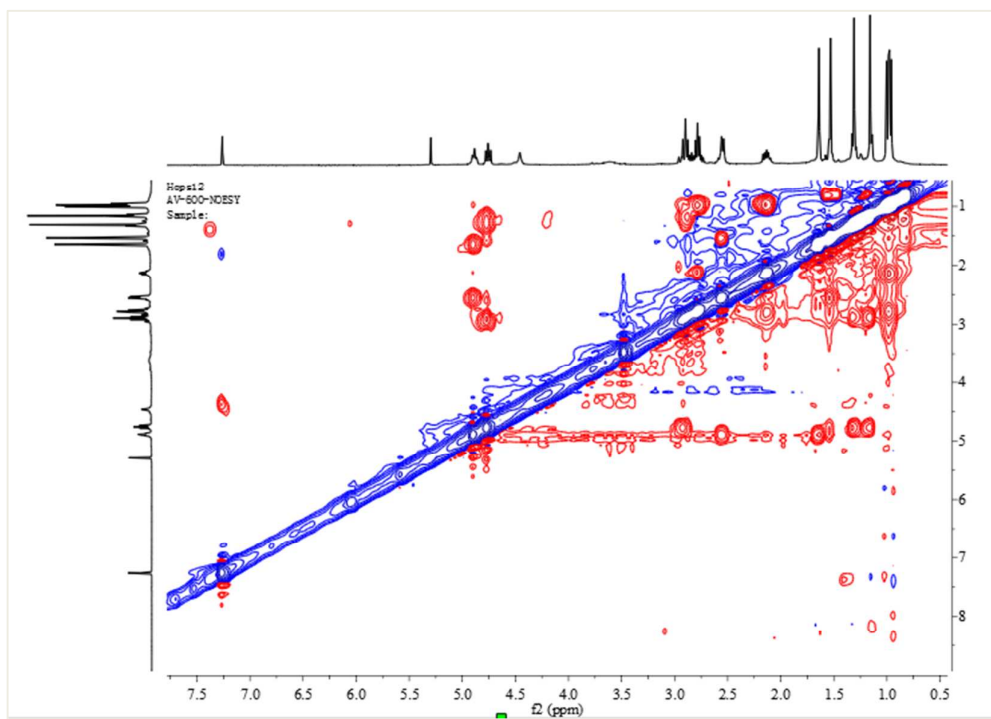
S31. HSQC (600 MHz, CDCl₃) spectrum of (2*R*, 7*S*)-humulone B (**5**).



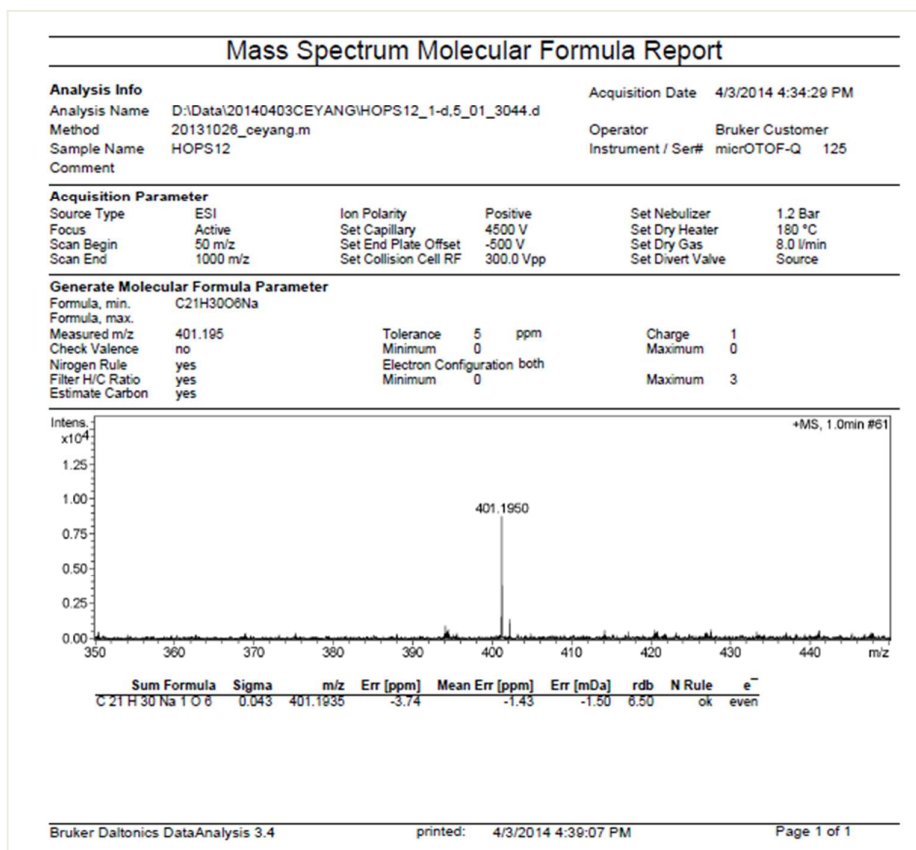
S32. HMBC (600 MHz, CDCl₃) spectrum of (2*R*, 7*S*)-humulone B (**5**).



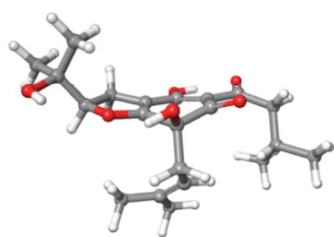
S33. NOESY (600 MHz, CDCl₃) spectrum of (2*R*, 7*S*)-humulone B (**5**).



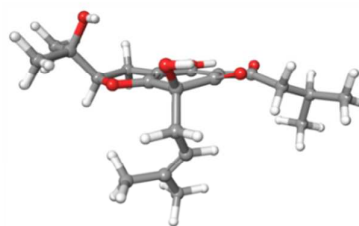
S34. HRESIMS spectrum of (2*R*, 7*S*)-humulone B (**5**).



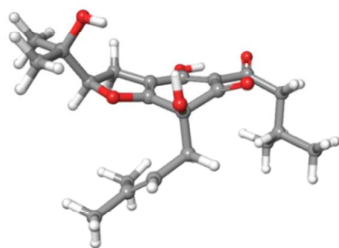
S35. Selected structures and population of the low-energy B3LYP/6-31G (d) in *vacuo* conformers of (2*R*,7*S*)-**5** based on experimental NOE correlations.



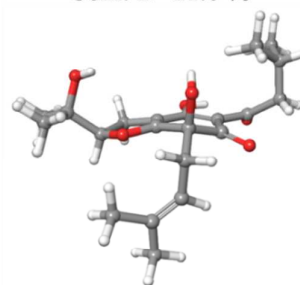
Conf. A 28.4 %



Conf. B 21.6 %

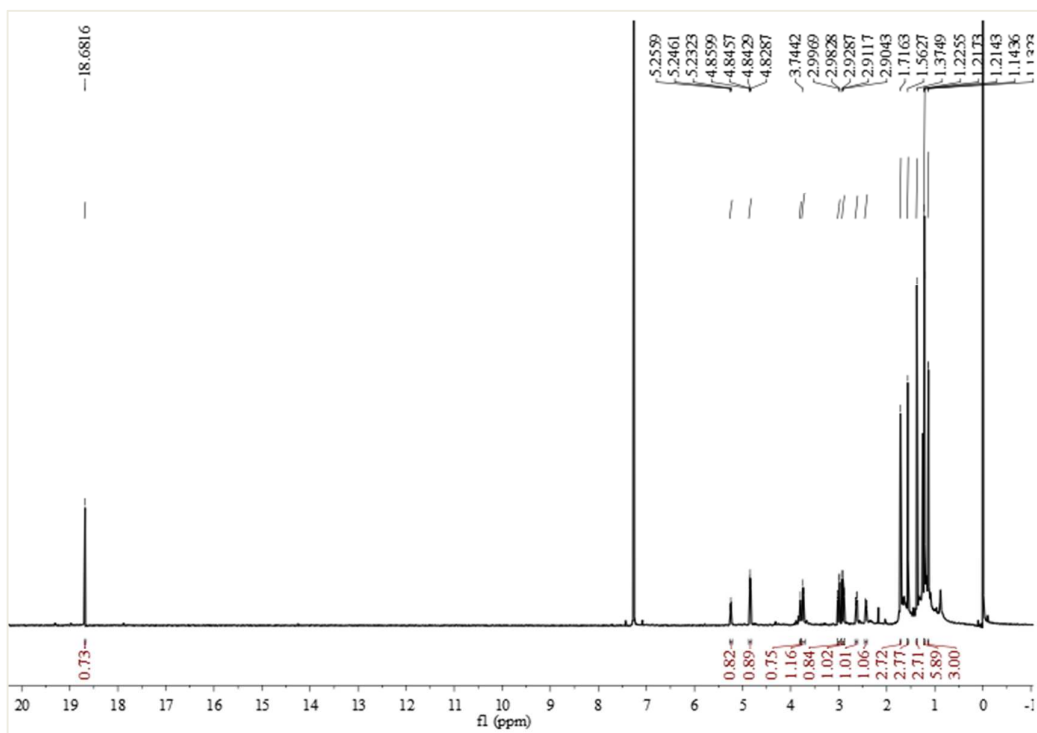


Conf. C 17.8 %

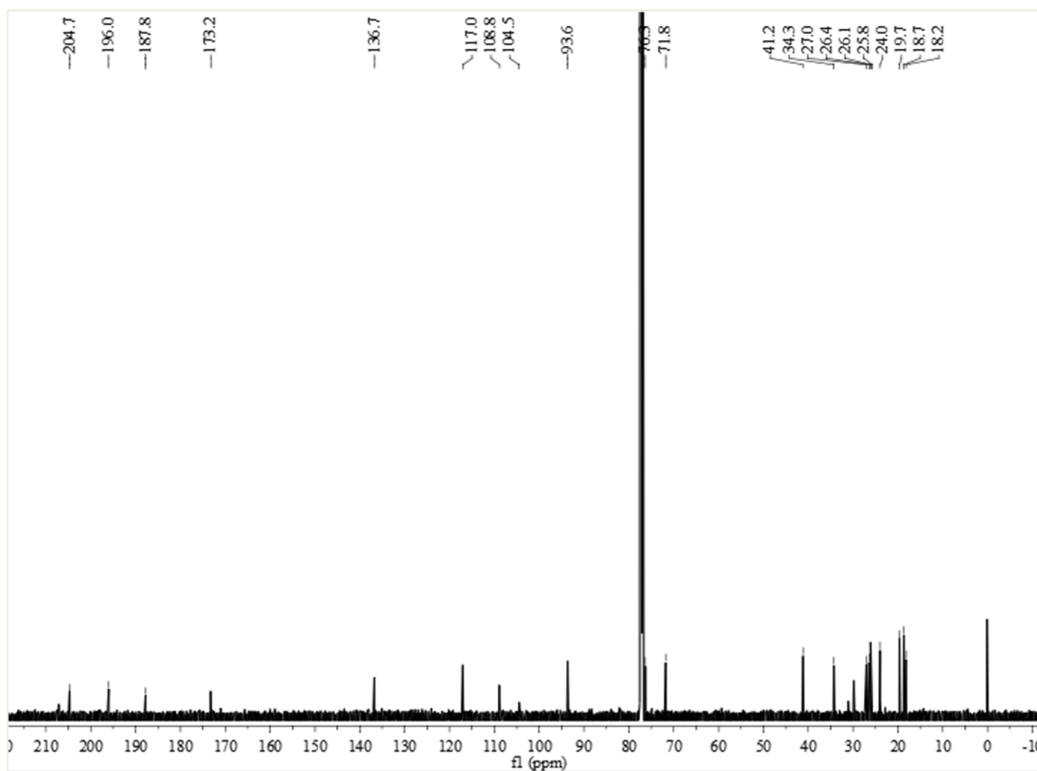


Conf. D 8.0 %

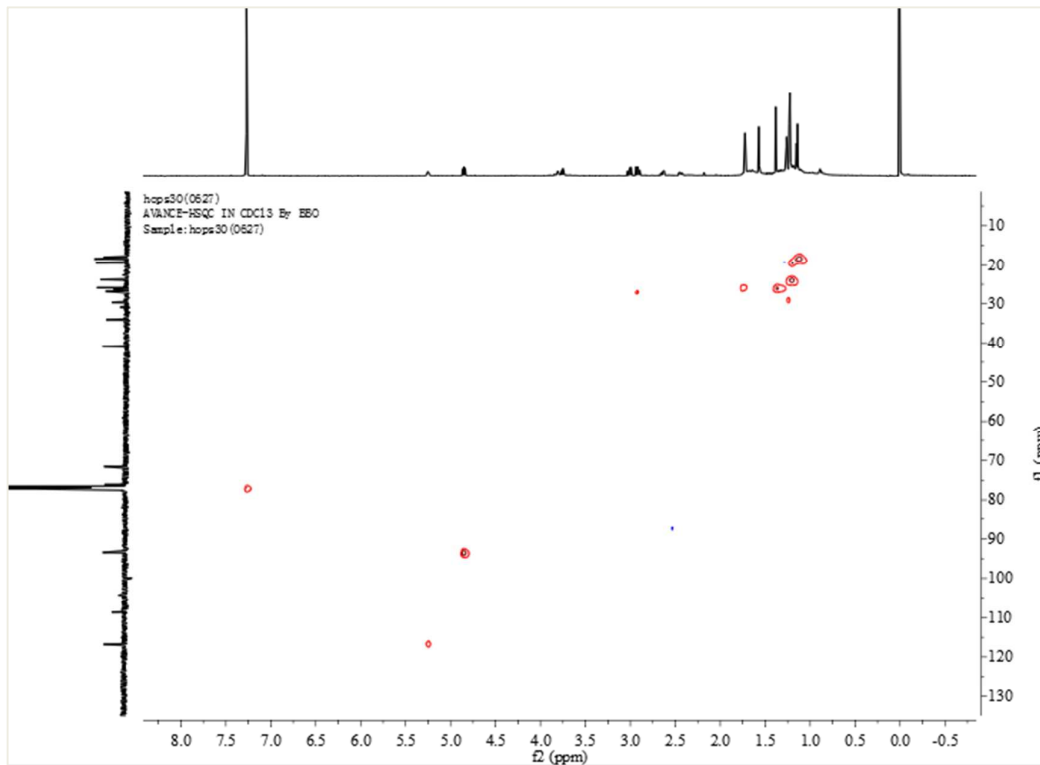
S36. ^1H NMR (400 MHz, CDCl_3) spectrum of (2*S*, 7*S*)-cohumulone B (**6**).



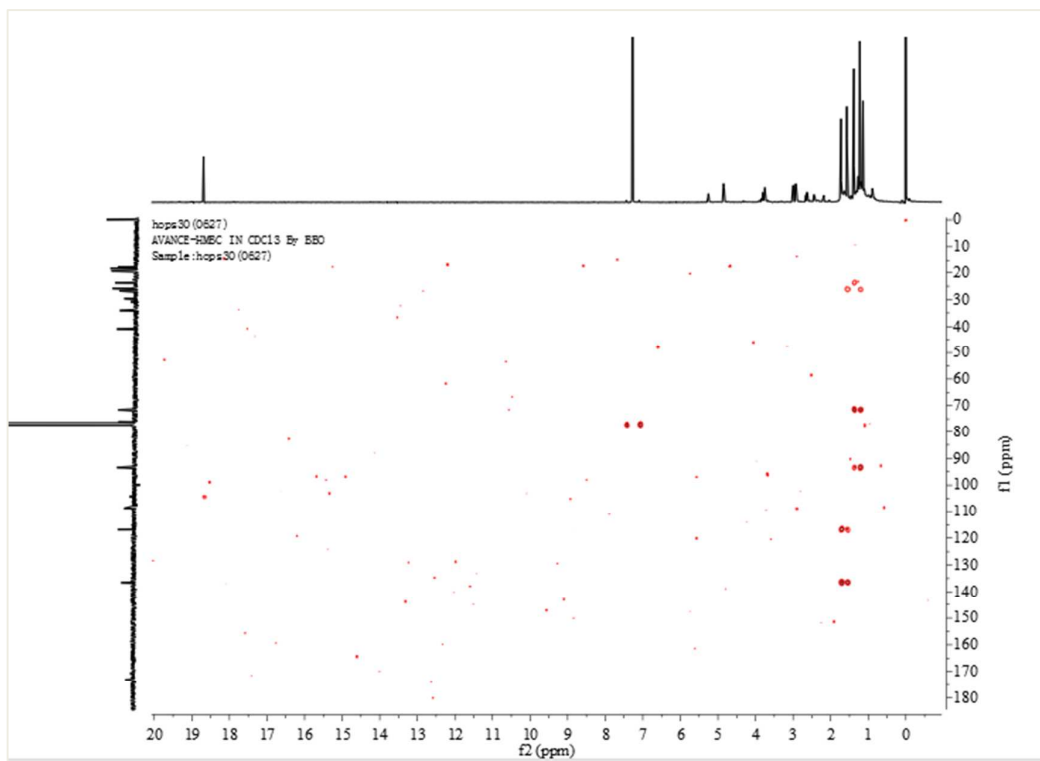
S37. ^{13}C NMR (100 MHz, CDCl_3) spectrum of (2*S*, 7*S*)-cohumulone B (**6**).



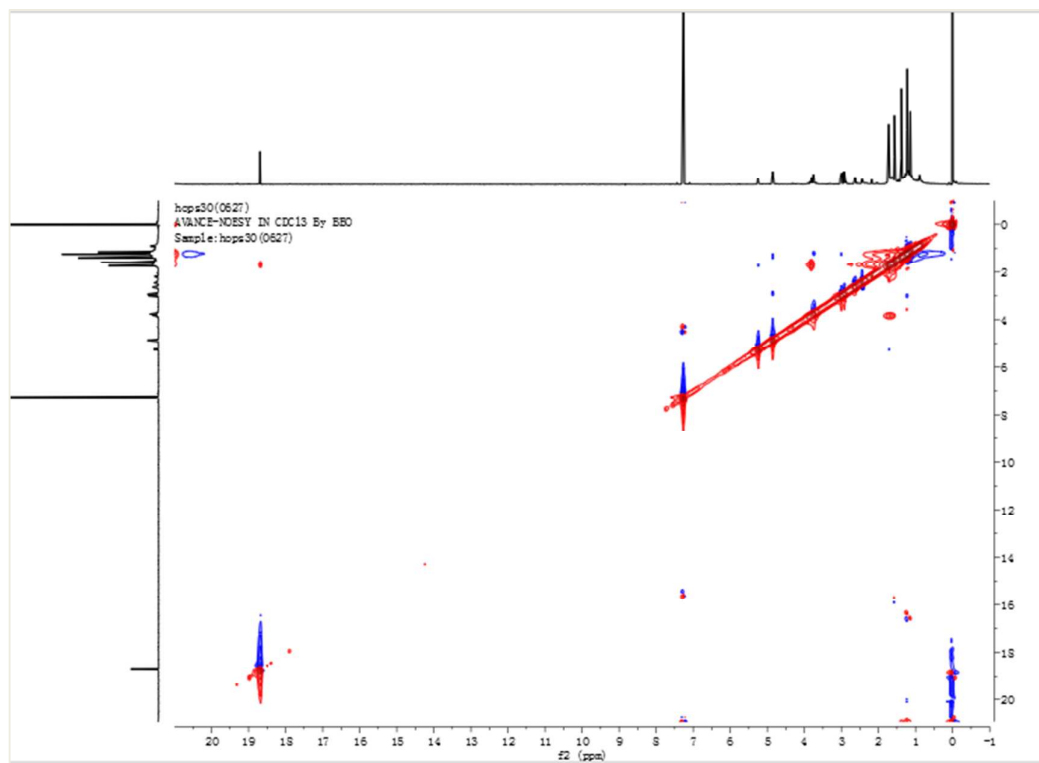
S38. HSQC (600 MHz, CDCl₃) spectrum of (2*S*, 7*S*)-cohumulone B (**6**).



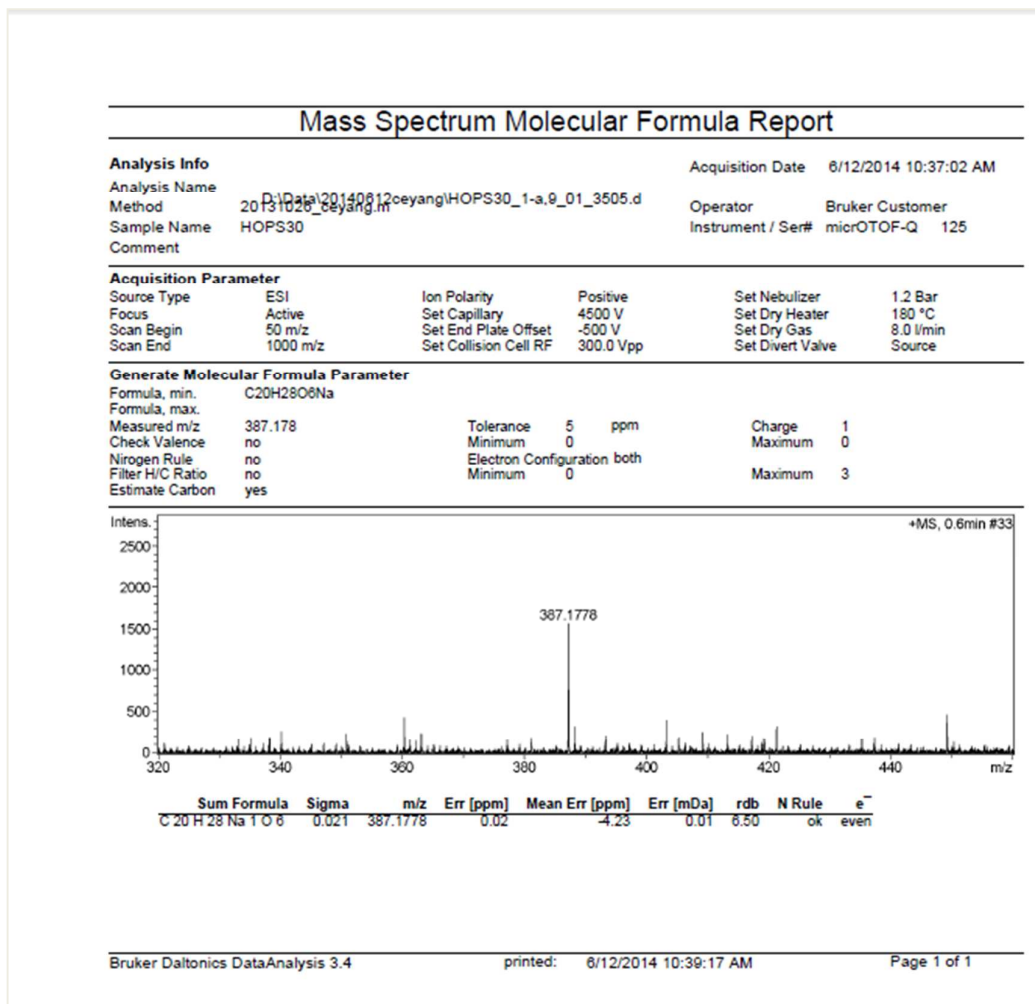
S39. HMBC (600 MHz, CDCl₃) spectrum of (2*S*, 7*S*)-cohumulone B (**6**).



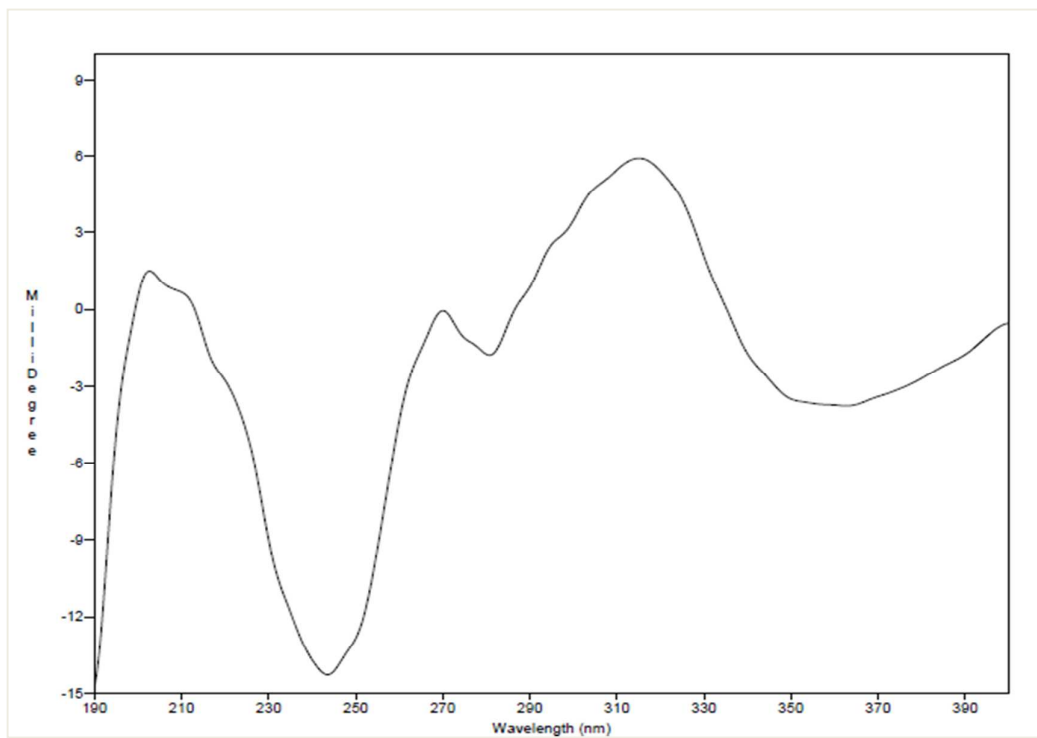
S40. NOESY (600 MHz, CDCl₃) spectrum of (2*S*, 7*S*)-cohumulone B (**6**)



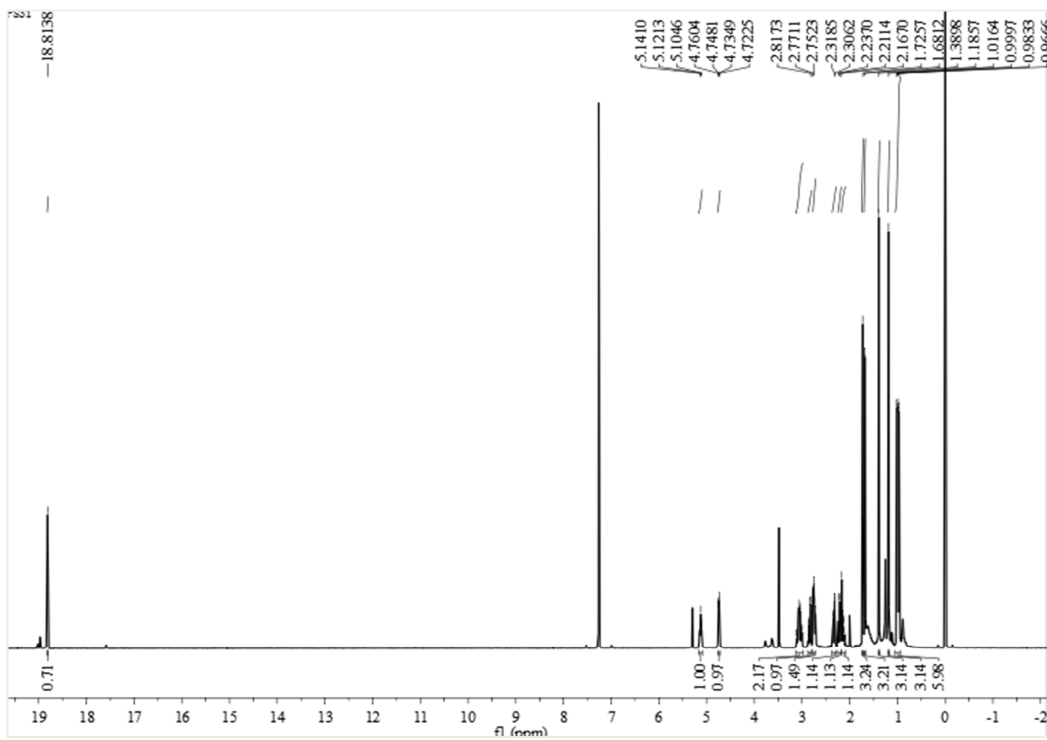
S41. HRESIMS spectrum of (2*S*, 7*S*)-cohumulone B (**6**).



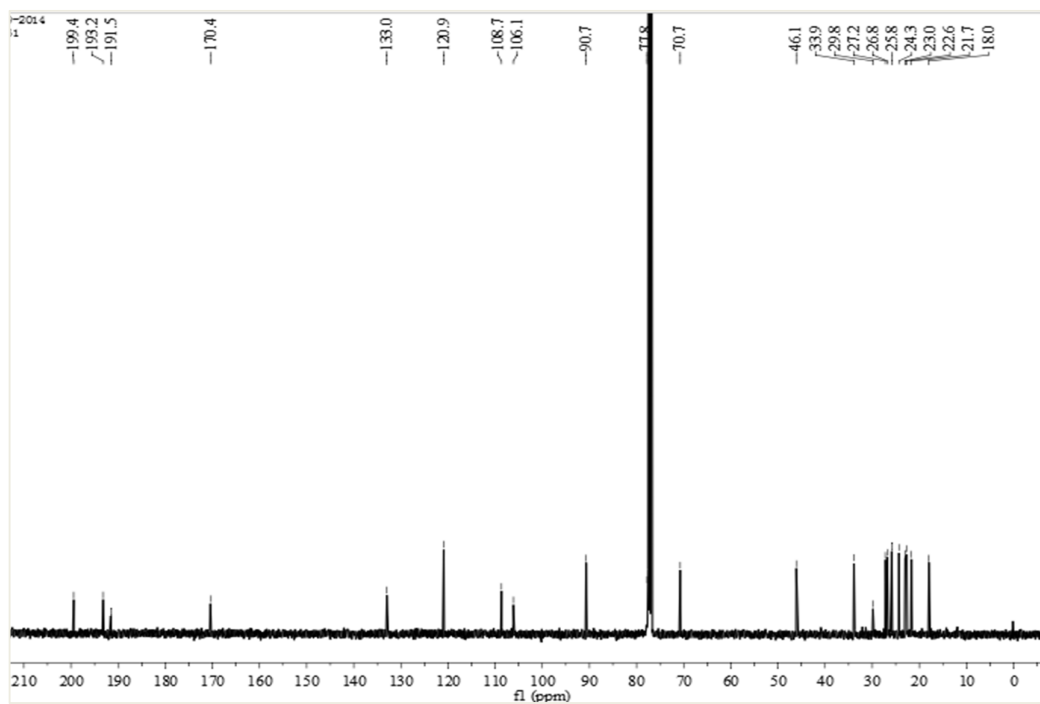
S42. Experimental CD spectrum of (2*S*, 7*S*)-cohumulone B (**6**).



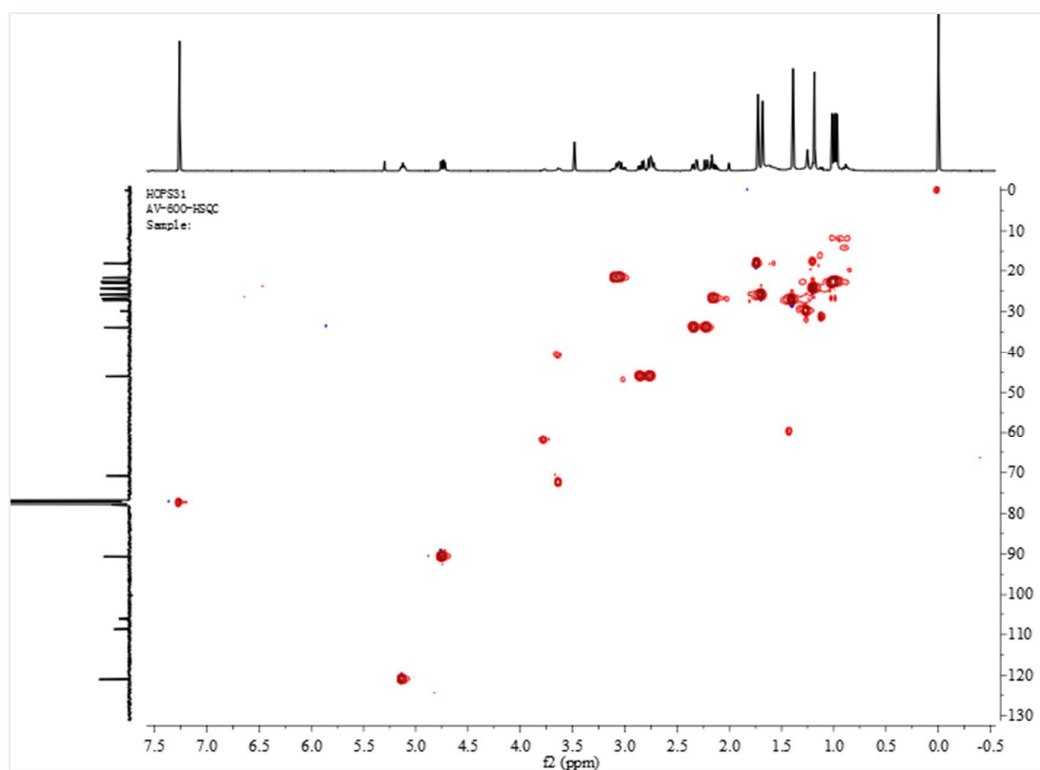
S43. ^1H NMR (400 MHz, CDCl_3) spectrum of (2*S*, 3*aS*)-humulone C (**7**).



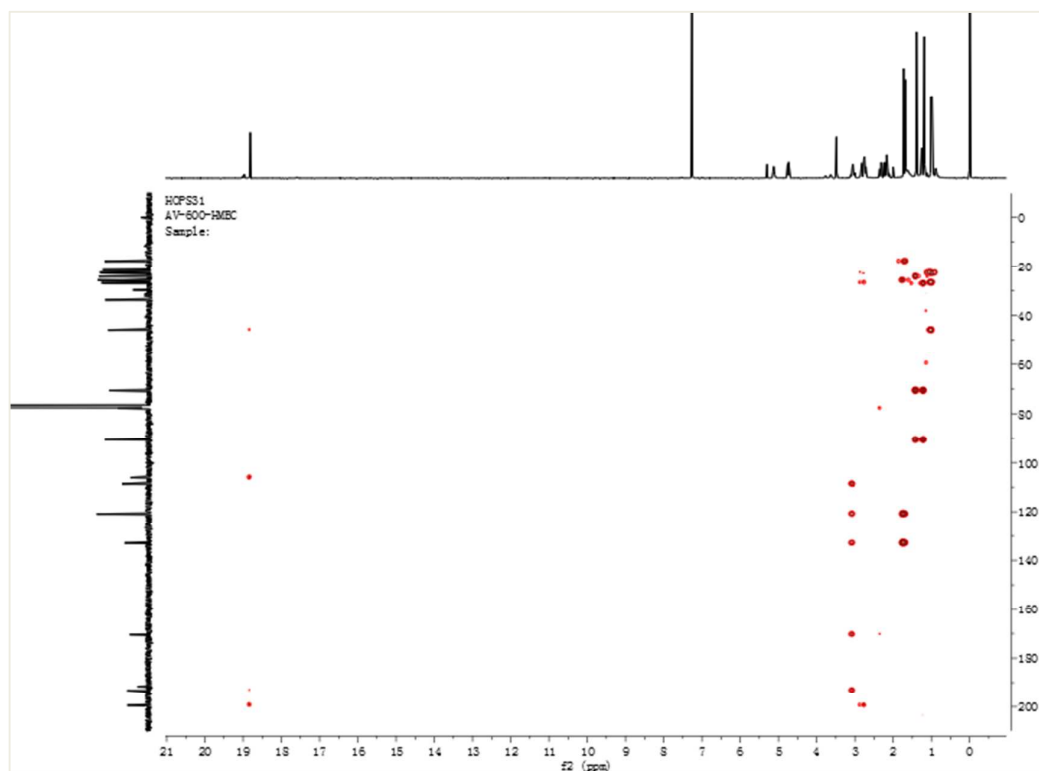
S44. ^{13}C NMR (100 MHz, CDCl_3) spectrum of (2*S*, 3*aS*)-humulone C (**7**).



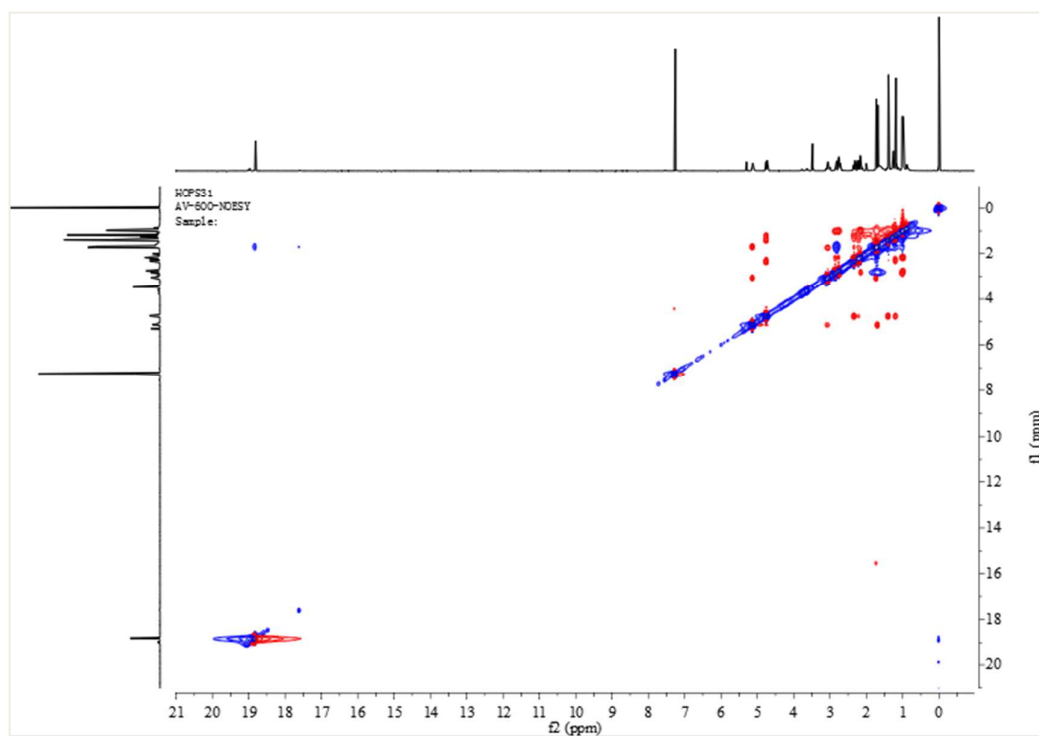
S45. HSQC (600 MHz, CDCl_3) spectrum of (2*S*, 3*aS*)-humulone C (**7**).



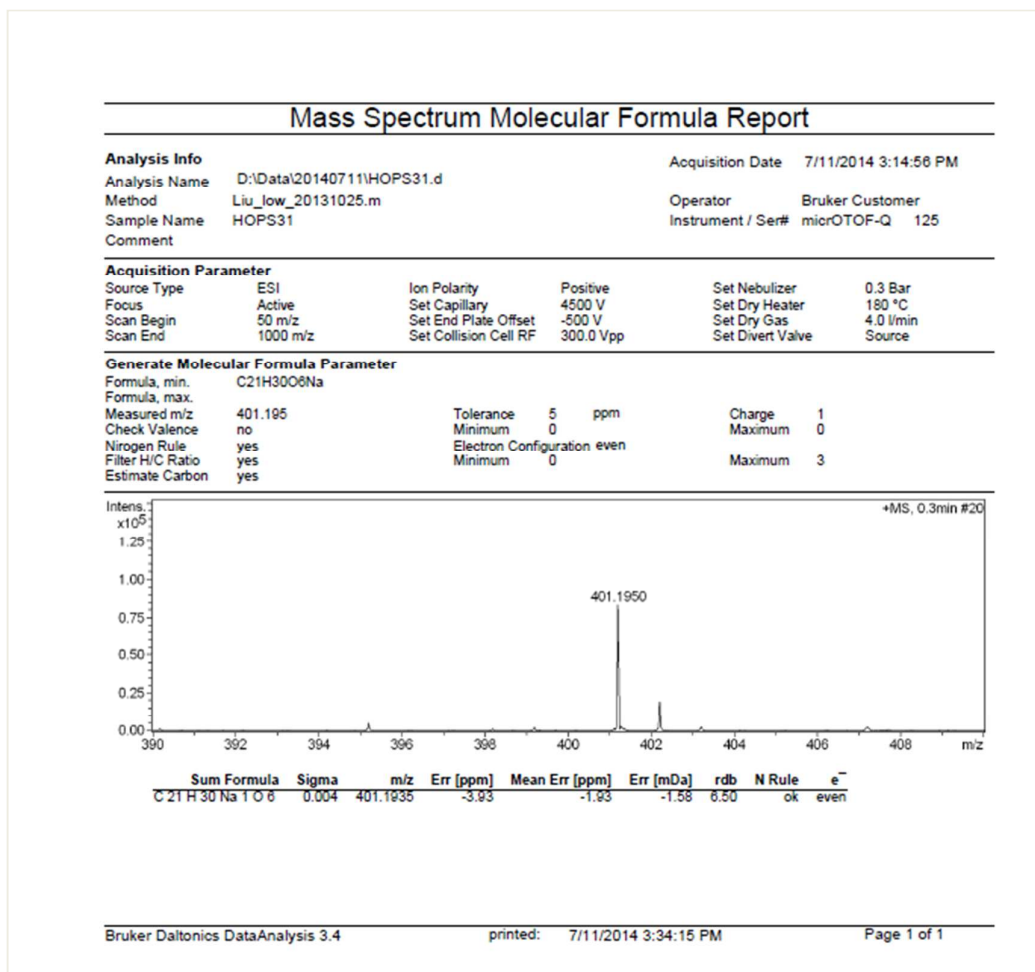
S46. HMBC (600 MHz, CDCl₃) spectrum of (2*S*, 3*aS*)-humulone C (**7**).



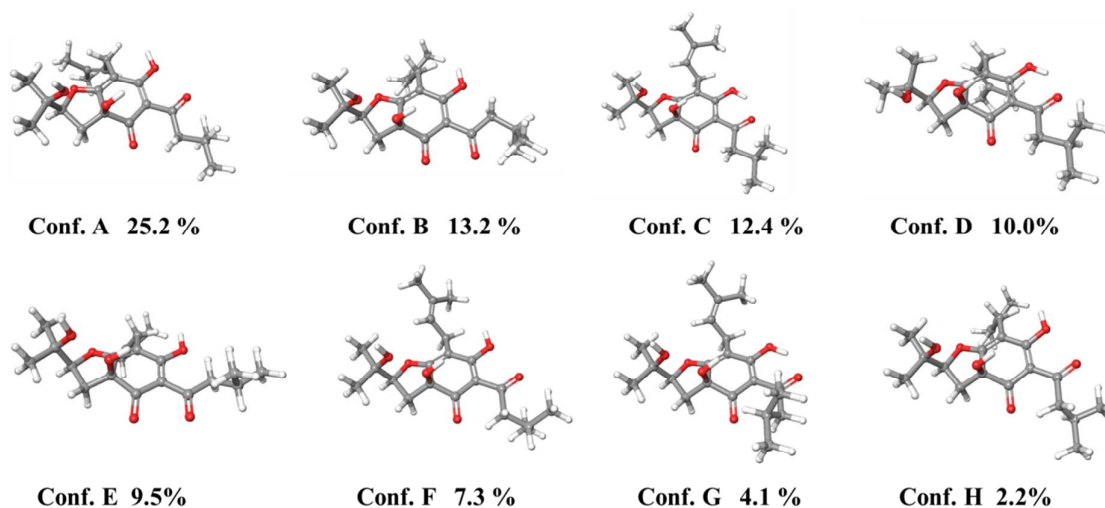
S47. NOESY(600 MHz, CDCl₃) spectrum of (2*S*, 3*aS*)-humulone C (**7**).



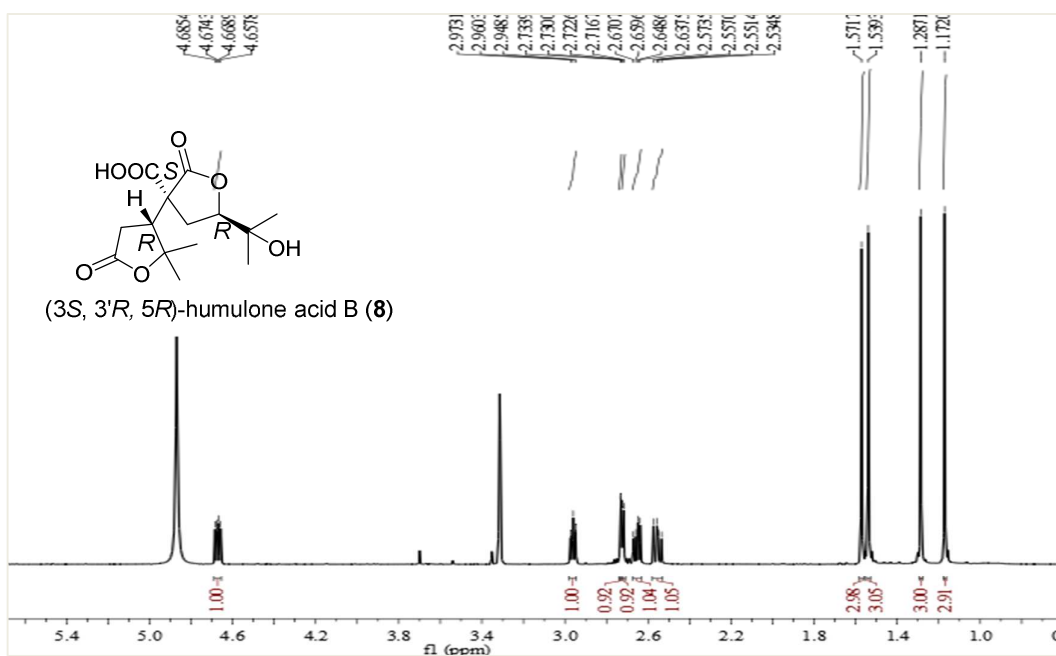
S48. HRESIMS spectrum of (2*S*, 3*aS*)-humulone C (7).



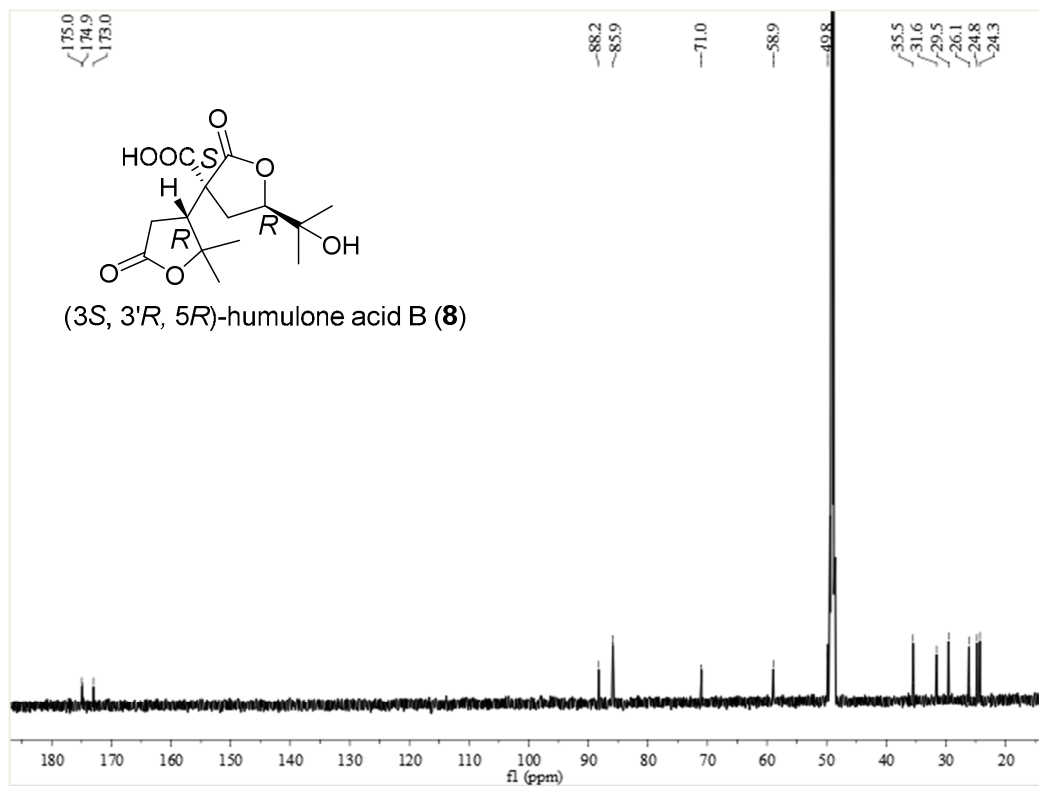
S49. Structures and populations of the low-energy B3LYP/6-31G (d) in *vacuo* conformers (>2%) of (2*S*, 3*aS*)-7.



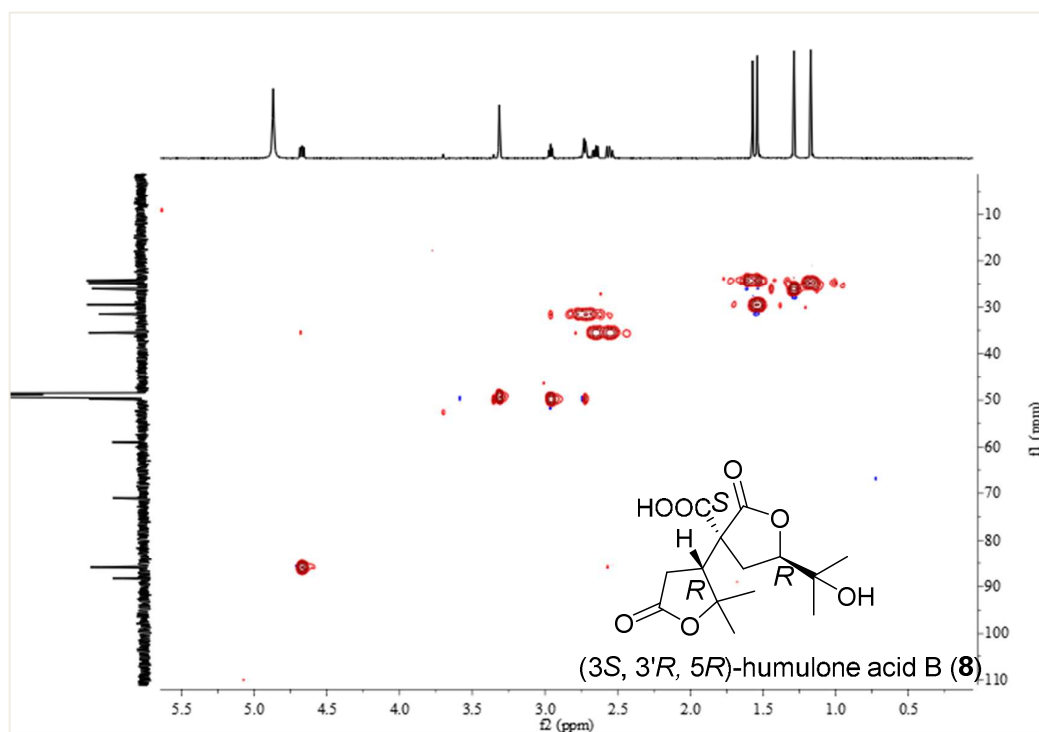
S50. ^1H NMR (600 MHz, CD_3OD) spectrum of (3*S*, 3'*R*, 5*R*)-humulone acid B (**8**).



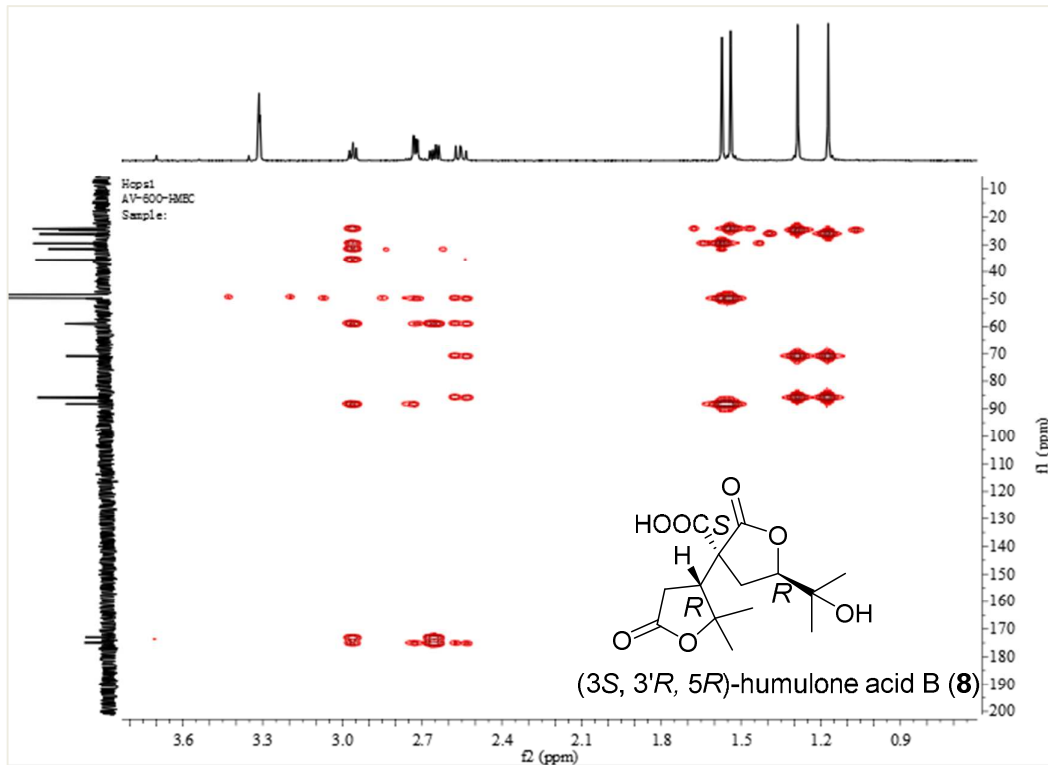
S51. ^{13}C NMR (150 MHz, CD_3OD) spectrum of (3*S*, 3'*R*, 5*R*)-humulone acid B (**8**).



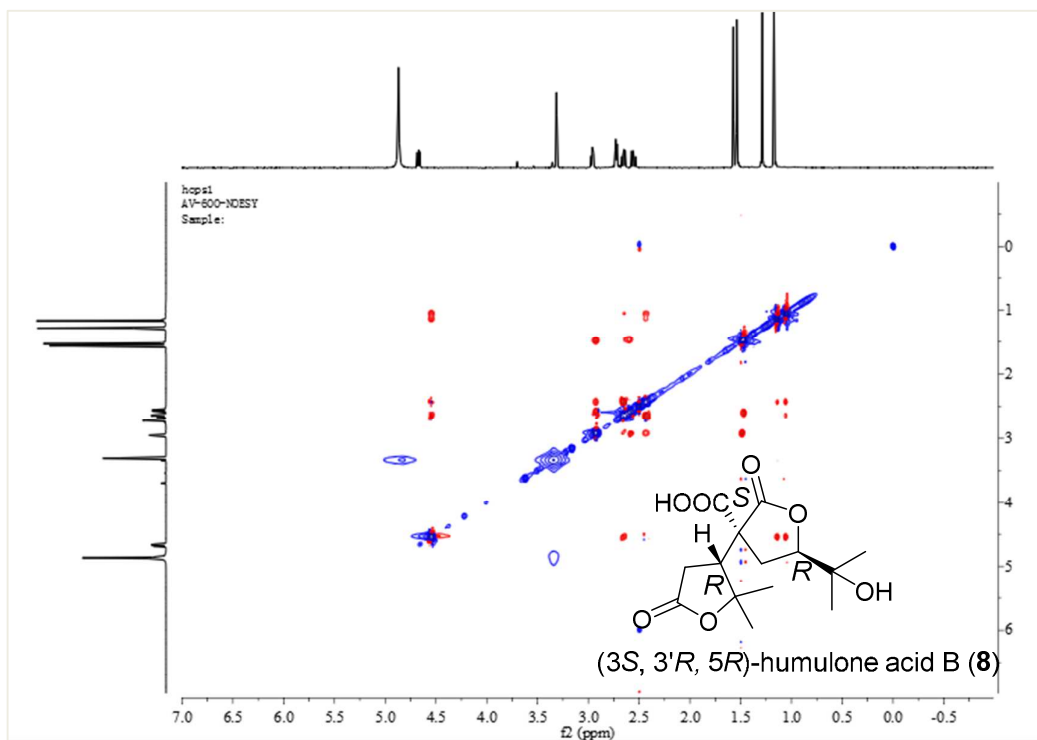
S52. HSQC (600 MHz, CD_3OD) spectrum of (3*S*, 3'*R*, 5*R*)-humulone acid B (**8**).



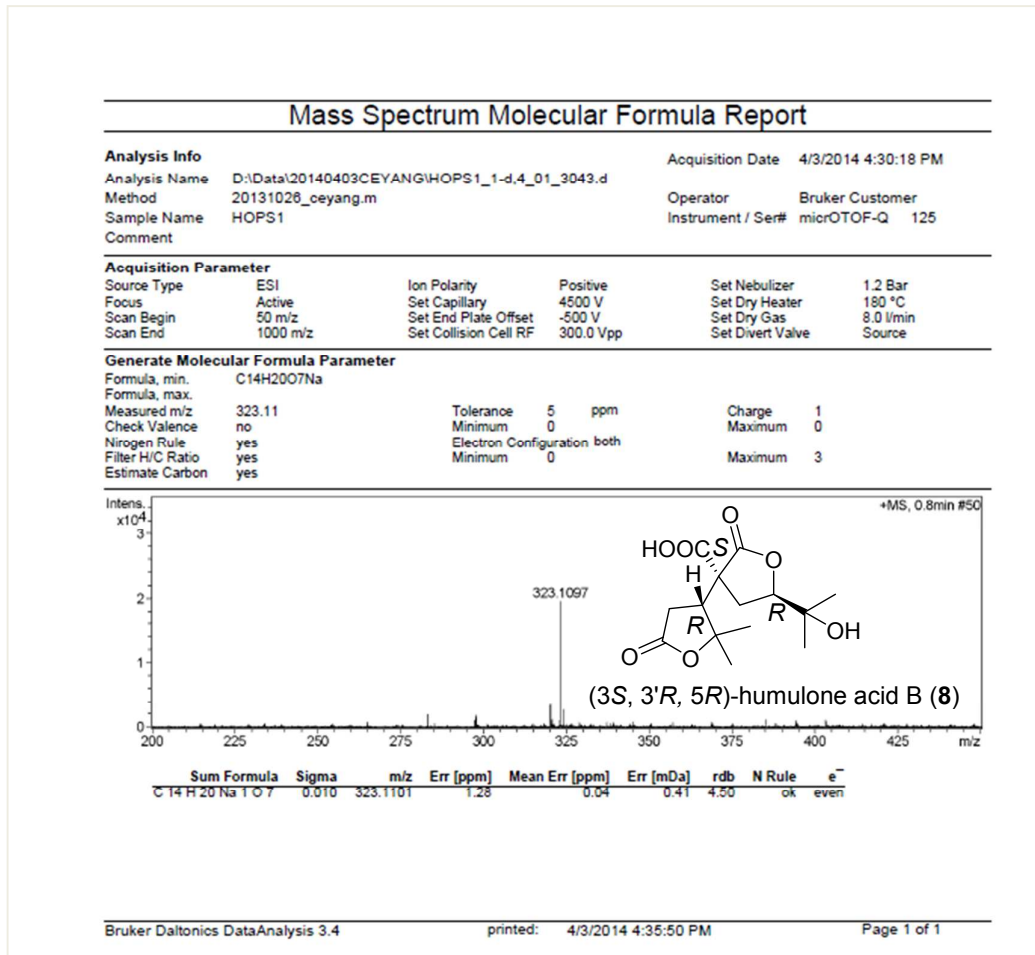
S53. HMBC (600 MHz, CD₃OD) spectrum of (3*S*, 3'*R*, 5*R*)-humulone acid B (**8**).



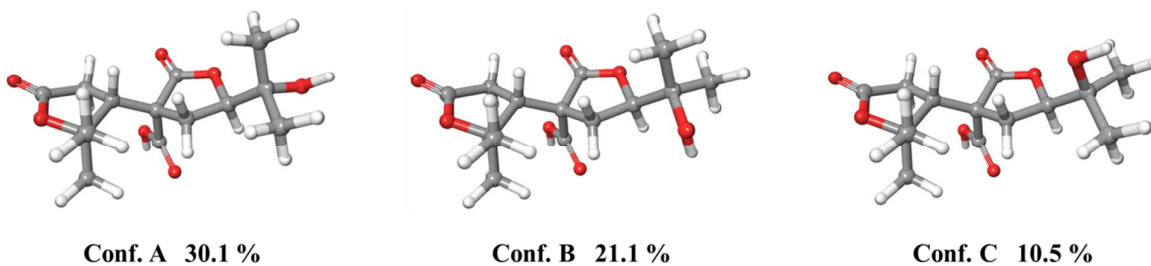
S54. NOESY (600 MHz, CD₃OD) spectrum of (3*S*, 3'*R*, 5*R*)-humulone acid B (**8**).



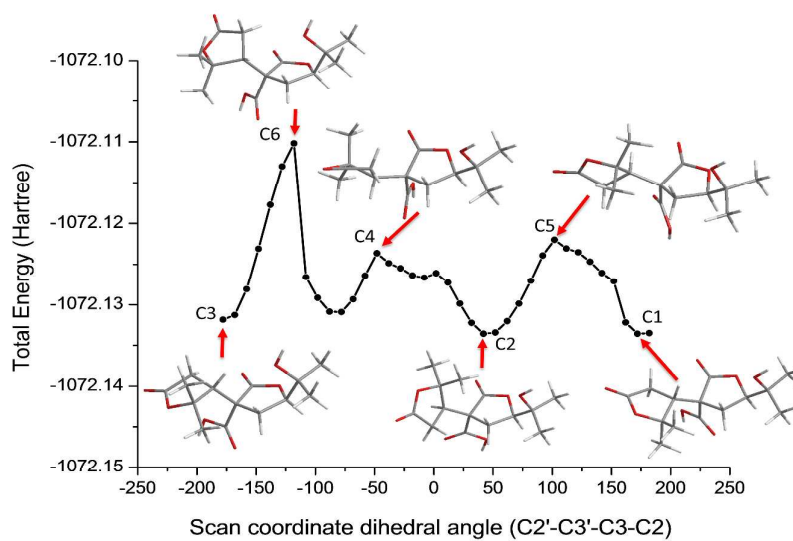
S55. HRESIMS spectrum of (3*S*, 3'*R*, 5*R*)-humulone acid B (**8**).



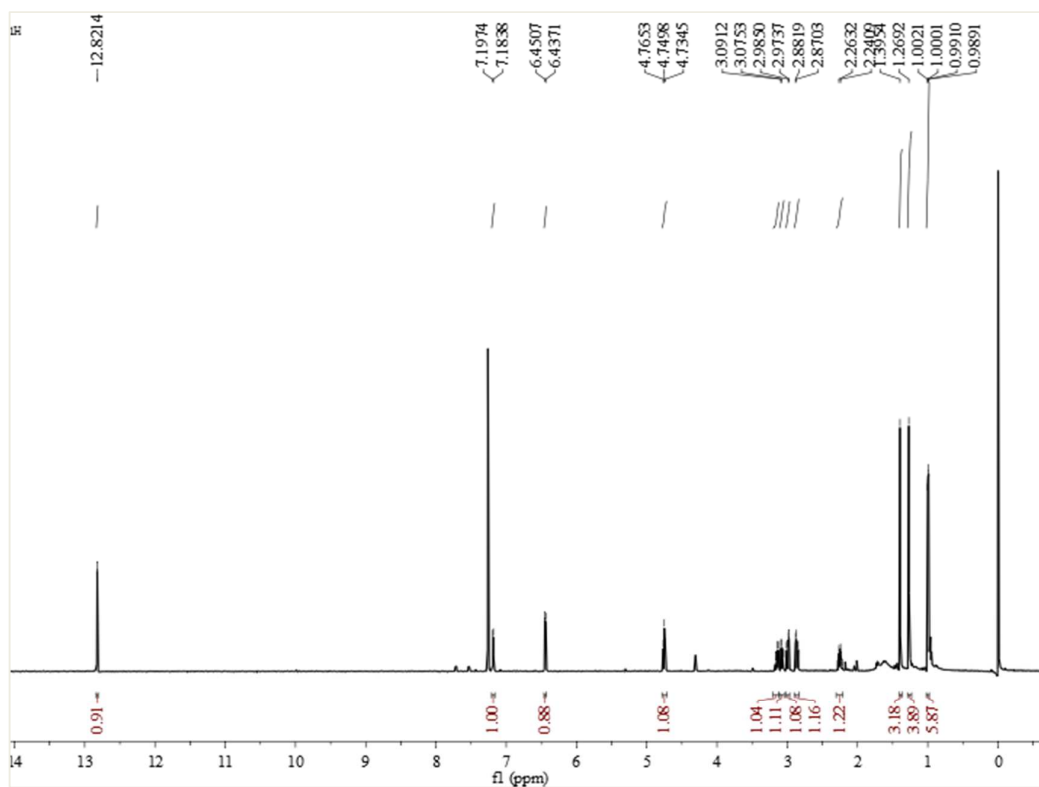
S56. Selected structures and population of the low-energy B3LYP/6-31G (d) *in vacuo* conformers of (3*S*, 3'*R*)-**8** based on experimental NOE correlations.



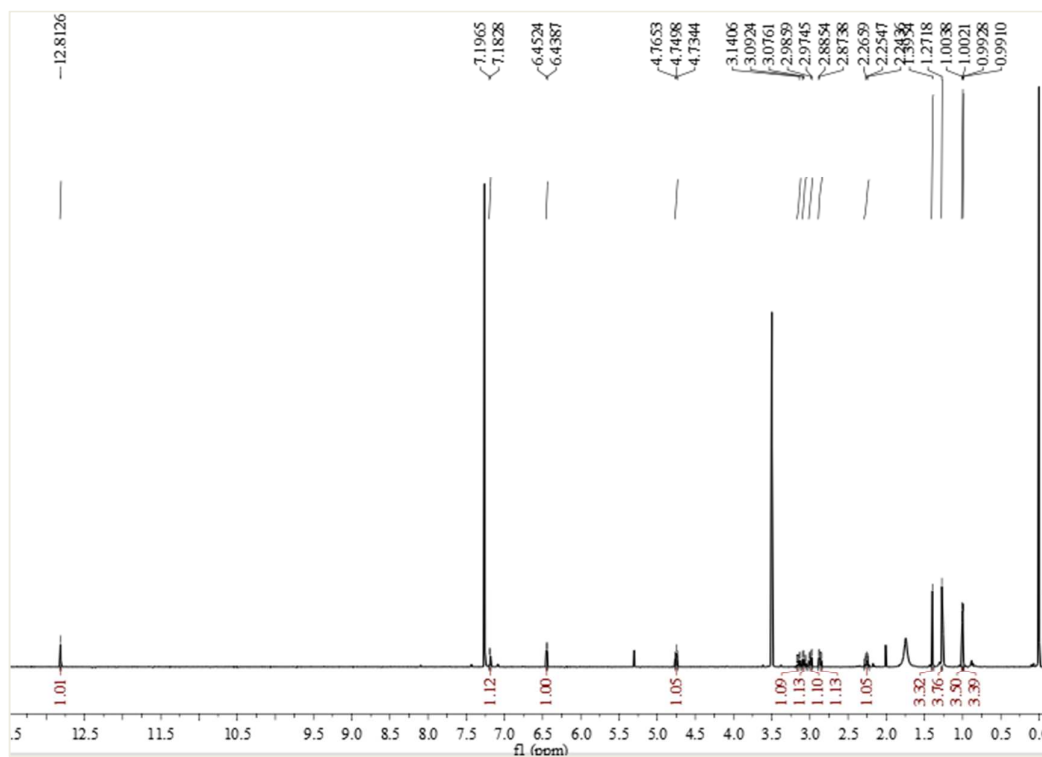
S57. The molecular energy profiles of conformational flexibility of compound **8**



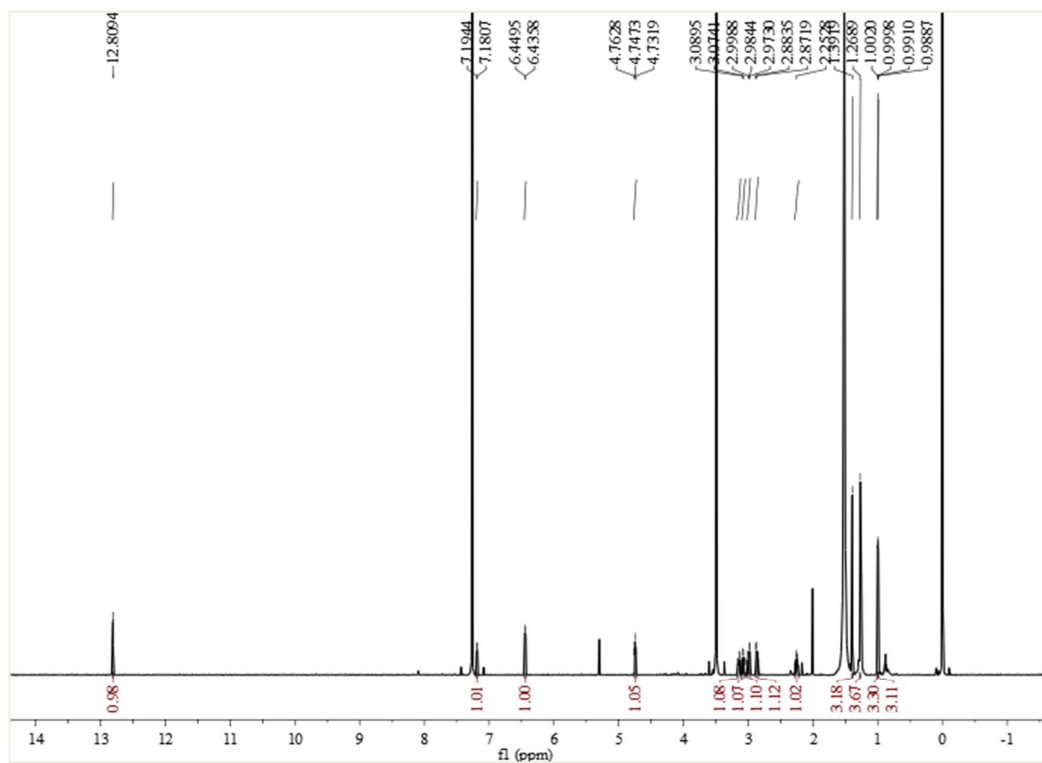
S58. ^1H NMR (400 MHz, CDCl_3) spectrum of lupulone H (**9**).



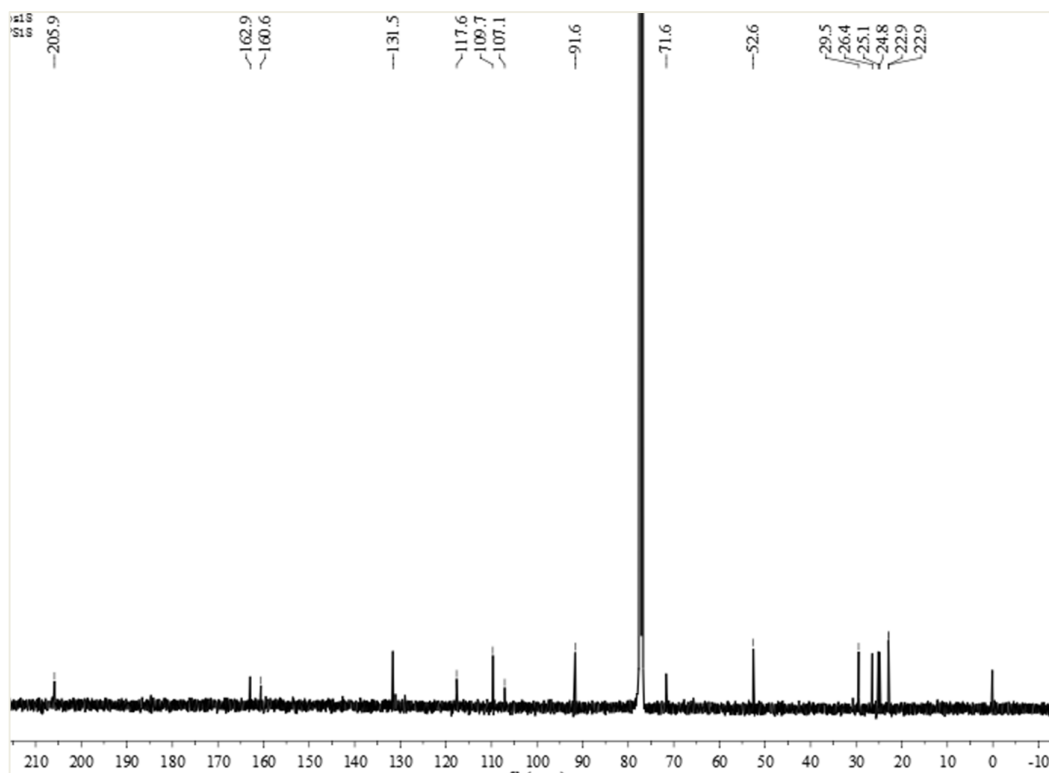
S59. ^1H NMR (600 MHz, CDCl_3) spectrum of (*R*)-lupulone H (**9a**).



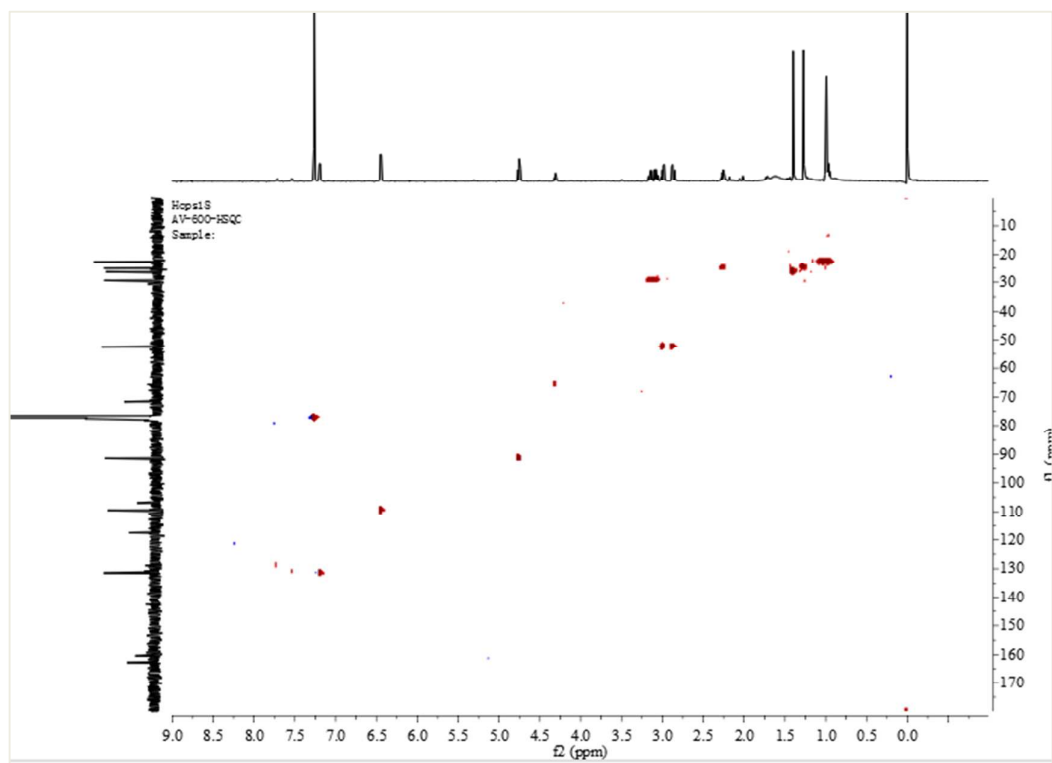
S60. ^1H NMR (600 MHz, CDCl_3) spectrum of (*S*)-lupulone H (**9b**).



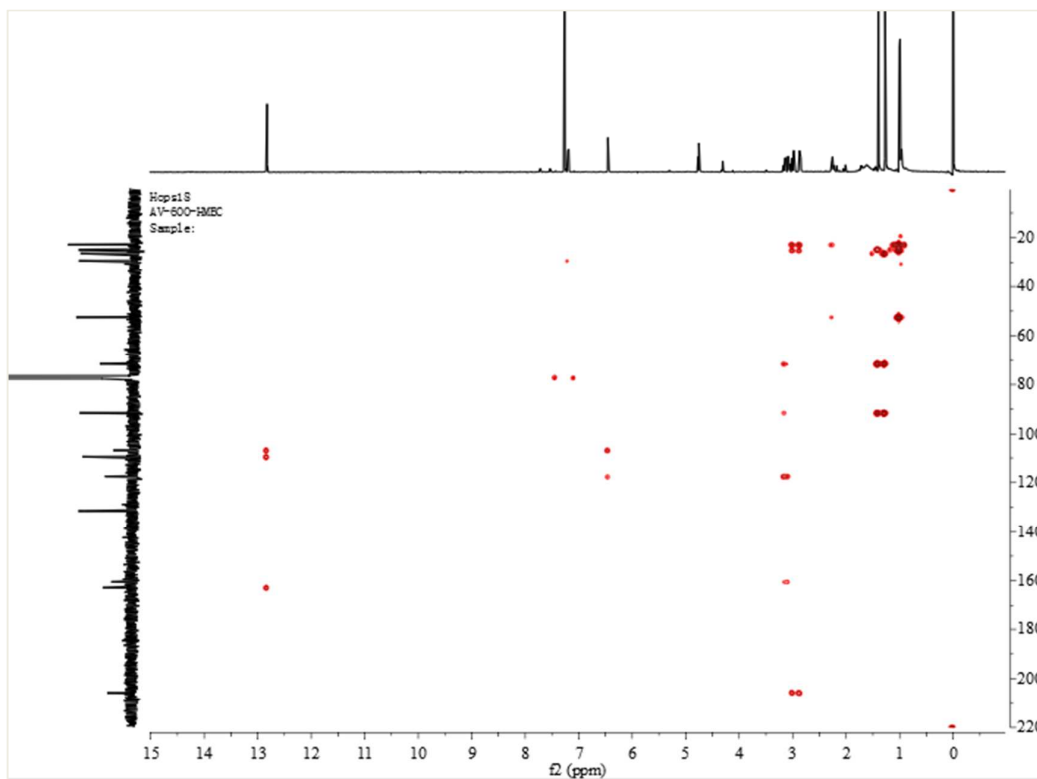
S61. ^{13}C NMR (100 MHz, CDCl_3) spectrum of lupulone H (**9**).



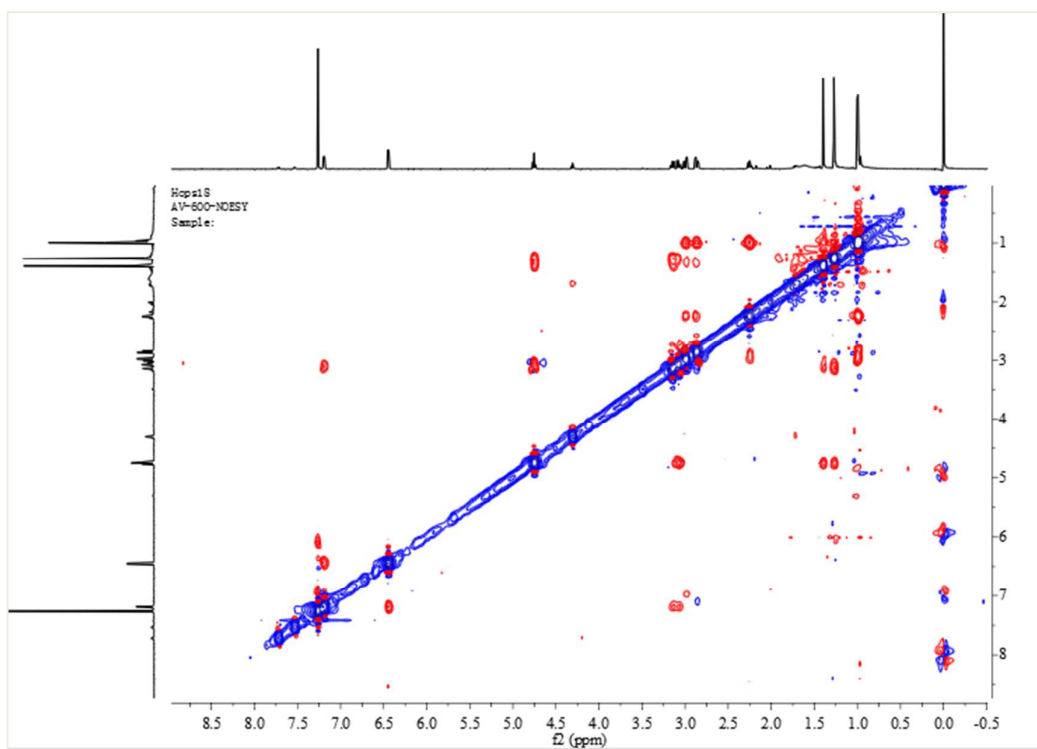
S62. HSQC (600 MHz, CDCl_3) spectrum of lupulone H (**9**).



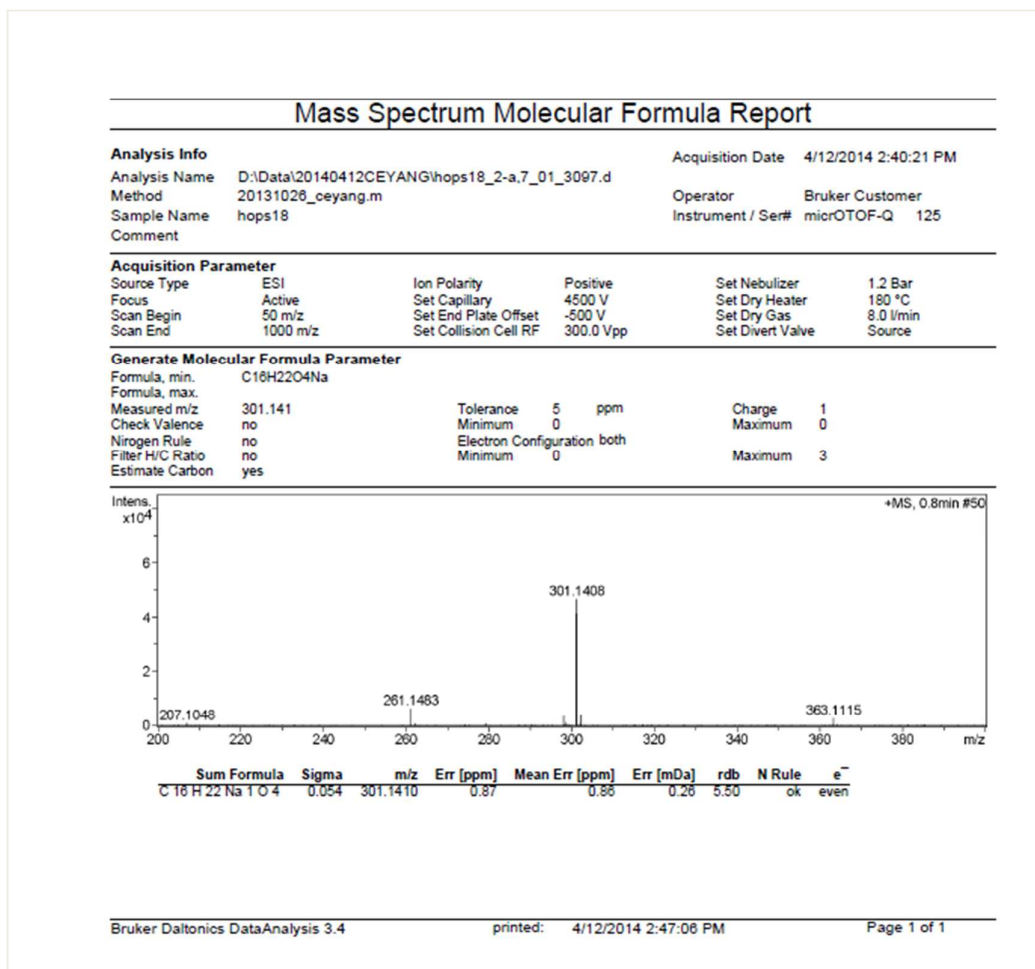
S63. HMBC (600 MHz, CDCl₃) spectrum of lupulone H (**9**).



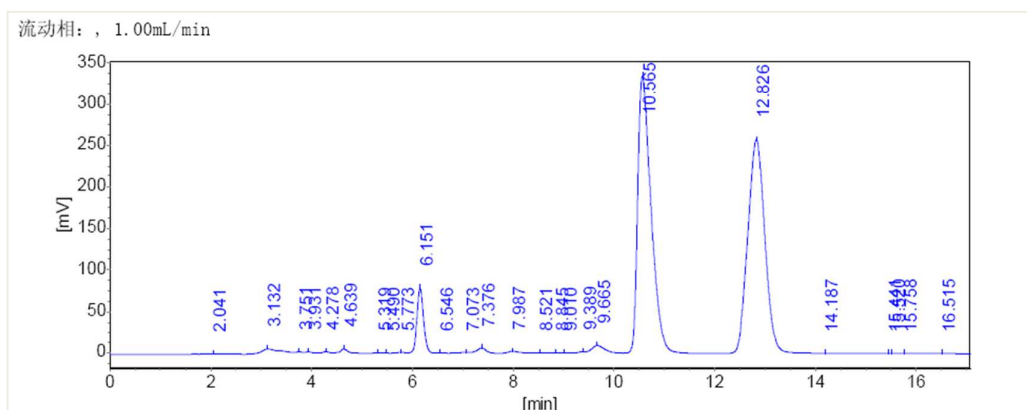
S64. NOESY (600 MHz, CDCl₃) spectrum of lupulone H (**9**).



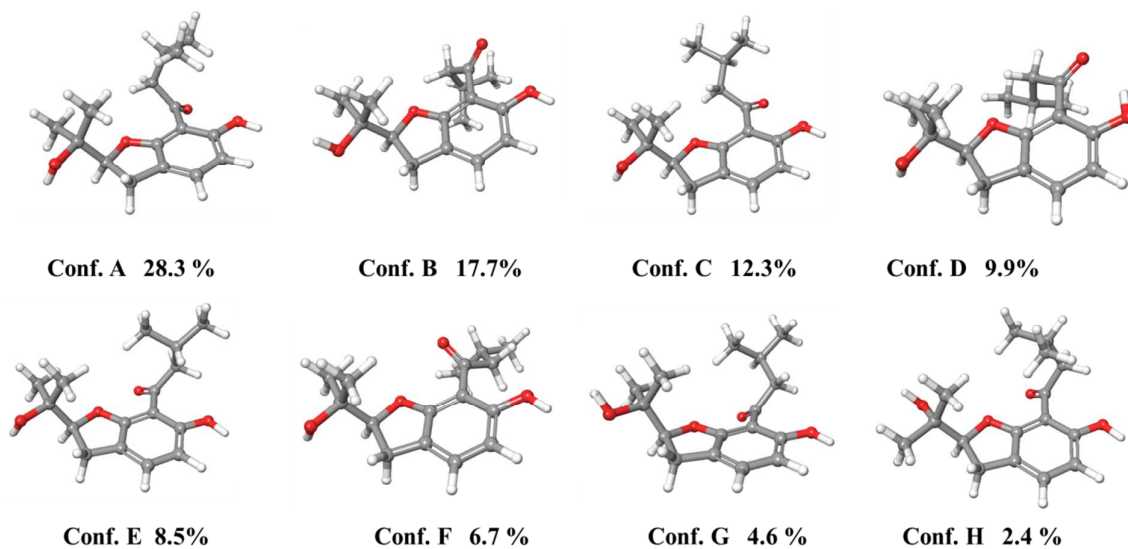
S65. HRESIMS spectrum of lupulone H (9).



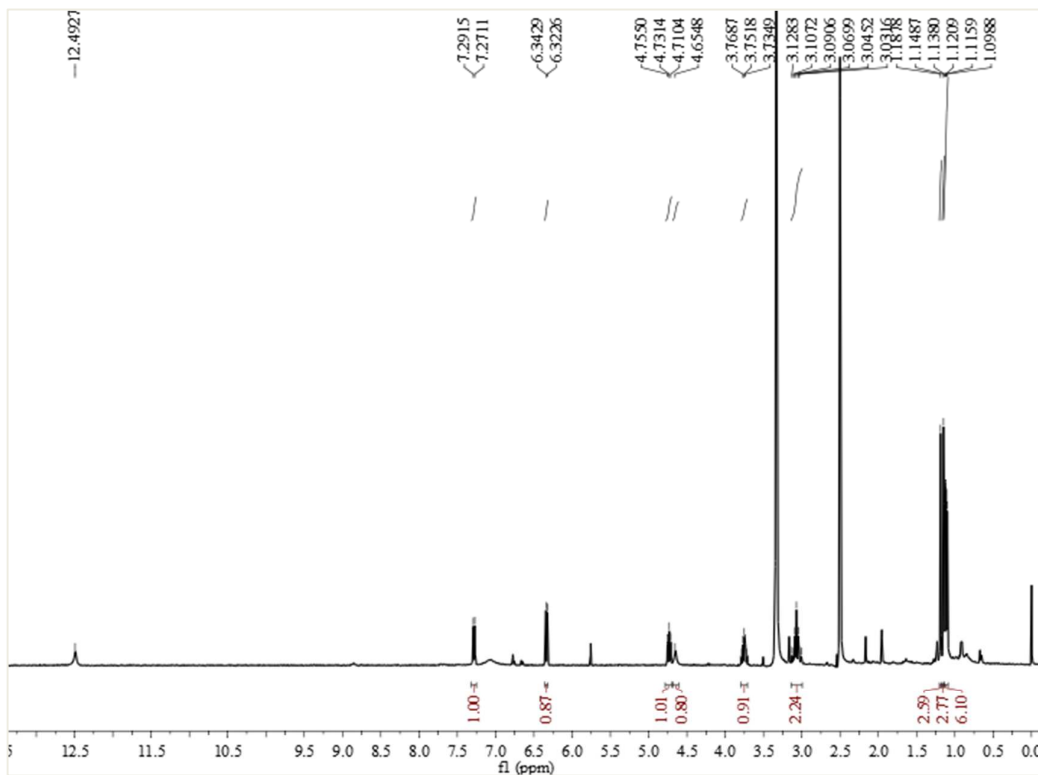
S66. The HPLC of chiral column analysis of lupulone H (9).



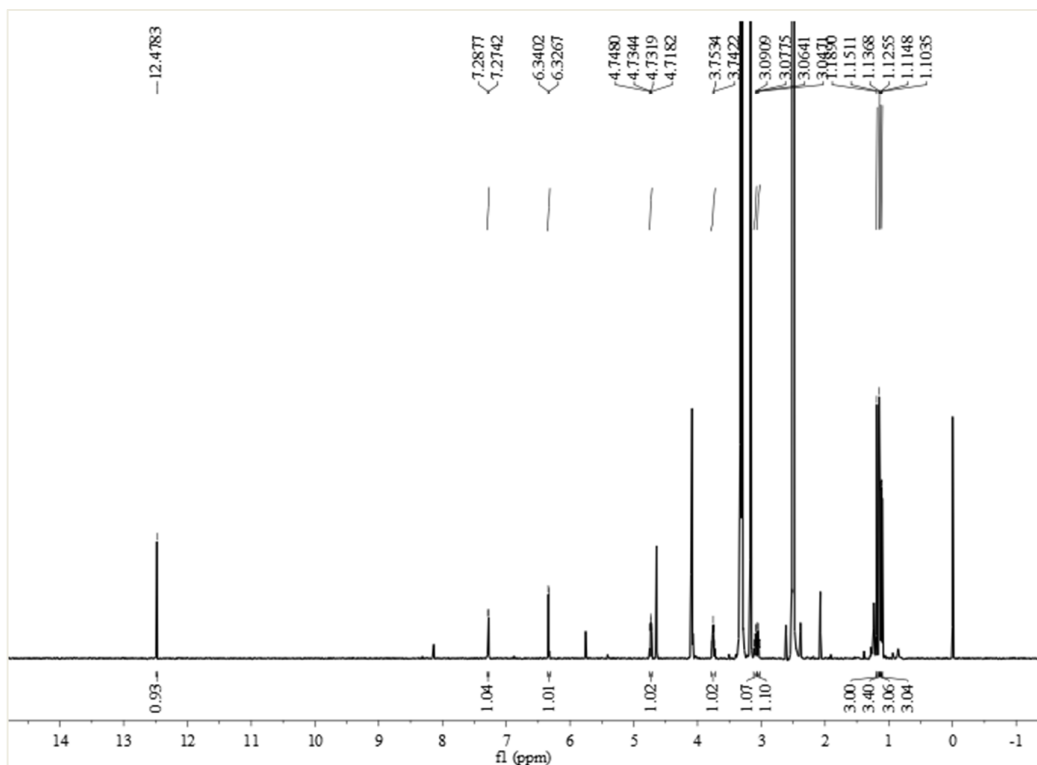
S67. Structures and populations of the low-energy B3LYP/6-31G (d) in *vacuo* conformers (>2%) of (2*S*)-9.



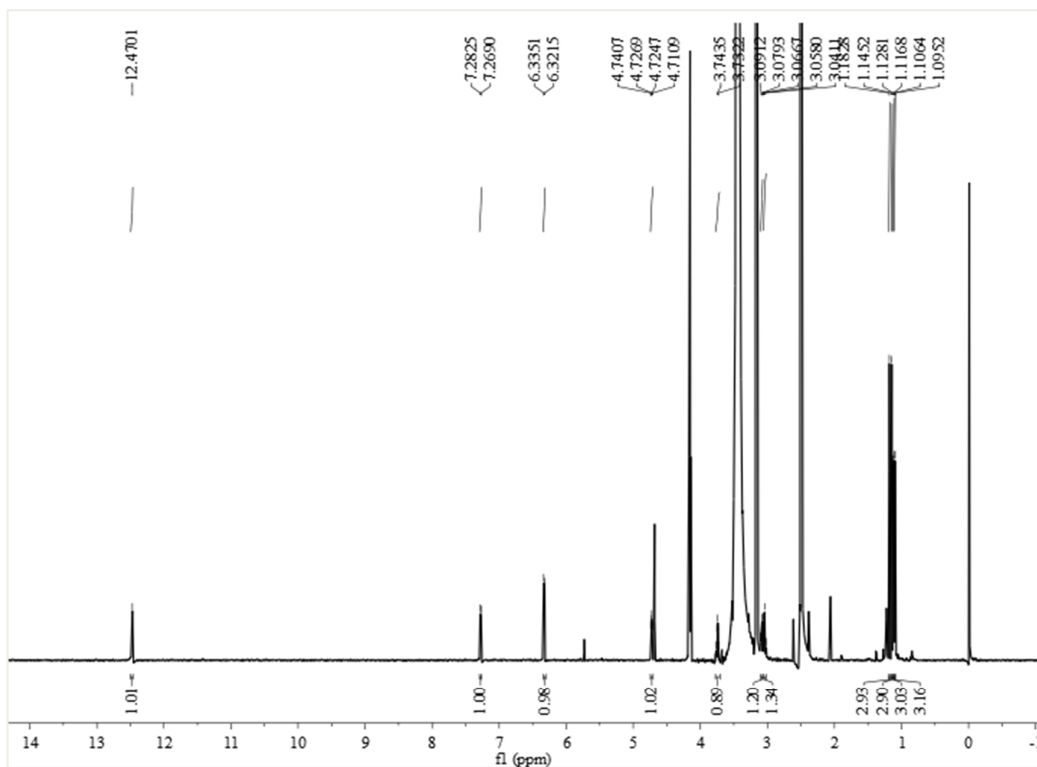
S68. ^1H NMR (400 MHz, $\text{DMSO-}d_6$) spectrum of lupulone G (**10**)



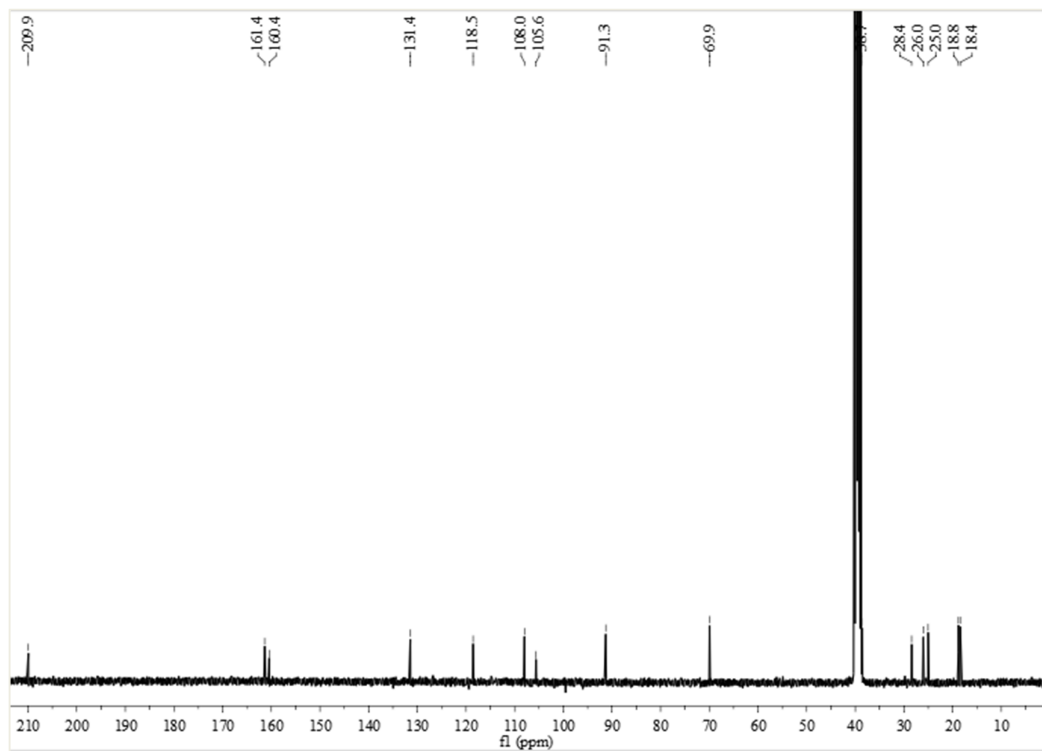
S69. ^1H NMR (600 MHz, $\text{DMSO}-d_6$) spectrum of (*R*)-lupulone G (**10a**)



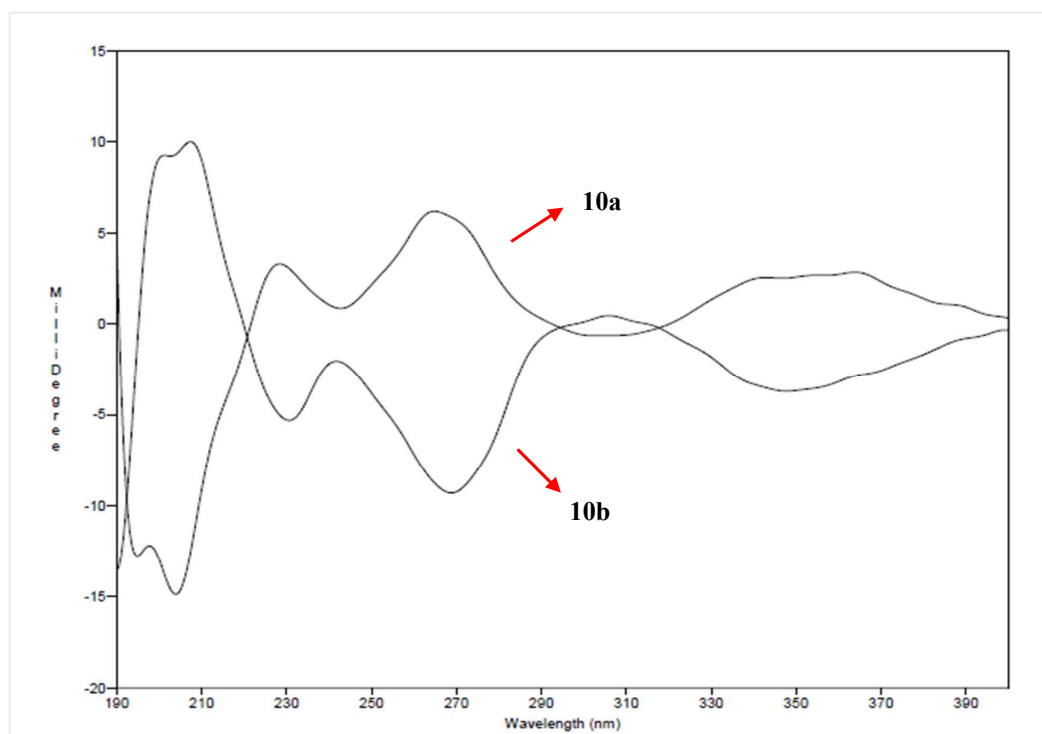
S70. ^1H NMR (600 MHz, $\text{DMSO}-d_6$) spectrum of (*S*)-lupulone G (**10b**)



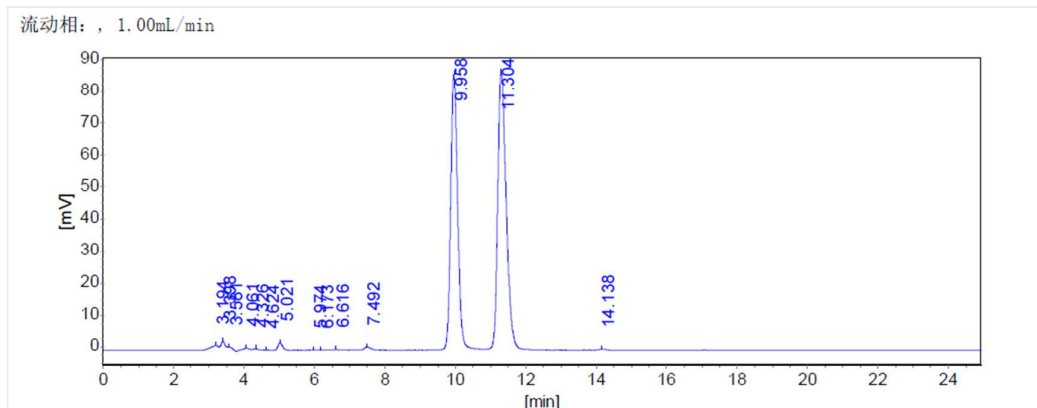
S71. ^{13}C NMR (100 MHz, $\text{DMSO}-d_6$) spectrum of lupulone G (**10**).



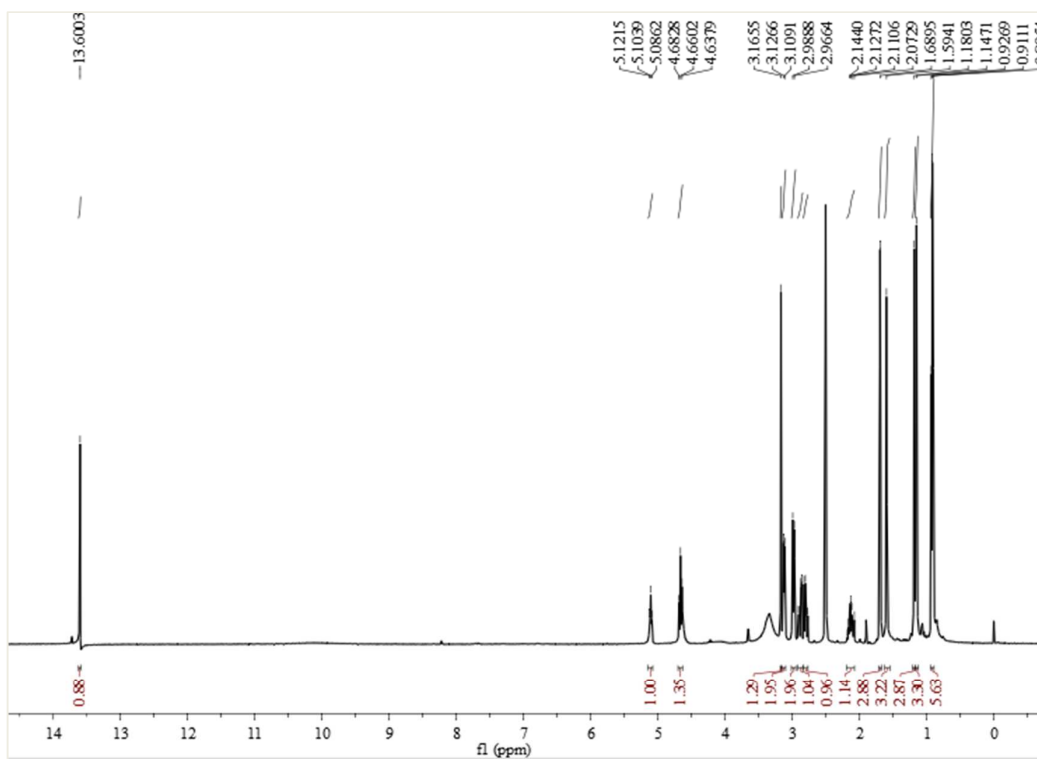
S72. Experimental CD spectrum of (*R*)-lupulone G (**10a**) and (*S*)-lupulone G (**10b**).



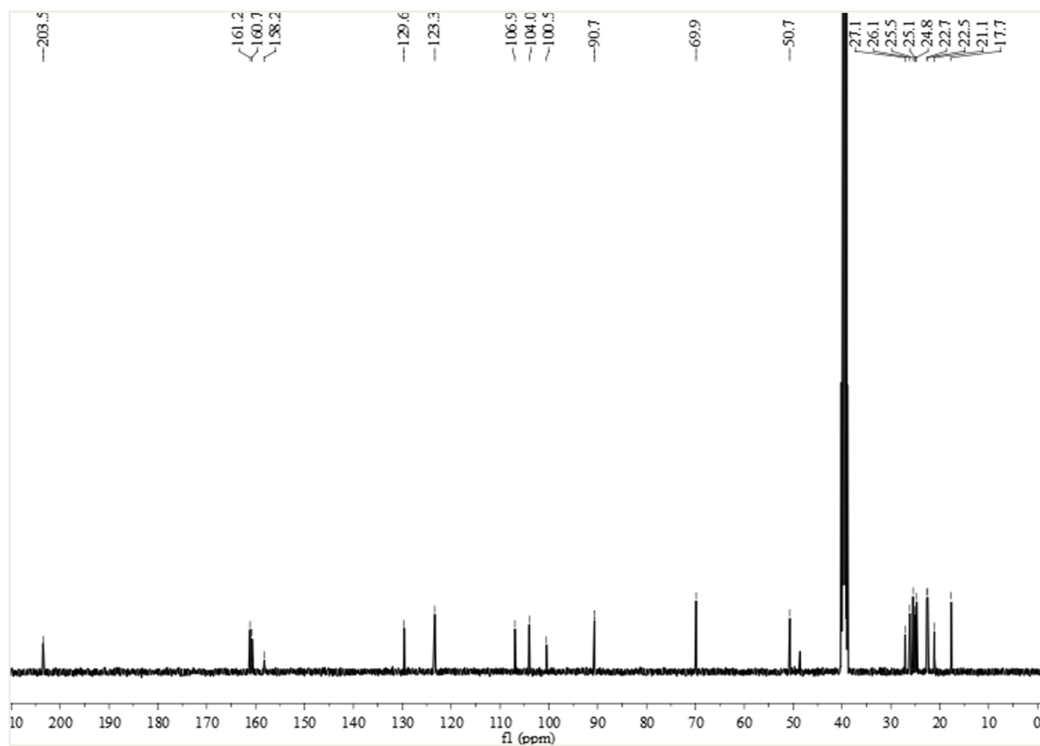
S73. The HPLC of chiral column analysis of lupulone G (**10**).



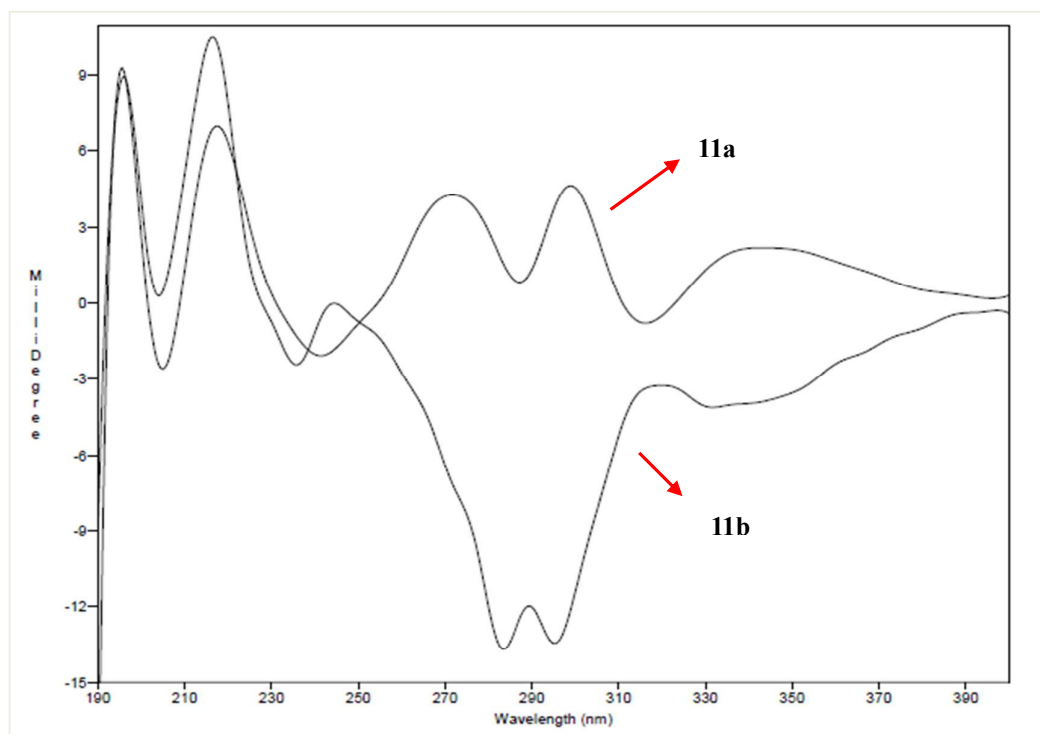
S74. ^1H NMR (400 MHz, $\text{DMSO}-d_6$) spectrum of 5-deprenyllupulonol C (**11**).



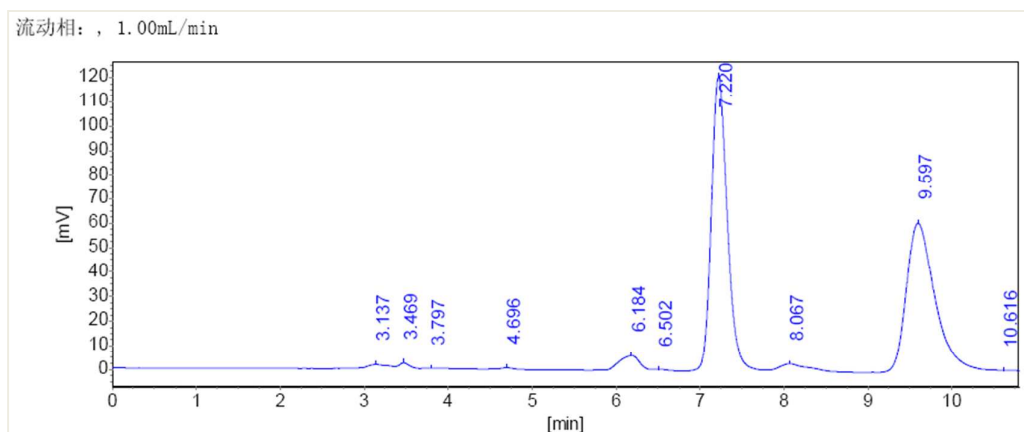
S75. ^{13}C NMR (100 MHz, $\text{DMSO}-d_6$) spectrum of 5-deprenyllupulonol C (**11**).



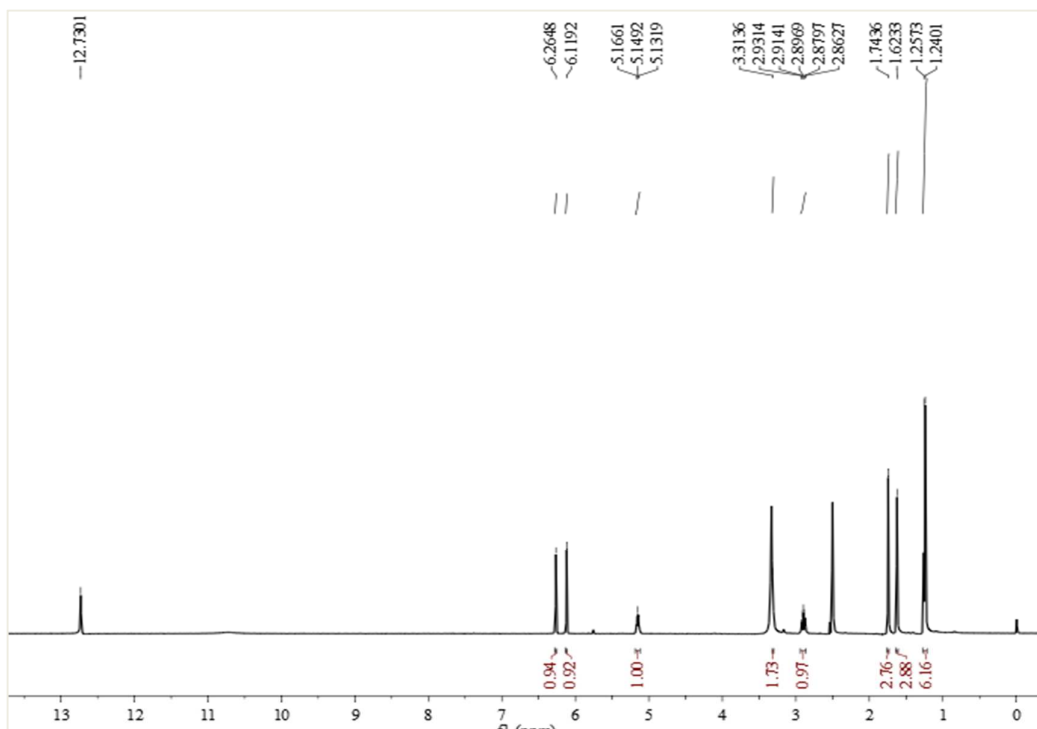
S76. Experimental CD spectrum of (*R*)-5-deprenyllupulonol C (**11a**) and (*S*)-5-deprenyllupulonol C (**11b**).



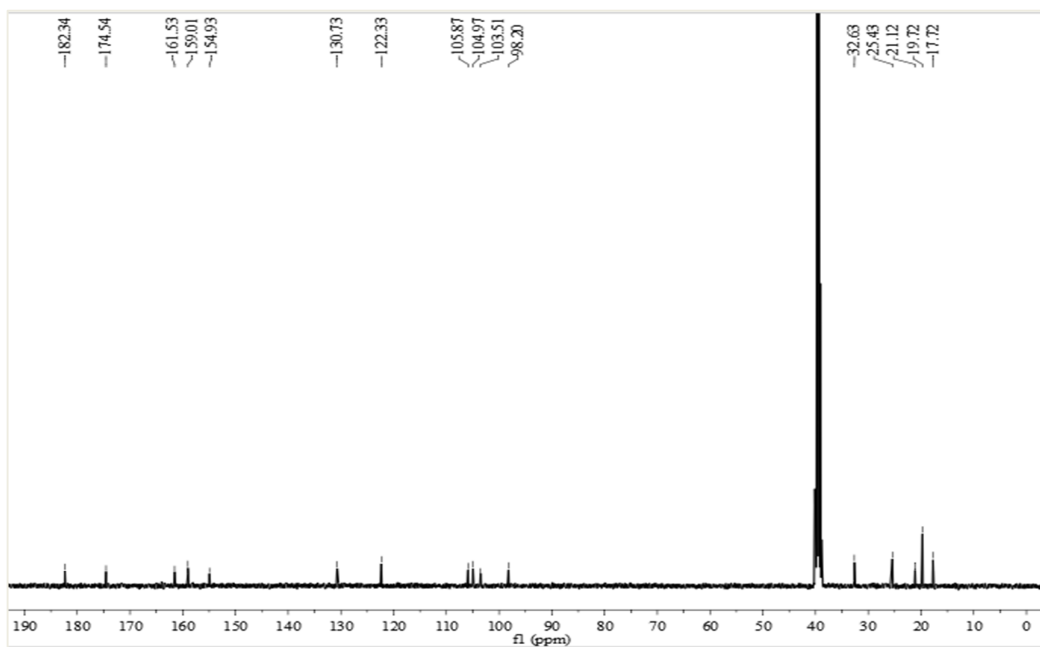
S77. The HPLC of chiral column analysis of 5-deprenyllupulonol C (**11**).



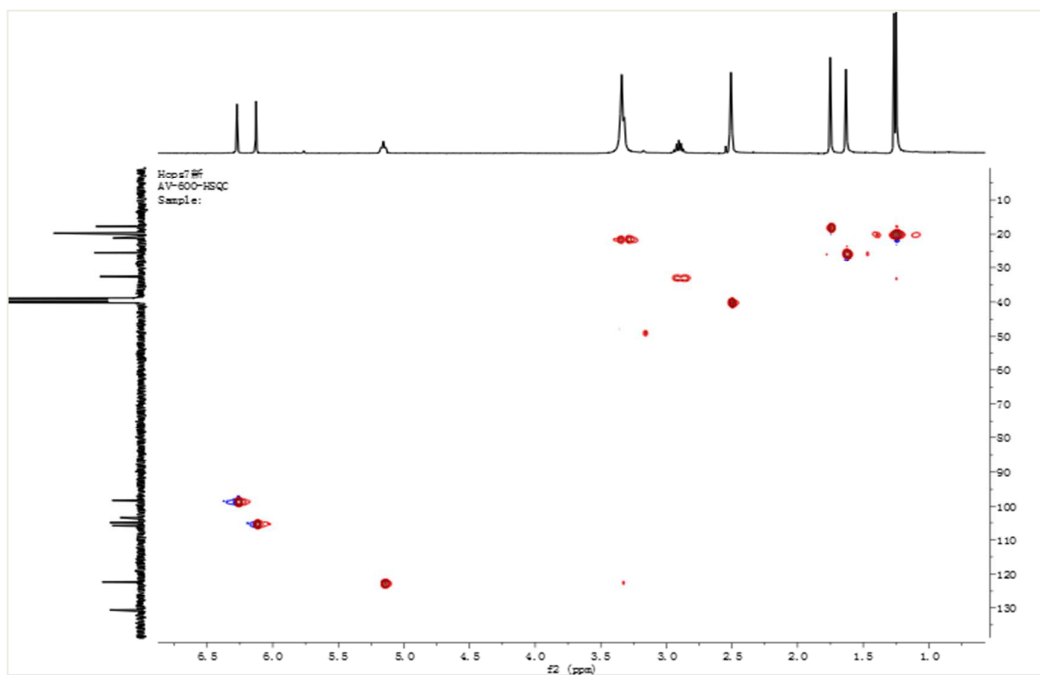
S78. ^1H NMR (400 MHz, $\text{DMSO}-d_6$) spectrum of 5,7-dihydroxy-2-isopropyl-8-prenylchromone (**12**).



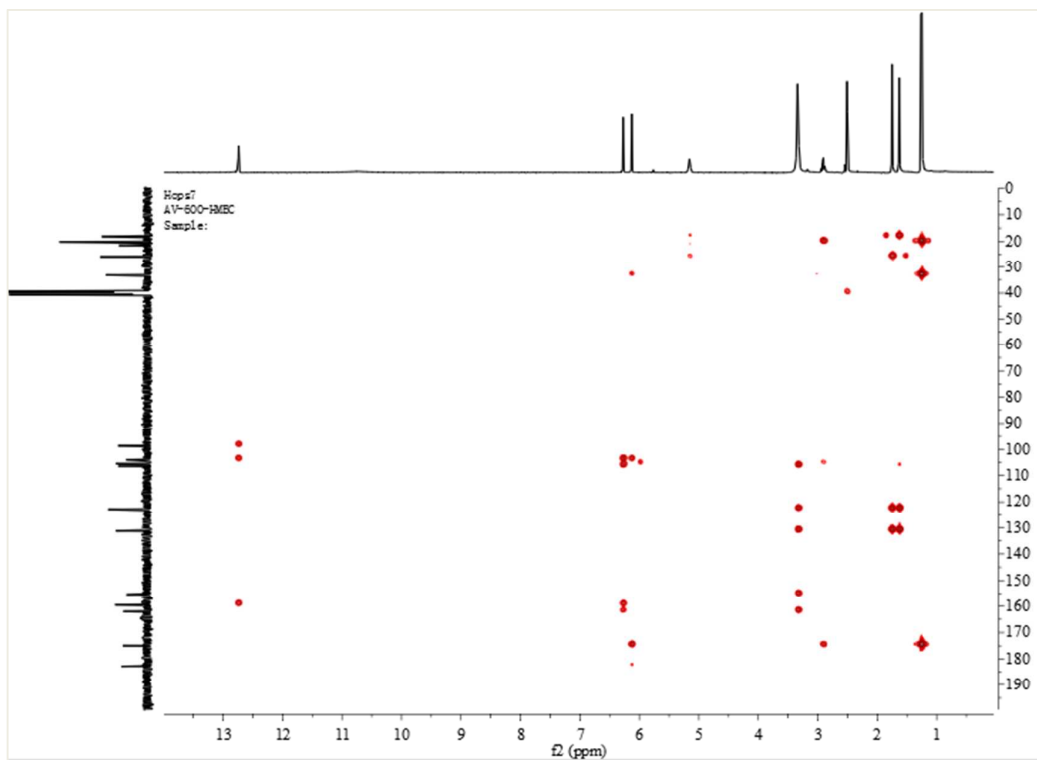
S79. ^{13}C NMR (100 MHz, $\text{DMSO}-d_6$) spectrum of 5,7-dihydroxy-2-isopropyl-8-prenylchromone (**12**).



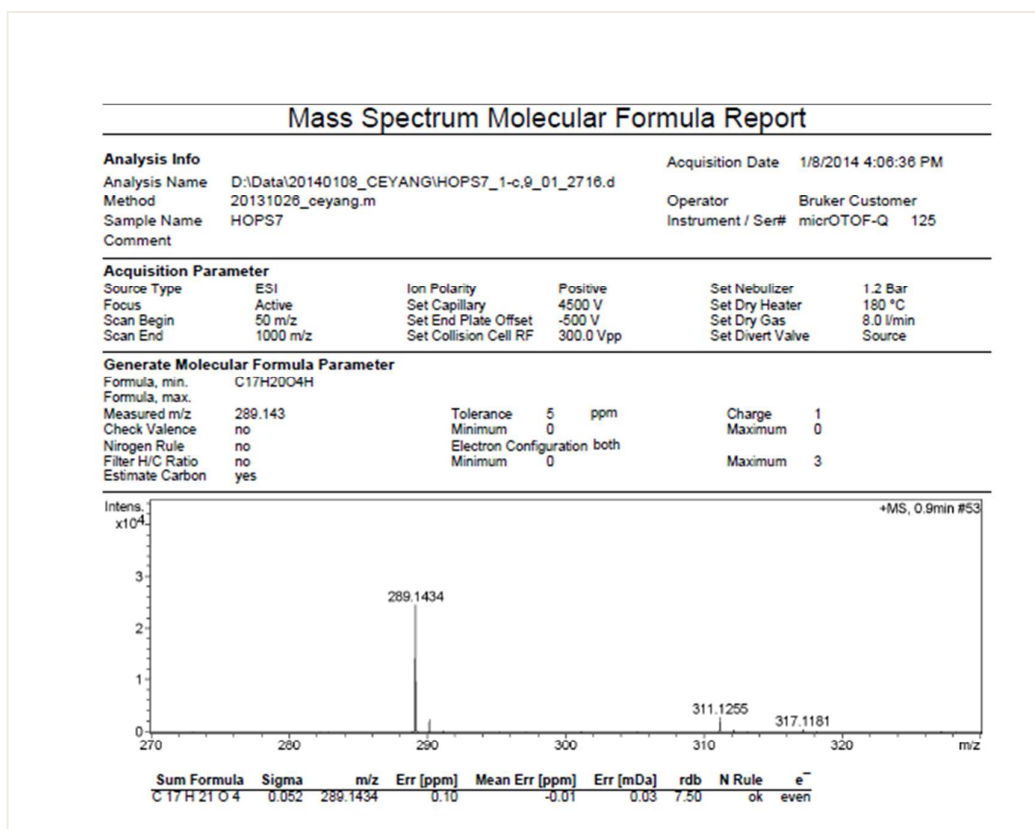
S80. HSQC (600 MHz, $\text{DMSO}-d_6$) spectrum of 5,7-dihydroxy-2-isopropyl-8-prenylchromone (**12**).



S81. HMBC (600 MHz, DMSO- d_6) spectrum of 5,7-dihydroxy-2-isopropyl-8-prenylchromone (**12**).



S82. HRESIMS spectrum of 5,7-dihydroxy-2-isopropyl-8-prenylchromone (**12**).



S83. The experimental method used for ECD calculations of compounds **1**, **4**, **5**, **7**, **8** and **9**

All structures were established by Schrodinger 2013 package. Conformational searches were performed using the bioactive search function of conformational search protocol of the Schrodinger 2013 package with 50 target conformers. The conformers generated from conformational search were optimized at the B3LYP/6-31G (d) level using Gaussian09 package. The optimized conformers were aligned using the flexible ligand alignment protocol to examine if there were identical conformers for some structurally similar conformers would lead to the totally identical conformer after structure optimization. After merging the identical conformers, the remaining conformers were subjected to frequent analysis at the B3LYP/6-31G (d) level and the population of each conformer was determined based on Boltzmann distribution. For compound **7** and **9**, eight conformers that contributes over 2 % of the population were used for ECD calculation. For compounds with high flexibility, the geometries from

the conformational searches studies would not represent the real geometries in the solution. Whereas NOE correlations were tested in liquid environments, giving more detailed information of a stereo-structure. Thus, for compounds **1**, **4** and **5**, the optimized geometries were subjected to intensive NOE analysis for the relative location of the isopentenyl at C-8 versus C-2'/C-1' of **1** and isopentenyl at C-7 versus the -C(CH₃)₂OH group at C-2 of **4** and **5** could predominate the ECD curves as the isopentenyl at C-8 was a large group besides the chromophore composed of C-8a, 4a, 5, 6, 7 in compound **1** (C-3a, 7a, 4, 5, 6 in compound **4** and **5**). The geometries that did not match the experimental NOE correlations were excluded for ECD calculations and finally 6 conformers for **1** and **4** (4 conformers for compound **5**) were used for further ECD calculation. For compound **8**, the conformational flexibility of the molecule was depicted in the molecular energy profiles (Figure S57 Supporting Information) with respect to the dihedral angle C2'-C3'-C3-C2, ranging from -180° to 180° at the B3LYP/6-31G(d) level of theory. As can be seen from Figure S57, the most stable conformer is obtained for 170° having energy of -1072.13358515 Hartree. Keeping C2'-C3'-C3-C2 at 170°, the conformer of lowest energy (170°) was used to perform conformational search, structure optimization and identical conformer merging studies by the same way as compounds **1**, **4**, **5**, **7** and **9** did and finally 3 conformers were generated for ECD calculation. ECD computations for all conformers were carried out at the B3LYP/6-31G (d) level in the gas phase. The calculated ECD spectrums were visualized and Boltzmann averaged using speedis software¹⁻³.

REFERENCES

- (1) Bruhn, T.; Schaumlöffel, A.; Hemberger, Y.; Pescitelli, G. Berlin. Germany, 2017.
- (2) Bruhn, T.; Schaumlöffel, A.; Hemberger, Y.; Bringmann, G. *Chirality*. **2013**, *25*, 243-249.
- (3) Pescitelli, G.; Bruhn, T. *Chirality*. **2016**, *28*, 466-47.

S84. BV-2 cell viability assay and effect of the extracts and isolated compounds **1-8**, **13-17** on LPS-induced NO production in BV-2 microglial cells.

